สำนักหอสมุดกลาง พระจอมเกล้าลาดกระบัง

ASSESSMENT ON PRACTICAL ESTIMATION FOR THE STATE OF CHARGE OF BATTERY IN ELECTRIC VEHICLE

E077279

NATHAPOL TAWEEWONG

เลขหมู่.....
เลขทะเบียน.077279
วัน.เดือน.ปี.-2 ส.ค. 2558

b 12671216
i.....

A THESIS SUBMITTED IN PARTIAL FULFILLMENT
OF THE REQUIREMENT FOR THE DEGREE OF
MASTER OF ENGINEERING IN AUTOMOTIVE ENGINEERING
(INTERNATIONAL PROGRAM)
INTERNATIONAL COLLEGE
KING MONGKUT'S INSTITUTE OF TECHNOLOGY LADKRABANG
2014
KMITL-2014-IC-M-004-008

This material is reserved for educational use only, not allowed for commercial use.
Forbidden to modify the content, and cite the document when use.

COPYRIGHT 2014
SCHOOL OF GRADUATE STUDIES
KING MONGKUT'S INSTITUTE OF TECHNOLOGY LADKRABANG

This material is reserved for educational use only, not allowed for commercial use.
Forbidden to modify the content, and cite the document when use.

Thesis	Assessment on Practical Estimation for the State of Charge of Battery in Electric Vehicle
Student	Mr. Nathapol Taweewong
Student ID	52600904
Degree	Master of Engineering in Automotive Engineering (International Program)
Year	2013
Thesis Advisors	Dr. Chi-na Benyajati
	Asst. Prof. Dr. Chinda Charoenphonphanich
	Prof. Masaki Yamakita

ABSTRACT

In order to use electric vehicles (EVs) and get the most efficiency out of it, the information about the battery status is important for drivers, since it helps them to know whether the battery is going to run out and also notifies how much further the vehicle can go. The accurate information about State of Charge (SoC) of each individual cell is one of important factors in developing a reliable battery monitoring system. However, unlike other physical properties of battery, SoC cannot be measured directly from a battery. The method for determining SoC varies depending on the battery type and on the application in which the battery is used.

The aim of this research was to present a battery estimation technique of two types of deep cycle Lead-Acid battery i.e. Flooded Lead-Acid battery and VRLA battery that was appropriated with an electric bus prototype. Various driving factors that directly affect the battery consumption of electric bus prototype were studied. The data was collected in both laboratory scale and real driving conditions. The results of the preliminary test, including specific gravity of battery electrolyte (S.G), open-circuit voltage (OCV), and α correcting factor, were used as a battery reference data for SoC estimation in real driving conditions. The real driving tests were conducted by different drivers in many driving situations with the resulting current flows from batteries measured and collected at every second. Then, a factor α was introduced to improve the accuracy of ampere-hour counting method.

The results revealed that by using mixed estimation techniques of Ampere-hour with correcting factor, the result of battery estimation tends to get closer to the referenced value from the OCV technique and, hence more accurate that the general ampere-hour counting technique. Nevertheless, the research also showed that the battery type, traffic conditions or even the driver's driving style were the factors that could not be neglected in order to get more accurate results.

This material is reserved for educational use only, not allowed for commercial use.
Forbidden to modify the content, and cite the document when use.

ACKNOWLEDGEMENTS

This thesis is the conformation of the kind hospitality from all who are involved. I sincerely thank you Dr. Chi-na Benyajati, Asst. Prof. Dr. Chinda Charoenphonphanich, and Assoc. Prof. Masaki Yamakita, for kindly be my advisors. Thank you for all information, knowledge, suggestions, and recommendations, which are always given unconditionally. They are all so invaluable. Mr. Piyapong Premvaranon, Mr. Jenwit Soparat, and Mr. Apichart Teralapsuwan thank you for helping and making all the tests and experiments finished successfully. Moreover, I am delight and grateful for all friendships given; you all make the time more interest and pleasant.

Additionally, for all supportive institutions: Materials Technology Center (MTEC) National Science and Technology Development Agency (NSTDA) for offering the scholarship and all required research facilities, TAIST Tokyo Tech for supporting the special education and research advises, and thank you King Mongkut's Institute of Technology Ladkrabang (KMITL) for kindly occur the academic program and staff.

Finally, again for my family, Ms. Thanyanart Saranyanitikul, and all of you and whom I may not mention, I really cannot thank you enough. "Thank you."

Nathapol Taweewong

March 2014

This material is reserved for educational use only, not allowed for commercial use.
Forbidden to modify the content, and cite the document when use.

CONTENTS

Page

ABSTRACT I

ACKNOWLEDGEMENTS II

TABLE OF CONTENTS III

LIST OF TABLES VI

LIST OF FIGURES VII

CHAPTER 1 INTRODUCTION 1

1.1 Background and problems 1

1.2 Objectives and Goal 2

1.2.1 Objectives 2

1.2.2 Goal 2

1.3 Scope of research 2

1.4 Motivations of research 3

1.5 Thesis organization 3

CHAPTER 2 LITERATURE REVIEW 6

2.1 Background of Electric Vehicles 6

2.1.1 Motivation for Electric vehicles 7

2.1.2 Types of electric vehicles 10

2.2 Background of Battery 12

2.2.1 Types of Battery for Automotive Applications 12

2.2.1.1 Lead-Acid Batteries 14

2.2.1.2 Nickel Based 15

2.2.1.3 Sodium Based 15

2.2.1.4 Lithium Based 16

2.2.2 Capacity 16

2.2.3 State of charge 17

2.2.4 Discharge current effects 18

2.2.5 Efficiency 19

2.2.6 Temperature effects 19

2.2.7 Aging effects 21

2.2.8 Self-discharge Effect on SoC 21

2.2.9 Some Technical Terms Related to Batteries 22

2.3 Previous study on State of Charge estimation techniques 22

2.3.1 Discharge test 24

This material is reserved for educational use only, not allowed for commercial use.

Forbidden to modify the content and cite the document when use.

CONTENTS (CONT.)

Page

2.3.2 Measurement of battery electrolyte 24
2.3.3 Open-circuit voltage 25
2.3.4 Ampere – hour Counting 25
2.3.5 Kalman filtering 26
2.3.5.1 Battery Model 26

CHAPTER 3 EXPERIMENTAL METHODOLOGY 27
3.1 Experimental setup 27
3.1.1 Battery 30
3.1.1.1 Flooded Lead-Acid battery 30
3.1.1.2 Valve regulated Lead-Acid (VRLA) battery 30
3.1.2 Experimental Tests 31
3.2 Laboratory Scale Experiment 33
3.2.1 Specific gravity Measurement 33
3.2.2 Ampere – hour Counting 34
3.2.3 Mixed estimations: Specific gravity Measurement and Ampere-hour Counting 34
3.2.4 Mixed estimations: Specific gravity Measurement and Ampere-hour Counting with correcting factor 35
3.3 Main Experiment in real driving conditions 36
3.3.1 Acceleration Test & Load Test 36
3.3.2 Fixed driving range test 37
3.3.3 Regenerative breaking test 37
3.4 Mixed estimation in real driving conditions 37

CHAPTER 4 RESULTS 42
4.1 Preliminary Test 42
4.1.1 Discharge test 42
4.1.2 Specific gravity test 43
4.1.3 Open Circuit Voltage (OCV) 44
4.1.4 Ampere-hour counting 46
4.1.5 Ampere-hour counting with correcting factor 47
4.2 Driving Test 49
4.2.1 Acceleration test 50
4.2.2 Fix driving range test 51

This material is reserved for educational use only, not allowed for commercial use.
Forbidden to modify the content and cite the document when use.

CONTENTS (CONT.)

Page

4.3 Battery State of Charge (SoC) 55

CHAPTER 5 DISCUSSIONS 60

5.1 Preliminary Test 60

5.1.1 Discharge test 60

5.1.2 Specific gravity test 61

5.1.3 Open Circuit Voltage 61

5.1.4 Ampere-hour counting - Ampere-hour counting with correcting factor 62

5.1.5 A comparison of State of Charge (SoC) estimation techniques 62

5.2 Driving Test 64

5.2.1 Acceleration test 64

5.2.2 Fix driving range test 65

5.2.2.1 Regenerative braking mode and Slippery mode 65

5.2.2.2 Effect of battery consumption 66

5.3 State of Charge (SoC) 66

CHAPTER 6 CONCLUSIONS AND SUGGESTIONS 69

6.1 Conclusions 69

6.2 Suggestions 70

REFERENCES 72

APPENDIX A: DATA ACQUISTION SPECIFICATIONS 74

APPENDIX B: PROCEEDINGS 80

BIOGRAPHY 105

This material is reserved for educational use only, not allowed for commercial use.

Forbidden to modify the content, and cite the document when use.

LIST OF TABLES

Table		Page
2.1	Status of Battery Systems for Automotive Applications	13
2.2	Comparison of Various Rechargeable Batteries	14
2.3	Effect of temperature on VRLA cell capacity	20
2.4	Summary of the different techniques for State of Charge estimation	23
3.1	Battery specifications	30
3.2	Example of the collecting data by Ah-counting and α corresponding factor	41
4.1	Variation of available capacity of flooded Lead-Acid battery	46
4.2	Variation of available capacity of VRLA battery	47
4.3	Available capacity and α corresponding factor (Flooded Lead-Acid battery)	47
4.4	Available capacity and α corresponding factor (VRLA battery)	48
4.5	The summarise of study cases in electric bus prototype	51
5.1	The available capacity of flooded lead-acid battery and VRLA battery	60
5.2	The estimation of maximum distance	66

This material is reserved for educational use only, not allowed for commercial use.
Forbidden to modify the content and cite the document when use.

LIST OF FIGURES

Figure		Page
1.1	MTEC Electric bus prototype	2
1.2	Research methodology flow chart	5
2.1	Electric Vehicle drive-train representation	7
2.2	Total emission of vehicle	8
2.3	World oil discovery, remaining reserves, and cumulative consumption	8
2.4	Ideal performance characteristics for a vehicle traction power plant	9
2.5	Typical performance characteristics of electric motors for traction	9
2.6	Tractive effort characteristics of a gasoline engine-powered vehicle	9
2.7	Possible EV configurations	11
2.8	Classification of hybrid electric vehicles	11
2.9	The reactions during the charge and discharge of the lead acid battery	15
2.10	Cut-off voltage of a typical battery	16
2.11	Discharge characteristics of a lead-acid battery	17
2.12	Discharge curves at 25°C for a 24V/37Ah SLA aircraft battery	18
2.13	Factors affecting the battery efficiency η	19
2.14	Effects of temperature on lead-acid batteries' discharge profile	20
2.15	Self-discharge rates versus time in NiH2 cell under open circuit	22
2.16	RC Battery Model schematic	26
3.1	Schematic diagram of laboratory-scaled experiment	27
3.2	EZ RED Hydrometer	28
3.3	LEM DHR100-C10 current transformer	28
3.4	Digital meter	28
3.5	National Instrument	28
3.6	The overall setup of preliminary experiment	28
3.7	MTEC Electric bus prototype	29
3.8	Replaceable Battery pack	29
3.9	The battery data of electric bus by data acquisition tools	29
3.10	GS Deep cycle lead-acid battery	30
3.11	Distilled water	30
3.12	Panasonic VRLA Battery	31
3.13	The internal structure of Panasonic EC-FV1260	31
3.14	Setup battery 5 steps charging system for VRLA battery	32
3.15	Battery 5 steps charging characteristic	32
3.16	The measurement of battery specific gravity by hydrometer	33

This material is reserved for educational use only, not allowed for commercial use.
Forbidden to modify the content and cite the document when use.

LIST OF FIGURES (CONT.)

Figure		Page
3.17	Constant current discharge test by adjusting the halogen light bulbs	34
3.18	Flowchart to determine SoC of lead acid battery	35
3.19	Flowchart to determine SoC of lead acid battery with correcting factor	36
3.20	Additional load 800kg during driving tests	37
3.21	Algorithm to determine SoC of Lead-acid battery in real driving condition	39
3.22	Characteristic of discharge current in real driving conditions	40
3.23	Example of the collecting data in real driving condition (VRLA Batteries)	40
4.1	Discharge Characteristic of Flooded Lead-acid Battery	42
4.2	Discharge Characteristic of VRLA Battery	43
4.3	Open circuit voltage versus Specific gravity and State of Charge	44
4.4	Measurement of electrolyte specific gravity between new battery and old battery	44
4.5	Battery voltage characteristics after open circuit	45
4.6	Open circuit voltage versus State of Charge of VRLA battery	45
4.7	The SoC estimation at different discharge rates by Ampere-hour counting method	46
4.8	The comparison of SoC estimation at different discharge rates of flooded lead-acid battery	48
4.9	The comparison of SoC estimation at different discharge rates of VRLA battery	48
4.10	The driving test of Flooded lead-acid battery in real traffic condition	49
4.11	The driving test of VRLA battery in real traffic condition	50
4.12	The acceleration test of flooded lead-acid battery	50
4.13	Battery terminal voltage of electric bus prototype (Regenerative braking)	52
4.14	Battery terminal voltage of electric bus prototype (Slippery)	52
4.15	VRLA battery consumption (with regenerative breaking)	53
4.16	VRLA battery consumption without regenerative breaking (Slippery)	53
4.17	Flooded Lead-Acid battery consumption (with regenerative breaking)	54
4.18	Flooded Lead-Acid battery consumption without regenerative breaking (Slippery)	54
4.19	VRLA battery consumption at different drivers	55
4.20	Flooded Lead-Acid battery consumption at different drivers	55
4.21	Battery parameters and SoC of VRLA battery (Regenerative braking mode)	56
4.22	Battery SoC and OCV of VRLA battery	56
4.23	Battery parameters and SoC of VRLA battery	57
4.24	Battery parameters and SoC of flooded Lead-Acid battery (Regenerative braking mode)	57
4.25	Specific gravity of flooded Lead-Acid battery (Regenerative braking mode)	58
4.26	Battery parameters and SoC of flooded Lead-Acid battery (Slippery mode)	58

This material is reserved for educational use only, not allowed for commercial use.
Forbidden to modify the content and cite the document when use.

LIST OF FIGURES (CONT.)

Figure		Page
4.27	Specific gravity of flooded Lead-Acid battery (Slippery mode)	59
5.1	The comparison of available capacity between flooded lead-acid and VRLA battery	61
5.2	A comparison of SoC estimation technique (flooded lead-acid battery)	63
5.3	A comparison of SoC estimation technique (VRLA battery)	63
5.4	Motor characteristics of electric bus at various driving conditions	64
5.5	A comparison of state of charge estimation (VRLA battery)	67
5.6	Flowchart to determine SoC of lead acid battery with correcting factor	67
5.7	A comparison of state of charge estimation (VRLA battery)	68

This material is reserved for educational use only, not allowed for commercial use.

Forbidden to modify the content and cite the document when use.

CHAPTER 1
INTRODUCTION

1.1 Background and problems

Nowadays, the lacking of natural resources has become one of the world's largest problems. Oil is one of the most important resources that has been involved and been used in everyday life, utilities, and industrials; with the higher number of demand, the number of resources are totally opposite. The number of the active oil fields is dramatically decreased. Thus, the volume of oil needed is higher than the supply, which causing the shortage of the energy and oil price crisis. Therefore, the seeking and invention of renewable energy is crucial.

Transportation sector is one of the most simply known having high number of oil consumption. Consequently, the research and development in alternative energy of that sector is significant in order to lessen the problem. According to the trend of the relating industries, the essential of the vehicles' innovation for the next generation could mainly be powered by electricity.

In internal combustion vehicles, a fuel gauge is an important part for displaying the remaining fuel in the fuel tank of vehicle. Similarly for electric vehicles, it is also necessary to know the amount of remaining charges in battery and to be able to display how far the vehicle can still travel. Thus, a significance of a battery monitoring system to electric vehicle is equivalent to how a fuel gauge is to internal combustion vehicles.

The State of Charge (SoC) is one of the important factors in a battery monitoring system. SoC could be defined as the percentage of the maximum possible charge that is presented inside a rechargeable battery [1]. Many techniques can be used to estimate SoC in lead-acid such as the specific gravity measurement, the coulomb counting technique, the open circuit voltage test, the model based technique, the Kalman filter, and etc. There are also many other factors for estimating SoC such as battery voltage, battery current, battery temperature, battery life, etc.

In 2008, the automotive laboratory of National Metal and Materials Technology Center (MTEC) has started the EVs project with the goal of developing a medium-size bus prototype that can be produced in Thailand (Figure1.1). In this prototype, 24 units of 12V, 130Ah lead acid batteries were used as power source for AC drive motor (maximum rated power 90kW) and the other 24 units of batteries were used for other electrical devices in the bus. The AC inverter needs high voltage for operates. Therefore, batteries were connected in series to achieve nominal 288V DC source and 130Ah.

This material is reserved for educational use only, not allowed for commercial use.
Forbidden to modify the content, and cite the document when use.

Figure 1.1 MTEC Electric bus prototype

1.2 Objectives and Goal

1.2.1 Objectives

The overall objective of the research is to study the State of Charge (SoC) estimation techniques of battery that appropriately used with electric bus prototype. This objective can be further specified into the following aspects:

1) To gain a deeper understanding of the SoC estimation techniques.
2) To obtain a SoC for estimate a remaining battery capacity i.e. remain SoC, run-time and ranges of electric vehicles.
3) To study the driving factors that directly effect to the battery consumption of an electric bus prototype.

1.2.2 Goal

The goal of this project is to study the most practical and accurate State of Charge estimation technique for electric bus prototype.

1.3 Scope of research

In general, there are various battery SoC estimation techniques, but the scope of this research is to study a practical and more accurate SoC estimation technique by using data acquisition tools and LabVIEW Signal Express. The data acquisition hardware by National Instrument (NI) is widely used for measuring and acquiring raw data while LabVIEW Signal Express is a software tool to acquire, analyze, and present data.

This material is reserved for educational use only, not allowed for commercial use.
Forbidden to modify the content, and cite the document when use.

The ampere-hour counting is the closest concept idea for battery State of Charge. However, the main problem of ampere-hour counting technique is an initial SoC and a battery life. Since the SG is relatively easy to be measured in flooded lead-acid battery, the SG data will be the key for accuracy of estimation technique of flooded lead-acid battery. Moreover, the open circuit voltage (OCV) is also an important physical parameter of VRLA battery. Nonetheless, the discharge rate is directly effect to capacity of battery; a factor α was presented to improve the accuracy of estimation technique.

This thesis presents a new progressive SoC estimation of lead-acid battery by using data acquisition tools and LabVIEW Signal Express. Apart from battery current, voltage, and temperature, the Specific Gravity (SG) values and OCV of battery will be used as parameter for SoC estimation. By using factor α combine with ampere-hour counting method, the progressive SoC estimation technique will be presented.

1.4 Motivations of research

This research is motivated by the assumption that electric vehicles signify as alternative vehicles for future transportation. Electric vehicles have many advantages over internal combustion engine vehicles such as; zero emissions vehicles, self-sufficiency from petroleum crisis, and high efficiency. In the near future, electric vehicles can become increasingly popular due to an imminent shortage of fossil fuel resource. The main cause of global emissions comes from pollutions by internal combustion engine in transportations. To reduce global emissions and solve petroleum price crisis, there has been a clear sign that majority of next generation vehicles will be powered by electricity.

As a battery monitoring system is a major part in electric vehicles, a high-accuracy State of Charge (SoC) monitor is needed. The results of proposed study can be used initially in an MTEC electric bus and can be used as a guideline for development of other electric vehicle projects in Thailand.

1.5 Thesis organization

This thesis presents and specifies the work done to study, analyze, and estimate a battery management system focusing on State of Charge (SoC) for an electric bus prototype. The content is divided into five main chapters: introduction, literature review, experimental methodology, result and discussion and conclusion. The first chapter, as shown above, it begins with the problem statement and general background, objectives and goal, scope, and motivation of this research. The outline of other sections are summarized as follow:

This material is reserved for educational use only, not allowed for commercial use.
Forbidden to modify the content, and cite the document when use.

Chapter 2: Literature review

In this chapter, the overview of the electric vehicles including the background information, the motivations, and the type of electric vehicles will be reviewed. Furthermore, the background, type and detail of batteries, and the previous study on State of Charge estimation techniques will be presented.

Chapter 3: Experimental methodology

A practical State of Charge (SoC) estimation will be discussed in this chapter. This will present a methodology and implementation of this work: software and hardware, experimental setup, the data acquisition tools, combined estimations and experiment in real driving condition.

Chapter 4: Results

In chapter 4, the experimental results both laboratory scale and real driving condition are shown, along with, the battery behaviors that are including; ability of discharge rate, available capacity, State of Charge (SoC), and battery behavior in real driving condition.

Chapter 5: Discussions

For chapter 5, the characteristics and behaviors of both flooded lead-acid and VRLA battery will be examined. Additionally, the numerical method of the appropriate State of Charge (SoC) estimation technique for electric bus prototype is explained. Nonetheless, the comparison and discussion of each estimation technique, advantages and drawbacks will be given. After, all result have been declared and discussed. Finally, in the last chapter (chapter 6) all results will be summarized and concluded.

This material is reserved for educational use only, not allowed for commercial use.
Forbidden to modify the content, and cite the document when use.

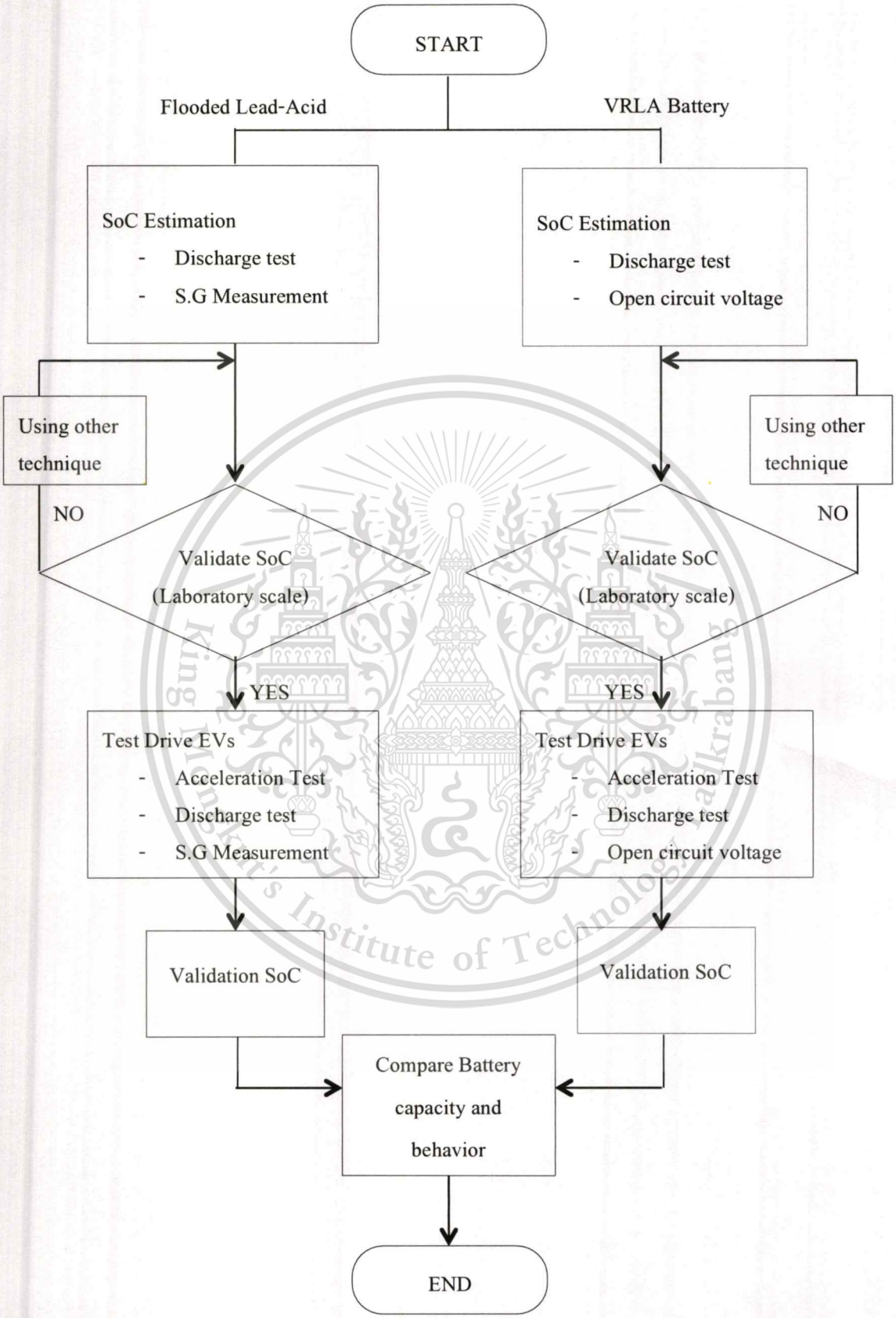

Figure 1.2 Research methodology flow chart.

This material is reserved for educational use only, not allowed for commercial use.
Forbidden to modify the content, and cite the document when use.

CHAPTER 2
LITERATURE REVIEW

The literature reviews are classified into three main topics: the background information of the electric vehicles; showing the innovation, motivations, and classified the type of the electric vehicles. The background of battery; declaring information of each type of battery, Lead-Acid Batteries, Nickel Based, Sodium Based, and Lithium Based, and also the other specific data relates the battery structures. Lastly, the previous study on State of Charge estimation techniques.

2.1 Background of Electric Vehicles

Because of recent global warming phenomena and oil price crisis, there has been a clear sign that majority of next generation vehicles will be powered by electricity. History of electric vehicles (EVs) development dated back to 1834 [2, 3]. French engineer, Gustave Trouvé, developed the first electric vehicle in 1881. It was a tricycle powered by lead-acid batteries for drive a 0.1hp DC motor [4]. Due to the improvements of the performance of internal combustion engine vehicles and lack of technology about battery and electric motor in electric vehicles, the interest in electric vehicles was reduced and temporarily ended in early 20th century. However, as petroleum price was increasing and environmental problems were more evident in late 20th century, the electric vehicles have become popular again.

Electric vehicles (EVs) use an electric motor for traction, instead of an engine in internal combustion engine vehicles (ICEVs), and use batteries as electricity storage for operation. Figure 2.1 is shown the essential concept of electric vehicles. The main components consist of an electric motor, energy storage unit (batteries), electronic control unit and drive train. Today, there are many various types and sizes of batteries such as; Lead-acid batteries (Pb-acid), Nickel- based batteries, Sodium-based batteries, and more recently, Lithium batteries. The different types of battery depended on different field of applications. There are some requirements for electric vehicles batteries such as; specific power, specific energy, efficiency, cost, maintenance, safety, and environmental friendly. At the present only few types of commercial battery are appropriate for use in electric vehicles, those types are lead-acid, nickel iron, nickel cadmium, nickel metal hydride, lithium polymer and lithium ion, sodium sulphur and sodium metal chloride [5].

This material is reserved for educational use only, not allowed for commercial use.
Forbidden to modify the content, and cite the document when use.

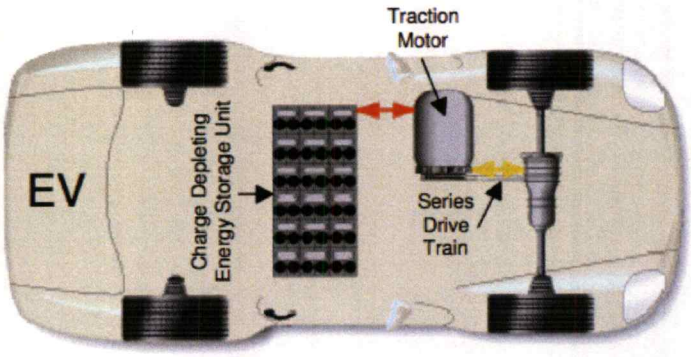

Figure 2.1 Electric Vehicle drive-train representation.

However, the limited travel range of electric vehicles is a serious drawback. Normally, electric vehicles could travel about 80km or so on a single charge (under good conditions) [2]. Travel range of electric vehicles usually depended on various types and sizes of rechargeable batteries. The major problem of rechargeable batteries is rechargeable time, several hours required to re-charge batteries, while only few minutes needed on a full-tank of gas.

2.1.1 Motivation for Electric vehicles

Electric vehicles have many advantages over internal combustion engine vehicles such as; zero emissions vehicles, self-sufficiency from petroleum crisis, high efficiency, and no sound pollutions.

Global warming, climate change and rising of sea level are also affect from emissions by mankind. Pollutions from internal combustion engine in transportation are a main cause of global emissions. Carbon dioxide (CO_2) and water vapor (H_2O) are produce of complete combustion in combustion engine. Normally, the complete combustion is not ideal, an incomplete combustion produce harmful emissions i.e. nitrogen oxides (NO_x), carbon monoxides (CO) and unburned carbon (HC) (Ehsani et.al, 2005). Electric vehicles are known as zero emissions vehicles, no emissions (CO_2, NO_x, CO, HC and other greenhouse gas) generated from the vehicles. However, emissions are generated in electricity generation process as shown in Figure 2.2.

Petroleum is non-renewable resource because it takes million of years to form. Due to the increasing of population, a lot of resources are used for living, industrial, and transportation. Figure 2.3 shown the petroleum discovery and consumption trends, the world petroleum will be run out in nearly future [4]. Impending petroleum exhaustion, an alternative energy source is necessary for future living.

This material is reserved for educational use only, not allowed for commercial use.
Forbidden to modify the content, and cite the document when use.

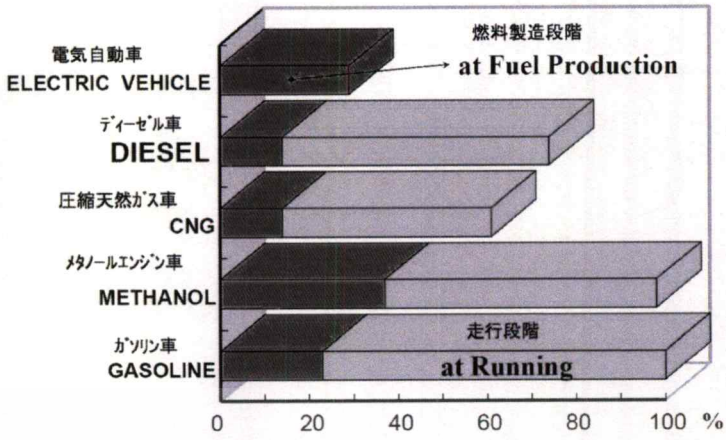

Figure 2.2 Total emission of vehicle.

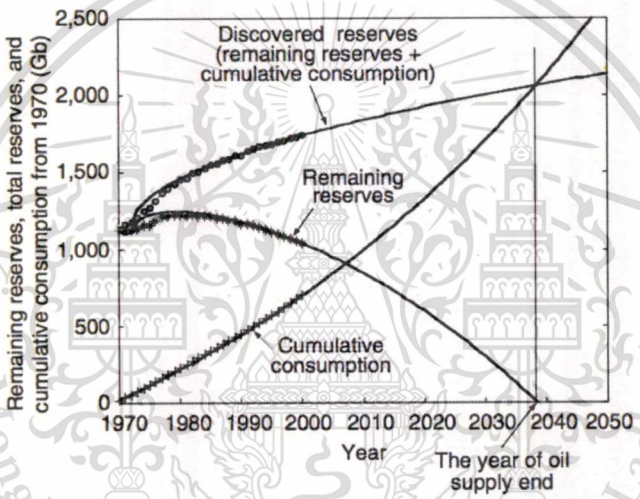

Figure 2.3 World oil discovery, remaining reserves, and cumulative consumption.

Normally, the efficiency of electric motor is about 70% to 85%, that higher than combustion engine. There are only few moving parts, so maintenance is also minimal. There are no engine-oil changes, timing, or tune-ups. Moreover, the ideal performance characteristics for vehicle traction (Figure 2.4) are matched to characteristics of electric motor (Figure 2.5). High torque requires for acceleration at low speed, then requires less torque as cruising speed is approached. An electric motor can develop maximum torque at low rpm, with torque declining with speed, mostly in step with a vehicle's natural demand [6]. A multi-gear transmission is necessary for internal combustion engine vehicles in order to modify the output traction properly match to ideal vehicle traction, as shown in Figure 2.6. Nonetheless, by changing the electric polarity input of motor, the reverse gear is unnecessary in electric vehicles.

This material is reserved for educational use only, not allowed for commercial use.
Forbidden to modify the content, and cite the document when use.

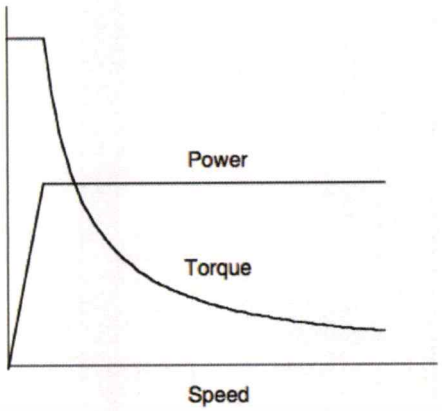

Figure 2.4 Ideal performance characteristics for a vehicle traction power plant.

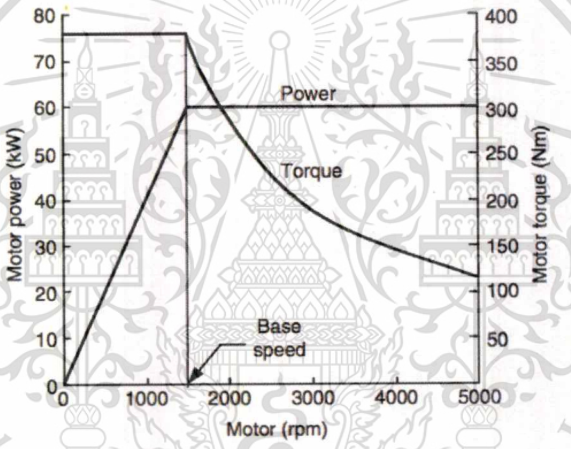

Figure 2.5 Typical performance characteristics of electric motors for traction.

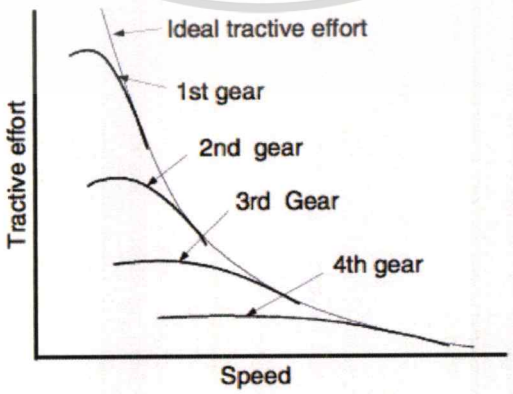

Figure 2.6 Tractive effort characteristics of a gasoline engine-powered vehicle.

This material is reserved for educational use only, not allowed for commercial use.
Forbidden to modify the content, and cite the document when use.

Another advantage of electric vehicles is the inherent bi-directionality of their energy loop [6]. In internal combustion engine vehicles a powertrain can only convert energy into vehicle motion, while electric vehicles can convert vehicle motion back into energy during braking by using regenerative breaking system. Due to energy conversion losses only 30% to 50% [7] of energy can be recover to energy storage.

2.1.2 Types of electric vehicles

From 19th century, the area of development in vehicles is not only focus on purely electric vehicles. There are many concepts of electric vehicles that may classify as follows.

Firstly there is an electric vehicle, which is a fully use battery as power source for drive motor. Varies possible concepts of electric vehicles configurations are shown in Figure 2.7 [8]. The second type is hybrid electric vehicle, which combine an internal combustions engine and an electric motor. In recent years, many automobile manufacturers launched their own hybrid vehicles to market, by many advantages (fuel consumptions, low pollution emissions, etc.) hybrid electric vehicles become more popular choice for customer. Hybrid electric vehicles can classify in to 4 kinds: series hybrid, parallel hybrid, series–parallel hybrid, and complex hybrid, as shown in Figure 2.8 [8]. Another type is a fuel cell vehicle, which almost the same principle as electric vehicles but only replace the energy source from batteries to fuel cell. By using hydrogen that is stored in liquid form, fuel cell can be produce electricity for drive the vehicle in longer range than battery. However there are many problems to overcome before they become a commercial: i.e. cost, hydrogen supply, cooling system, etc. And there are some types of electric vehicles; electric vehicles using supply line, solar powered vehicles, and electric vehicles that use flywheels of super capacitors.

This material is reserved for educational use only, not allowed for commercial use.
Forbidden to modify the content, and cite the document when use.

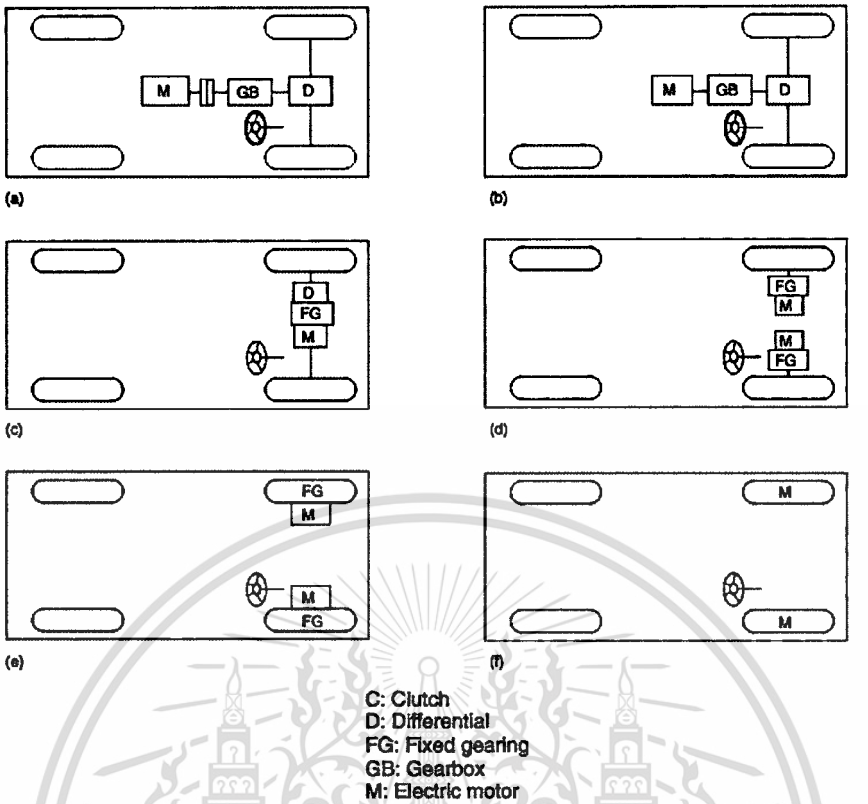

Figure 2.7 Possible EV configurations.

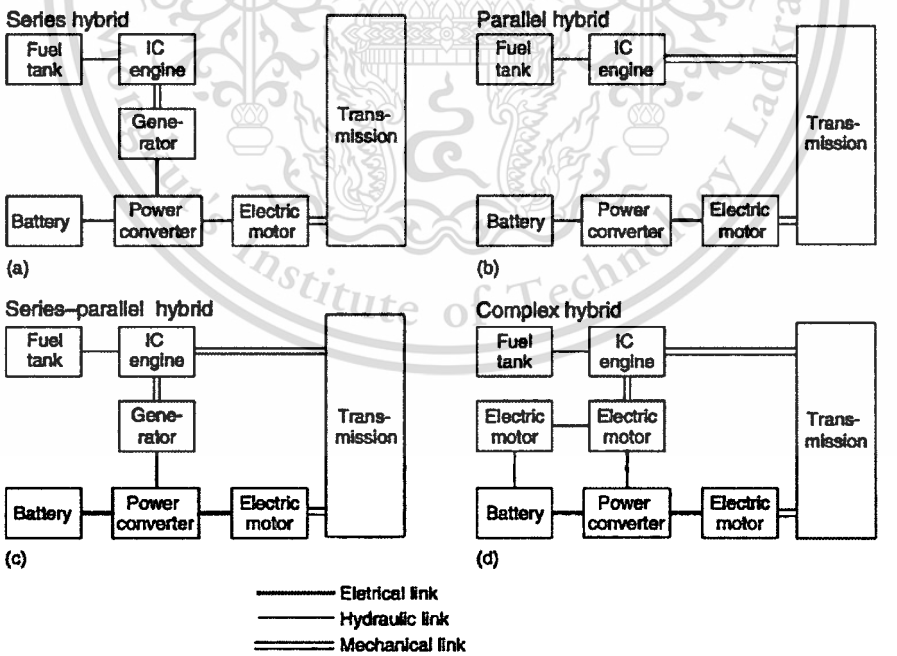

Figure 2.8 Classification of hybrid electric vehicles.

This material is reserved for educational use only, not allowed for commercial use.
Forbidden to modify the content, and cite the document when use.

2.2 Background of Battery

Nowadays, electric devices have become a major part of our life. All portable electric devices use battery as electricity storage for operation. Batteries are electrochemical devices that convert electrical energy into potential chemical energy during charging, and convert chemical energy into electric energy during discharging [9]. In the most basic terms, a battery is an electrochemical cell in which an electric potential (voltage) is generated at the battery terminals by a difference in potential between the positive and negative electrodes [10].

Batteries are mostly classified into 2 types: Primary Batteries and Secondary Batteries (Rechargeable Batteries). Primary batteries (non-rechargeable batteries) are battery in with electrochemical reaction is irreversible. It can be used only once and discarded, cannot reuse after full discharge. Normally, primary batteries have higher energy densities commonly used in portable devices that have low discharge current. Some examples of primary batteries are Alkaline battery, Aluminum battery, Silver Oxide battery, Zinc Carbon battery, Zinc Air battery, Zinc Chloride battery, Lithium battery, Mercury battery etc. [11]. Secondary batteries (rechargeable batteries) are battery in with electrochemical reaction can reversible. These batteries can be used multiple times and recharged very cheaply. It can be used in varies discharge current and many fields of applications; portable devices, uninterruptible power supplies (ups), automotive field and etc. Some examples of rechargeable batteries are Lead acid, Nickel Cadmium, Nickel Metal Hydride, Lithium ion, Lithium Polymer, Silver Zinc, Nickel Iron, Lithium Titanate, Lithium Sulphur etc. [11].

2.2.1 Types of Battery for Automotive Applications

Today, there are many various types and sizes of batteries such as; Lead-acid batteries, Nickel-based batteries, Sodium-based batteries, and more recently, Lithium batteries. The different types of battery depended on different applications. There are some requirements for electric vehicles batteries such as; specific power, specific energy, efficiency, cost, maintenance, safety, and environmental friendly. For automotive field, secondary batteries are chosen as power sources. In Table 2.1 and Table 2.2, a review of battery specification is presented [12].

This material is reserved for educational use only, not allowed for commercial use.
Forbidden to modify the content, and cite the document when use.

Table 2.1 Status of Battery Systems for Automotive Applications.

System	Specific Energy (Wh/kg)	Peak Power (W/kg)	Energy Efficiency (%)	Cycle Life	Self-Discharge (% per 48 h)	Cost (US$/kWh)
Acidic aqueous solution						
Lead/acid	35–50	150–400	>80	500–1000	0.6	120–150
Alkaline aqueous solution						
Nickel/cadmium	50–60	80–150	75	800	1	250–350
Nickel/iron	50–60	80–150	75	1500–2000	3	200–400
Nickel/zinc	55–75	170–260	65	300	1.6	100–300
Nickel/metal hydride	70–95	200–300	70	750–1200+	6	200–350
Aluminum/air	200–300	160	<50	?	?	?
Iron/air	80–120	90	60	500+	?	50
Zinc/air	100–220	30–80	60	600+	?	90–120
Flow						
Zinc/bromine	70–85	90–110	65–70	500–2000	?	200–250
Vanadium redox	20–30	110	75–85	—	—	400–450
Molten salt						
Sodium/sulfur	150–240	230	80	800+	0[a]	250–450
Sodium/nickel chloride	90–120	130–160	80	1200+	0[a]	230–345
Lithium/iron sulfide (FeS)	100–130	150–250	80	1000+	?	110
Organic/lithium						
Lithium-ion	80–130	200–300	>95	1000+	0.7	200

[a]No self-discharge, but some energy loss by cooling.

King Mongkut's Institute of Technology Ladkrabang

This material is reserved for educational use only, not allowed for commercial use.
Forbidden to modify the content, and cite the document when use.

Table 2.2 Comparison of Various Rechargeable Batteries.

S.No	Feature		Lead Acid	NiCd	NiMH	Li-ion	Li-Pol	Ag-Zn
1	Cell Voltage (V)		2.1	1.2	1.2	4.1	4.1	1.86
2	Specific Energy (MJ/Kg)		Low	Low	Moderate	High	High	Very High
3	Cost		Moderate	Low	Low	High	Very High	Very High
4	Load Current	Peak	5C	20C	5C	2C	2C	30C
		Best Result	0.2C	1C	0.5C or Lower	1C or Lower	1C or Lower	2C to 3C
5	Self Discharge Rate (Per Month)		Very Low	Moderate	Very High	Low	Low	Negligible
6	Memory Effect		No	Yes	Yes	No	No	No
7	Operating Temp.(°C)		-20 to 60	-40 to 60	-20 to 60	-20 to 60	0 to 60	-30 to 60
8	Internal Resistance		Low	Low	Moderate	High	High	Very Low
9	Efficiency (%)		70 to 92	70 to 90	62 to 70	80 to 90	85 to 95	94 to 98
10	Recharge Life (Cycles)		500 to 800	1300 to 1500	500 to 1000	1000 to 1200	800 to 1000	>4000
11	Environmental Impact		More	More	Less	Very Less	Very Less	Very Less
12	Overcharge Tolerance		More	Moderate	Less	Very Less	Less	Less
13	Maintenance Req. (Days)		90 to 180	30 to 60	60 to 90	Not Required	Not Required	Not Required

2.2.1.1 Lead-Acid Batteries

Lead-acid battery is the most popular type of battery for over century. It is a cheap battery compare to kilo-watt-hour of charge widely used for storage in applications such as; SLI (starting, lighting, ignition), UPS (uninterruptible power supply), and stationary applications. However, lead-acid battery has low specific power compared to other types of batteries. Overall reaction of Lead-acid can be generally expressed by

$$PbO2 + Pb + 2H2SO4 \rightleftharpoons 2PbSO4 + H2O \quad (2.1)$$

In the discharge of a lead-acid battery, the lead dioxide and lead react with the sulfuric acid in the electrolyte to form the lead sulfate on the positive and negative plates, respectively. During charge process, the sulfuric acid revert back into the solution state again as shown in Figure 2.9 [5, 13]

This material is reserved for educational use only, not allowed for commercial use.
Forbidden to modify the content, and cite the document when use.

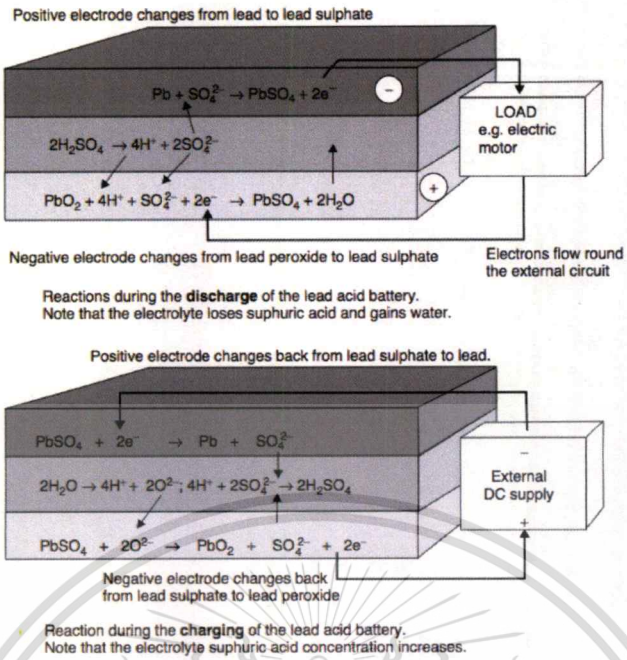

Figure 2.9 The reactions during the charge and discharge of the lead acid battery.

There are 2 types of lead-acid batteries; flooded lead-acid battery and valve regulated lead-acid (VRLA) battery (Sealed lead-acid battery). Flooded lead-acid battery requires watering with distilled water once to twice a month, while VRLA do not require addition water to the cells. VRLA battery can classify in to 2 types; there are the absorbed glass mat (AGM) based battery and the gel technology battery [10].

2.2.1.2 Nickel Based

Nickel Cadmium (Ni-Cd) batteries are already using in some EVs manufacturer. The advantages of Ni-Cd are high energy density, more cycle life and recharge very quickly. However, the cost of nickel is more expensive than lead-acid and highly toxic. Nickel Iron (Ni-Fe) batteries also have high energy density and high deep-discharge cycle. Though, the overcharge problem needs to be concern. Another type of nickel based is nickel-metal hydride (NiMH) battery. NiMH is environmental battery, all components are nontoxic recyclable materials. The cycle life of NiMH is twice of lead-acid batteries, maintenance free, and quickly charge.

2.2.1.3 Sodium Based

The specific energy of sodium sulfur (NaS) batteries is 5 times higher than lead-acid batteries. The cost of NaS may drop by high – volume production. Another type of sodium based batteries is sodium nickel chloride (NaNiCl2) batteries, which is being tested and developed by

This material is reserved for educational use only, not allowed for commercial use.
Forbidden to modify the content, and cite the document when use.

some Germany EVs manufacturer. However, the main problem of sodium based batteries is safety of battery. The melting point of sulfur, the battery must be kept at a temperature around 300C.

2.2.1.4 Lithium Based

Lithium-ion battery is the most commonly used in portable device, with the high specific power, high specific energy and more life cycles. Although it is very expensive and still has a problem about safety of battery during charge/discharge, a cooling system required for keep battery as operating temperature. Lithium-polymer battery is another interesting type of battery, the twice energy can supply by only 20% cost more than lead-acid battery. But it still has some problem, the battery need to scale up the size for use properly in EVs.

2.2.2 Capacity

By electrochemical reaction, batteries store and produce the electric energy during charging and discharging. Generally, batteries are rated by voltage and ampere-hour (Ah). Battery voltage is depended on the number of cells connected in series (about 2.0 volt/ cell for lead-acid) [14]. The most common voltage rating for EVs battery is 12 volts (6 cells). Battery manufacturers usually specify the battery with coulometric capacity (amp-hours), which is defined as the number of amp-hours gained when discharging the battery from a fully charged state to cut-off voltage as shown in Figure 2.10 [13].

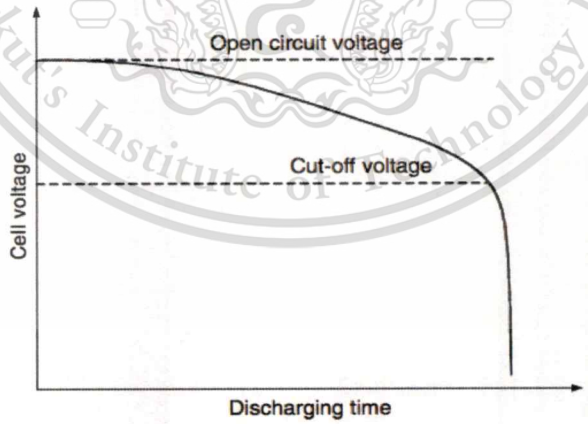

Figure 2.10 Cut-off voltage of a typical battery.

Technically, an ampere-hours (Ah), defined as the integral product of current (Amperes) and time (hours), as expressed below:

$$Ah = \int_0^t I\,dt \tag{2.2}$$

This material is reserved for educational use only, not allowed for commercial use.
Forbidden to modify the content, and cite the document when use.

สำนักหอสมุดกลาง พระจอมเกล้าลาดกระบัง

Nonetheless, available capacity of the same battery is depended on rate of discharge, temperature and age. The battery industry conventionally uses C- rate to scale the charge and discharge current of a battery [15]. For example, 10Ah battery can generate 1A for 10 hours (C_{10}), or 5A for 2 hours (C_2), or in theory 10A for 1 hour (1C). The common discharge rate for identify the specification of battery is measured at 20 hours (C_{20}) [2]. Normally, at higher discharge current rate the battery capacity will become smaller as shown in Figure 2.11 [4].

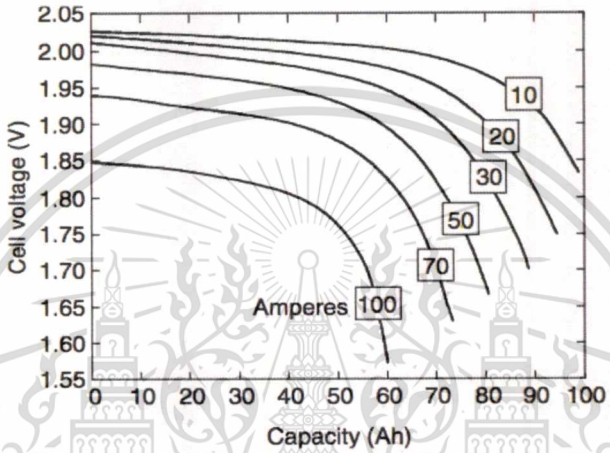

Figure 2.11 Discharge characteristics of a lead-acid battery.

2.2.3 State of charge

Another important parameter of a battery is the state-of-charge (SoC). The state-of-charge (SoC) of a battery is the percentage of available capacity relative to the capacity of battery when it is fully charged. At fully charged, battery has a 100% of SoC and a fully discharged battery has a 0% of SoC. Technically, there has been no general definition of SoC. This was mainly because SoC cannot be measured directly from battery. Accordingly, The SoC is defined as the percentage of the maximum possible charge that is present inside a rechargeable battery as expressed in equation (2.3) [1]. Furthermore, the method for determining state of charge varies depending on the battery type and on the application in which the battery is used.

$$\text{SoC} = \frac{\text{Actual amount of charge (Ah)}}{\text{Amount of total charge } (\text{Ah}_{\text{total}})} \times 100 \qquad (2.3)$$

However, 0% of SoC or fully discharged is sometimes causes confusion because of the discharge rate may effects to available capacity of battery and cut-off voltage. Manufacturers specified a reserve capacity of battery for automotive, in units of minutes during which a fully

This material is reserved for educational use only, not allowed for commercial use.
Forbidden to modify the content and cite the document when use.
077279

charged battery can be discharged at 25A without the terminal voltage dropping below 10.5 V [16]. At this voltage, the battery is treated as completely discharged.

2.2.4 Discharge current effects

Normally, battery discharge characteristics are presented by plotting battery voltage or power versus discharge time. The curve starting from a fully charged to fully discharged. The discharge performance data of batteries are shown in Figures 2.12. The graph shown that, the discharge current increases, the less total capacity of battery (Ampere-hours) could be withdrawn from the battery.

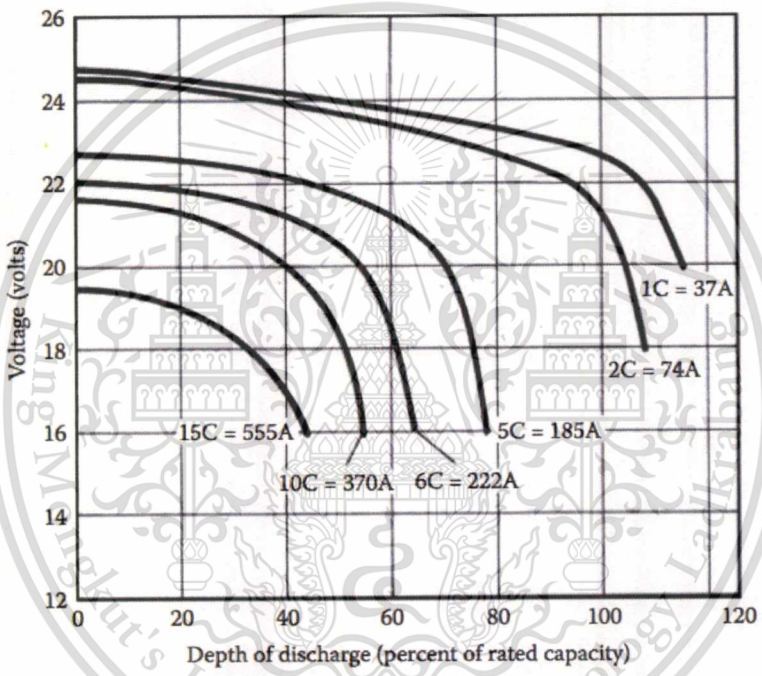

Figure 2.12 Discharge curves at 25°C for a 24V/37Ah SLA aircraft battery.

In 1987, German scientist W. Peukert present the Peukert's Law, expresses the capacity of a battery in terms of the rate at which it is discharged. This law explains why a battery discharged at 20A does not remove twice as much power as discharged at 10A. The equation showed the battery consumption at various discharge rates. When compare total battery discharge capacity at different rates, we can compute the efficiency as a percentage. Peukert's law is as follows:

$$C_p = I^k t \tag{2.4}$$

where C_p = The capacity according to Peukert, at a one-ampere discharge rate, expressed in Ampere-hour,

This material is reserved for educational use only, not allowed for commercial use.
Forbidden to modify the content, and cite the document when use.

I = The discharge current, expressed in Ampere,

k = The Peukert constant,

t = the time of discharge, expressed in hours.

The Peukert constant increases with age for any of the battery types, but generally ranges from 1.2-1.6 for Flooded Lead-Acid Batteries, 1.05 - 1.15 for VRLA batteries.

2.2.5 Efficiency

The factors that influence the battery efficiency of a traction battery (battery efficiency is defined as the ratio of the energy output of a battery to the input energy) are shown in Figure 2.13 [10]. Frequencies of charge/ discharge of batteries, discharge rate, temperature of charging and discharging, etc., are some of the factors that affect the battery efficiency. However, the key determinant of the EV battery system efficiency is the cycle life.

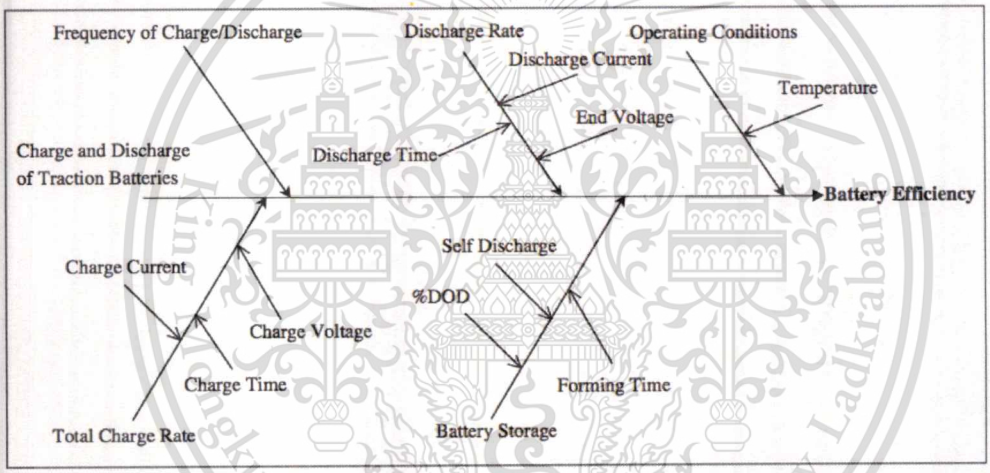

Figure 2.13 Factors affecting the battery efficiency η.

2.2.6 Temperature effects

Temperature has a direct effect on the performance of a lead-acid battery. The chemical reactions that occur in a battery are temperature dependent. The specific gravity of sulfuric acid in battery cell increases and decreases with temperature. Table 2.3 and Figure 2.14 presents the effects of temperature on a lead acid battery cell at a C_5 discharge rate. The most efficient temperature that battery manufacturers recommend is 77°F. This factor will limit the driving range of the electric vehicle significantly. The available capacity of battery at different temperature and may be represented by the following equation

$$C_t = C_{77} * (1-0.065(77-t)) \quad (2.5)$$

This material is reserved for educational use only, not allowed for commercial use.
Forbidden to modify the content, and cite the document when use.

Where C_t = the battery capacity,

t = the temperature in °F at t °F,

C_{77} = the capacity of the battery at 77°F (room temperature).

For example, C3 capacity at 32°F, for a 80Ahr VRLA battery is expressed as C_3 (32°F).

$C_3(32°F) = 80 * (1 - 0.0065(77 - 32)) = 56.6Ah$

Table 2.3 Effect of temperature on VRLA cell capacity

(assuming electrolyte density = 1.340kg/ltr).

Temperature (°F)	*Capacity (%)*
−10.4 (frozen)	9
23	57
33.8	68
50	82
59	87
68	94
77	100

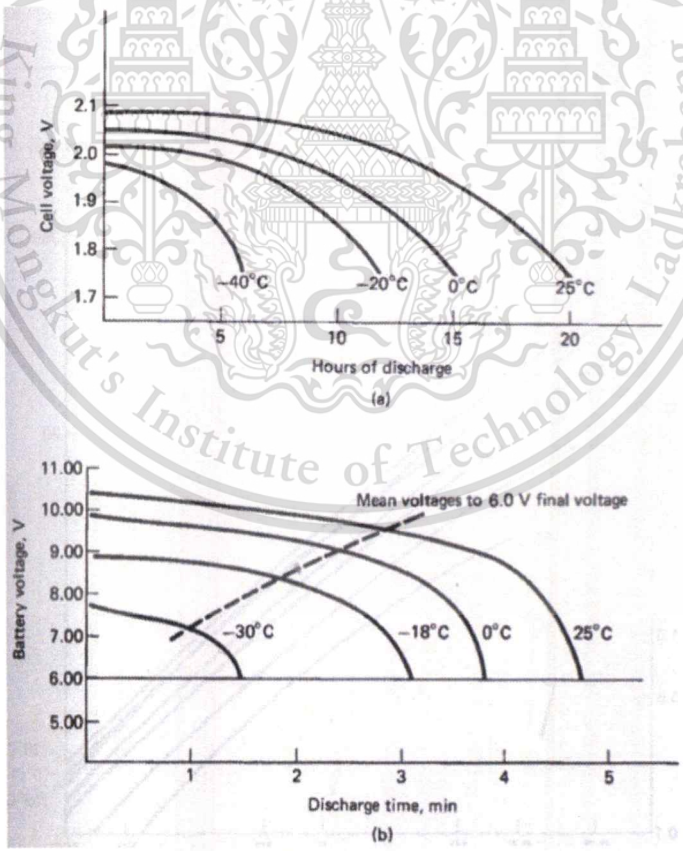

Figure 2.14 Effects of temperature on lead-acid batteries' discharge profile, (a) at C/20 rate, (b) at 340A. 12V 60A-h SLI battery.

This material is reserved for educational use only, not allowed for commercial use.
Forbidden to modify the content, and cite the document when use.

As the temperature varies, the SoC of a battery also varies. The operating temperature of a battery is a one factor that affects to SoC estimation. So, in order to determine the SoC of a battery accurately, the temperature effect should by considered.

2.2.7 Aging effects

When the rechargeable battery is being used repeatedly, the performance of the battery deteriorates. Most rechargeable batteries will only undergo a few hundred deep cycles to 20% of the battery charge [5]. The nominal capacity of the battery decreases and the impedance of the battery increases [2]. However, the exact number of cycles depends on the battery type, and also on the details of the battery design, and on how the battery is used. This is a very important figure in a battery specification, as it reflects in the lifetime of the battery. The State of Health (SoH) of the battery is known as parameter to monitor the effects of battery aging. This is because of the sulfate formation on the plates of the electrodes in the battery, which decreases the net concentration of the electrolyte concentration in the battery. This reduces the full-charge capacity of the battery, which in turn affects the SoC calculations. Since the nominal capacity of a battery has a direct relation with the SoC, it affects SoC estimation of battery.

2.2.8 Self-discharge Effect on SoC

In general, the battery slowly self-discharges even without any connection between the electrodes or open-circuit. This self-discharge is a function of the cell chemistry reactions and the temperature environment experienced by the cell, the self-discharge of Ni-H_2 shows a proportionate loss as seen in Figure 2.15 [17]. This rate is usually less than 1% per day for most electrochemistry in normal working conditions. This becomes more significant the longer the periods between charging. Self-discharge decreases the useful capacity of batteries and causes them to have less capacity than expected when actually put to use. The temperature is sensitivity of the self-discharge reactions, relatively small differences in storage temperature result in large differences in self- discharge rate. Since the self-discharge of a battery is abnormal behavior, it also affects the SoC estimation.

This material is reserved for educational use only, not allowed for commercial use.
Forbidden to modify the content, and cite the document when use.

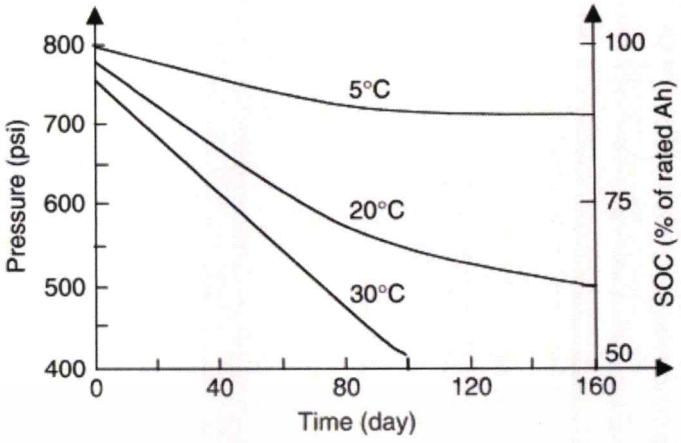

Figure 2.15 Self-discharge rates versus time in NiH2 cell under open circuit.

2.2.9 Some Technical Terms Related to Batteries

Some technical terms are used while discussing the characteristics of batteries. These are important in determining or verify which battery should be used for a particular application. A short description of these battery characteristics is presents in following section.

Specific Energy

Specific energy is an important factor in determining range. Specific energy, defined as the gravimetric energy density, which is the energy stored per unit mass (Wh/kg).

Energy Density

Energy density refers to the amount of energy a battery has in relation to its size, defined as the volumetric energy density, which is the energy stored per unit volume (Wh/l). Batteries that have high energy density are smaller in size.

Specific Power or Power Density

Specific power and power density, defined as the power the battery can practically deliver per kilogram of mass and liter of volume, respectively. Specific power is highest when the battery is fully charged. As the battery is discharged, the specific power decreases and acceleration also decreases. Specific power is usually measured at 80% depth of discharge.

Cycle Life

Cycle life, defined as the number of charge and discharge cycles the battery can deliver while maintaining the cut-off voltage. When the battery can no longer hold a charge over 80%, its cycle life is considered to be finished.

2.3 Previous study on State of Charge estimation techniques

The most common SoC estimation technique is Ampere-hour counting, which is the remaining charge calculated by integrating the current entering or leaving the battery over time.

This material is reserved for educational use only, not allowed for commercial use.
Forbidden to modify the content, and cite the document when use.

However, it requires initial SOC [18]. Another popular method for SoC estimation technique is an Open-circuit voltage (OCV). However, the measurement of OCV requires a several time of rest before the terminal voltage converges to the actual OCV. A decent overview of SoC estimation methods was presented in [19]. Some methods are appropriated with electric vehicles while some techniques are not. This is because they cannot estimate the value in real time and require disconnection of the battery. In this work, SoC estimation method for lead-acid batteries was a purpose of study and would be described below.

In Table 2.4, a review of literature [19, 20] methods is presented. Some techniques are appropriated with electric vehicles while some techniques are not. This is because they cannot estimate the value in real time and require disconnection of the battery.

Table 2.4 Summary of the different techniques for State of Charge estimation.

Technique	**Field of Application**	**Advantages**	**Drawbacks**
Discharge test	All battery systems. Used for capacity determination in the beginning of life	Easy and accurate; independent of SOH	Offline, time intensive, modifies the battery state, loss of energy
Ampere-hour Counting (Coulomb Counting)	All battery systems, most applications	Online, easy, accurate if enough recalibration points are available and with flawless current measurement	Sensitive to parasite reactions; needs regular recalibration points
Physical properties of electrolyte (density, concentration, color)	Lead, possibly Zn/Br and Va	Online, Give information about SOH	Error if acid stratification, low dynamic. Problem of stability of sensors in electrolyte. Sensitive to temperature and impurities.
Open circuit voltage (OCV)	Lead, lithium, Zn/Br and Va	Online, cheap, OCV prediction	Low dynamic, Needs long rest time (Current= 0A) for lead system.
Linear Model	Lead PV	Online, easy	Needs reference data for fitting parameter.

This material is reserved for educational use only, not allowed for commercial use.
Forbidden to modify the content, and cite the document when use.

Impedance spectroscopy	All systems	Gives information about SOH	Temperature sensitive, cost intensive
DC internal resistance	Lead, Ni/Cd	Gives information about SOH	Accuracy only for a short time interval.
Artificial Neural Networks	All battery systems	Online	Needs training data of a similar battery, expensive to implement.
Fuzzy logic	All battery systems	Online Robust	Large amount of memory in real world applications
Kalman Filters	All battery systems, even strongly dynamic applications (such HEV)	Accurate Flexible Online	Needs strong hypothesis on battery model. Difficult to implement the filtering algorithm that considers all features as,e.g. nonlinearities

2.3.1 Discharge test

Discharge test under controlled conditions is one of the most reliable tests for determining the SoC. A test usually includes a sequence recharge, is too time consuming to be considered for most applications. So, in this discharge test the battery should be continuous discharge until fully discharge, cannot be interrupted. The battery is usually discharged at 10% of its rated capacity (C_{10}, e.g., 10 A for a 100 A-h battery).

2.3.2 Measurement of battery electrolyte

When considering flooded lead-acid cells, the specific gravity (S.G.) of the electrolyte is known to be a good measure of SoC [21]. During the discharge of a lead-acid battery, the discharge consumes sulfuric acid (H_2SO_4) and converts it to water (H_20). In charge process, the

This material is reserved for educational use only, not allowed for commercial use.
Forbidden to modify the content, and cite the document when use.

sulfuric acid reverts back into the solution state again [3, 19]. Overall reaction of lead-acid battery can be generally expressed by

$$PbO_2 + Pb + 2H_2SO_4 \rightleftharpoons 2PbSO_4 + H_2O \quad (2.6)$$

The S.G. measurement with the use of a hydrometer is a simple and easy way, with a high accuracy, to indicate SoC of battery. The relationship between sulfuric acid's specific gravity and SoC is almost linear. The general S.G of H_2O and H_2SO_4 is 1 and 1.28 respectively [8]. However, it is impossible to measure the specific gravity of each battery cells during a driving period wild the method can also be used only in a flooded-type lead-acid.

2.3.3 Open-circuit voltage

The open circuit voltage (OCV) of battery varies almost linearly to the battery SoC. The specific relationship of OCV and SoC of each battery is usually identified by manufacturer in data sheet. However, a direct measurement of OCV cannot be operated under loading condition. Because of surface charge, the voltage measured just after discharge would drop lower than an actual voltage of a battery. If the surface layers of the plates have a much lower concentration of charged chemical species than deeper in the plate, it may take several hours before a charge is evenly distributed through the electrode [22]. Especially in valve-regulated lead-acid (VRLA) batteries, considerable amount of times, such as several hours, are needed to reach a steady state after loading [23]. In [24], the individual cell open circuit voltage (OCV) was measured and the S.G. was calculated using the following equation:

$$OCV = S.G. + 0.845 \quad (2.7)$$

2.3.4 Ampere – hour Counting

Ampere-hour counting or Coulomb counting is a method to measure and summing the amount of delivered current during charge or discharge. By using Ampere counting, SoC of battery can be expressed as:

$$SoC(t) = SoC(0) - \frac{1}{Ah_{total}} \int_0^t I(t)dt \quad (2.8)$$

Where: SoC(0) is initial SoC value,

$Ah_{(total)}$ is amount of total charge,

I(t) is the measured current.

This material is reserved for educational use only, not allowed for commercial use.
Forbidden to modify the content, and cite the document when use.

A current is measured by current sensor, which is inserted into the loop and integrated over time. The current sensor is generally either a Hall-Effect sensor or a current shunt [25]. However, this technique could present only a change in battery capacity. Lack of knowledge of initial value of SoC and an accumulated error results in a limited accuracy of the estimation.

2.3.5 Kalman filtering

Kalman filter theory was introduced In 1960 [26]. Kalman Filters are an optimal-means for estimating a present value of the time-varying "state" of a dynamic system [22].

2.3.5.1 Battery Model

To use Kalman Filter techniques to estimate battery SOC, a mathematical state-space model of the cell is needed. A dynamic model of lead-acid battery that was necessary for Kalman Filter technique to predict the SoC is shown in "Fig.2.16" [23]. The battery model is consisted of two capacitors and three resistors; C_{bulk}(bulk capacitor), $C_{surface}$(surface capacitor),R_t(terminal resistance), R_s(surface resistance), and R_e(end resistance). The V_{Cb} and V_{Cs}, are voltage across the bulk capacity and surface capacitors respectively. The SoC can then be determined from the voltage present across the bulk capacitor (V_{Cb}).

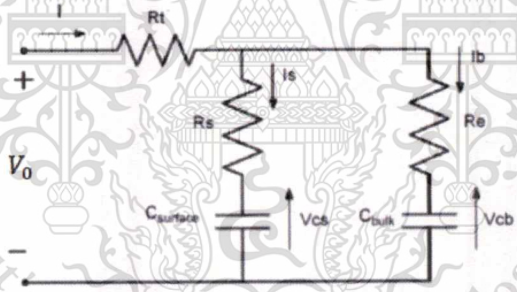

Figure 2.16 RC Battery Model schematic [23].

From RC battery model schematic "Figure 2.16", the characteristics equation of voltages and currents can be express as:

$$V_0=IR_t+I_bR_e+V_{Cb} \quad (2.9)$$

$$V_0=IR_t+I_sR_s+V_{Cs} \quad (2.10)$$

After some algebraic manipulation and Kirchoff's laws application, the complete state variables of the model were presented in [23].

This material is reserved for educational use only, not allowed for commercial use.
Forbidden to modify the content, and cite the document when use.

CHAPTER 3
EXPERIMENTAL METHODOLOGY

In this chapter, the details of methods using to evaluate the topic will be explained. The setup processes and both testing types that were used in the research processes will be clarified. The research processes was divided into a laboratory scale and real driving scale tests, with two types of batteries used in each test. The laboratory scale test is determined and performed as preliminary experiment; thus, the results of the test would be used as a battery reference data. For the driving scale test, the experiment was held in a fixed distance on real traffic conditions, in order to monitor behavior of the batteries.

3.1 Experimental setup

The first part of the test was performed in a laboratory. The two types of batteries chosen to use in the test were flooded lead-acid battery GS BV-130, and VRLA battery Panasonic EC-FV1260. These two batteries were selected because they are wildly used and also have been using on the MTEC electric bus prototype. The laboratory-scaled experiment was set up as shown in Figure 3.1.

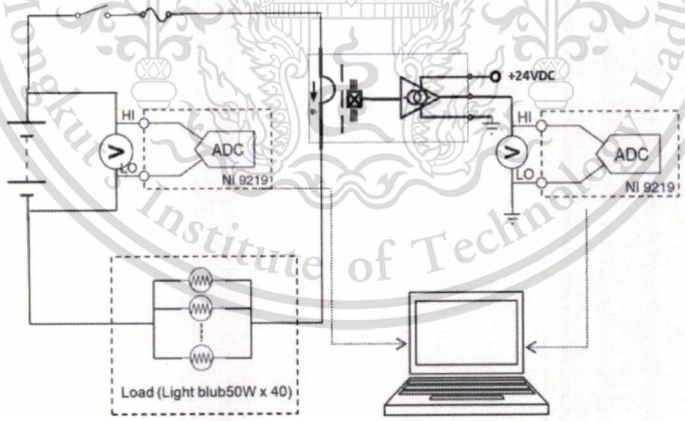

Figure 3.1 Schematic diagram of laboratory-scaled experiment.

The constant current discharge was used as loads of battery; 40 units of Halogen Light Bulb rated 12V, 50W were connected in parallel to achieve a maximum discharge current of 132A. A hydrometer (Figure 3.2) was used to measure the concentration of electrolyte in battery after battery being charged and during discharge process. However, a direct measurement of battery specific gravity could not be done in a high current discharge rate test and VRLA Battery. Therefore, the LEM DHR100-C10 current transformer was equipped to measure the current flow

This material is reserved for educational use only, not allowed for commercial use.
Forbidden to modify the content, and cite the document when use.

(Figure 3.3). The K-type thermocouple was installed to measure battery temperature. Two units of digital meter were set for displaying battery voltage and current flow (Figure 3.4). The data acquisition hardware by National Instrument (NI 9219) was used to measure battery data. Signal Express by National Instruments was used as software for monitoring and collection of the battery data (Figure 3.5). The overall setup of preliminary experiment is shown in Figure 3.6.

Figure 3.2 EZ RED Hydrometer.

Figure 3.3 LEM DHR100-C10 current transformer.

Figure 3.4 Digital meter.

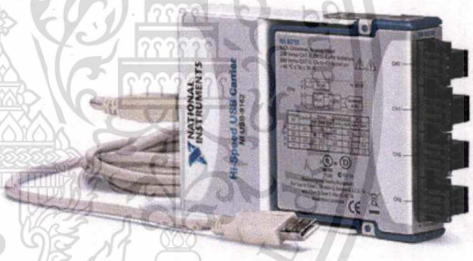

Figure 3.5 National Instrument (NI 9219).

Figure 3.6 The overall setup of preliminary experiment.

This material is reserved for educational use only, not allowed for commercial use.
Forbidden to modify the content, and cite the document when use.

In the second part, a test drive of MTEC electric bus prototype (Figure 3.7) was carried out in controlled driving conditions. Due to the high voltage consumption of the drive motor invertor, the flooded lead-acid batteries were connected in series to achieve nominal 288V DC source and 130Ah. In this bus, 24 units of 12V, 130Ah lead acid batteries were installed as main power source for AC drive motor (maximum rated power 78kW) and the other 24 units of batteries were used for other electrical devices in the bus (Figure 3.8). In another part, 26 units of VRLA battery (312V DC, 60Ah) were also used as a power source. The data acquisition tools from Azure dynamic were used to collect battery discharging data such as battery voltage, battery current, battery temperature, motor revolution, and torque as shown in Figure 3.9.

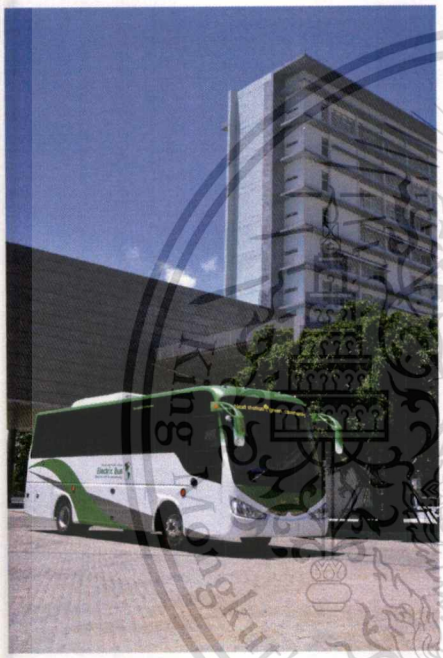

Figure 3.7 MTEC Electric bus prototype.

Figure 3.8 Replaceable Battery packs.

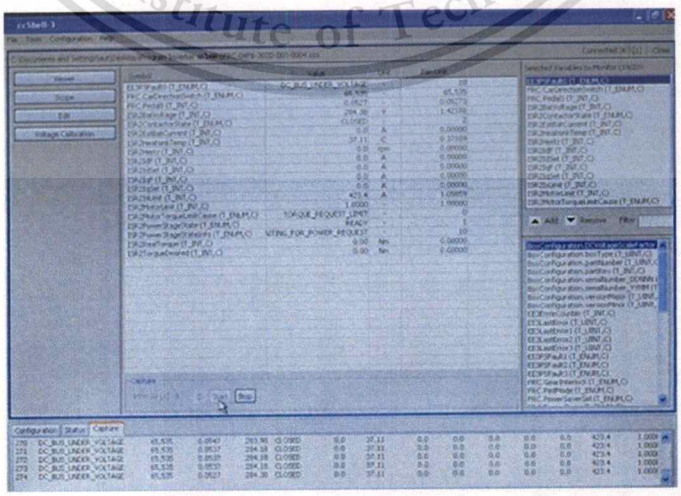

Figure.3.9 The battery data of electric bus by data acquisition tools.

This material is reserved for educational use only, not allowed for commercial use.
Forbidden to modify the content, and cite the document when use.

3.1.1 Battery

As stated above, there were 2 types of battery employed in this study i.e. flooded lead-acid battery and valve regulated lead-acid (VRLA) battery. These two types of battery offer different profits and consequences that would affect to the experiment in the different ways, therefore the testing results from both types of batteries will be explored and to compared in our study.

3.1.1.1 Flooded Lead-Acid battery

The most obvious advantage of flooded lead-acid battery is high nominal capacity (Ampere-hour). In this test, lead-acid battery from GS (GS-BV130Z) was used (Figure 3.10). The specifications of battery are shown in Table 3.1. For this battery, it requires refilling with distilled water (Figure 3.11) at least once to twice a month.

Figure 3.10 GS Deep cycle lead-acid battery.

Figure 3.11 Distilled water.

Table 3.1 Battery specifications.

Type of Battery	Nominal Voltage	Nominal Capacity	Capacity (25°C)		Size (mm)			Mass (kg)
					Width	Length	Height	
BV130Z	12V	130Ah	105Ah @ C_5	NA	173	407	209	34
EC-FV1260	12V	60Ah	53Ah @ C_3	43Ah @ 1C	116	388	175	21

3.1.1.2 Valve regulated Lead-Acid (VRLA) battery

Because of high discharge rate and stable discharge current, Panasonic 12V, 60Ah VRLA battery was selected as test samples (Figure 3.12). This VRLA battery type is the absorbed glass mat (AGM) based battery. The overall structure of battery is shown in Figure 3.13. The specifications of EC-FV1260 are also presented in Table3.1. The main advantage of VRLA

This material is reserved for educational use only, not allowed for commercial use.
Forbidden to modify the content, and cite the document when use.

battery is higher discharge rate comparing to flooded lead-acid battery. About 3C discharge rate is available for VRLA with only 1C for another type of battery. However, only half of battery nominal capacity might have a significant effect on the total operating range of an electric vehicle. Because of structural design and the lack of additional water content, the total weight of VRLA could be reduce by 40% and with maintenance-free feature.

Figure 3.12 Panasonic VRLA Battery.

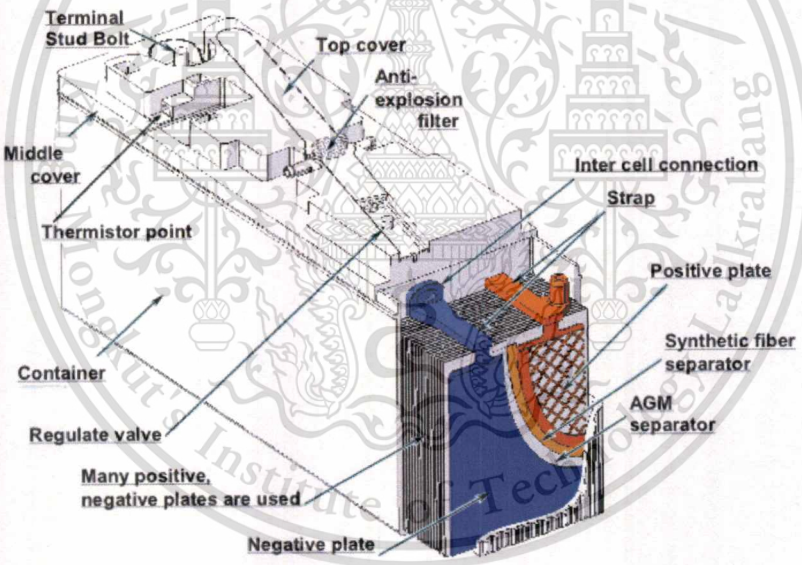

Figure 3.13 The internal structure of Panasonic EC-FV1260.

3.1.2 Experimental Tests

Charging

For flooded lead-acid battery, constant current AC/DC charger was used to charge the test samples. Normally, it would take 6-8 hours for a fully-charged state. When fully charged (100% SoC), the presented battery voltage was 12.3V while corresponding specific gravity (SG) was measured to be 1.26. Moreover, from the recommendation of VRLA manufacturer, the 5-steps charger was used for charging the VRLA battery (Figure 3.14) and a charging profile is shown in

This material is reserved for educational use only, not allowed for commercial use.
Forbidden to modify the content, and cite the document when use.

Figure 3.15. By using 5 steps charger, it has been claimed to get more charging efficiency and extended battery life.

Technically, battery characteristics change due to aging and directly affect the maximum capacity of battery. However, the discharge test was started at a fully charged condition where the SoC was considered to be 100%.

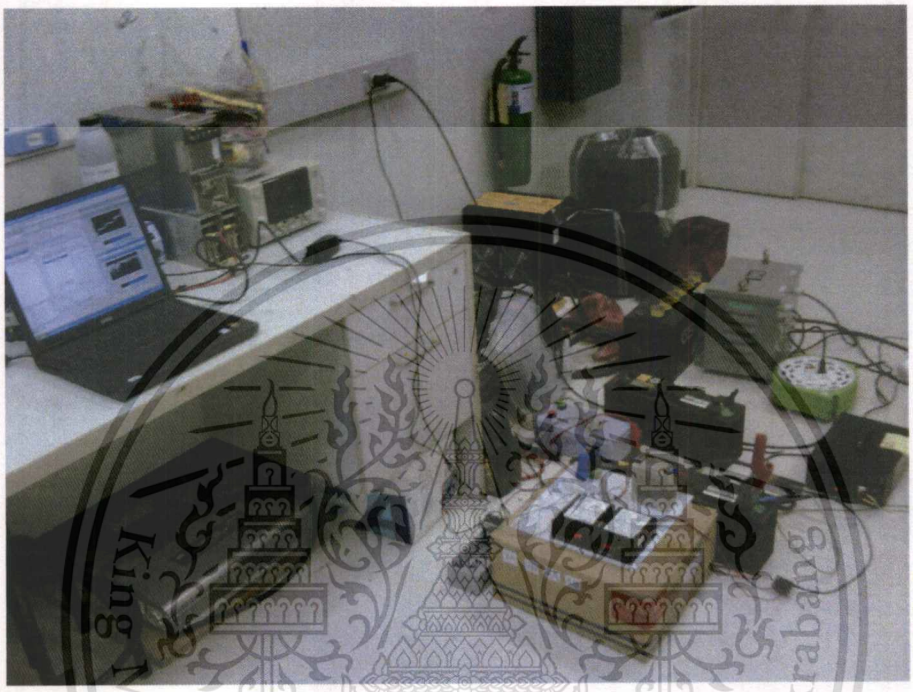

Figure 3.14 Setup of battery 5-steps charging system for VRLA battery.

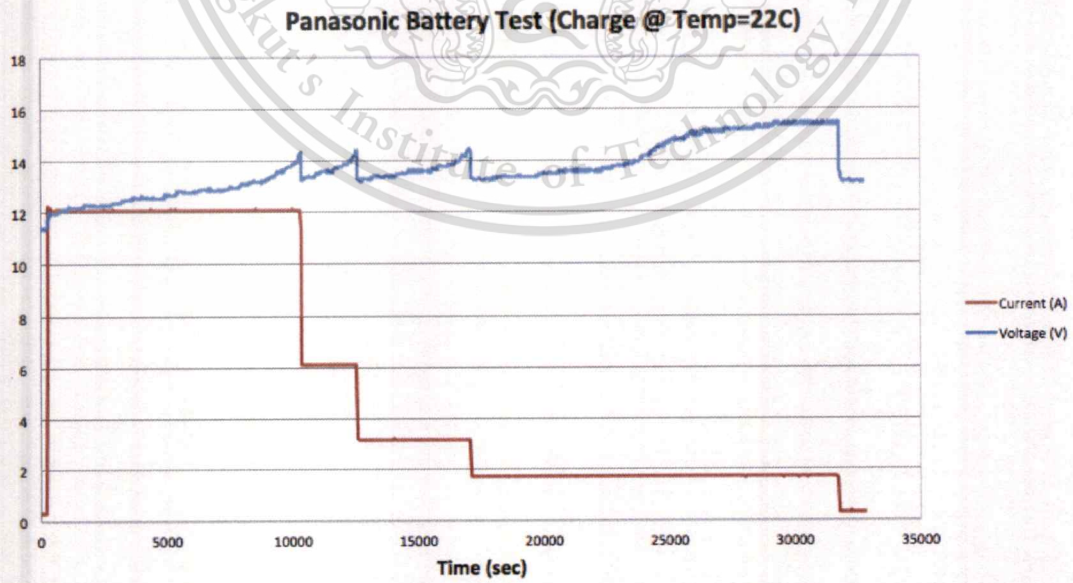

Figure 3.15 Battery 5 steps charging characteristic.

This material is reserved for educational use only, not allowed for commercial use.
Forbidden to modify the content, and cite the document when use.

Discharging

In order to conveniently calculate the percentage of the maximum possible charge that was presented inside a rechargeable battery, a constant current discharge was used as battery loads. The different rates of discharge were employed i.e. C_{10}, C_5, C_3, and1C among which the C_5 rate was a common discharge rate for electric vehicles. The battery was discharged until the cut off voltage was reached, as presented in the battery datasheet (GS battery data sheet). Normally, the battery was considered to be completely discharged when the voltage reached 10.2V.

3.2 Laboratory Scale Experiment

This methodology can be further specified into the following aspects:

1. Validated battery consumption behavior using discharge test.
2. Used Hydrometer for measuring specific gravity of battery (Flooded lead-acid battery).
3. Used data acquisition hardware to collect battery referenced data.
4. Varied the discharge current by adjusting the illumination load.

3.2.1 Specific gravity Measurement

The measurement of electrolyte specific gravity could be done on only flooded type. In Figure 3.16, the measurement of battery specific gravity by hydrometer is shown. In preliminary tests, the measurement of specific gravity was carried out every 30 min during discharge tests and was recorded as reference data.

Figure 3.16 The measurement of battery specific gravity by hydrometer.

This material is reserved for educational use only, not allowed for commercial use.
Forbidden to modify the content, and cite the document when use.

3.2.2 Ampere – hour Counting

Furthermore, by using Ampere-hour counting method, a flow of current could be directly obtained. The discharge test was started at fully charged condition where the SoC was considered to be 100%. The battery was discharged until the cut off voltage as presented in the battery datasheet was reached. Therefore, the LEM DHR100-C10 current transformer and the data acquisition hardware NI 9219 were used to measure the current flow, battery voltage and temperature at every second during the test. Signal Express was used as software for monitoring and collect the battery data (Fig.3.4). The constant current discharge tests were done at 4 different discharge rates C_{10}, C_5, C_3 and C_1 for Flooded Lead-Acid battery and 5 different discharge rates C_{10}, C_5, C_2, 1C and 2C for VRLA battery by means of adjusting the halogen light bulbs (Figure 3.17). The halogen light bulb consumes 50W -12V or about 4 Ampere-hour/bulb.

Figure 3.17 Constant current discharge test by adjusting the halogen light bulbs.

By using Ampere counting, SoC of battery can be expressed as:

$$SoC(t) = SoC(0) - \frac{1}{Ah_{total}} \int_0^t I(t)dt \qquad (3.1)$$

3.2.3 Mixed estimations: Specific gravity Measurement and Ampere-hour Counting

By using specific gravity and open circuit voltage data, the initial SoC of battery could be estimated. Then, the ampere-hour counting discharge rate was used. The flowchart of the explained method is shown in Figure 3.18

This material is reserved for educational use only, not allowed for commercial use.
Forbidden to modify the content, and cite the document when use.

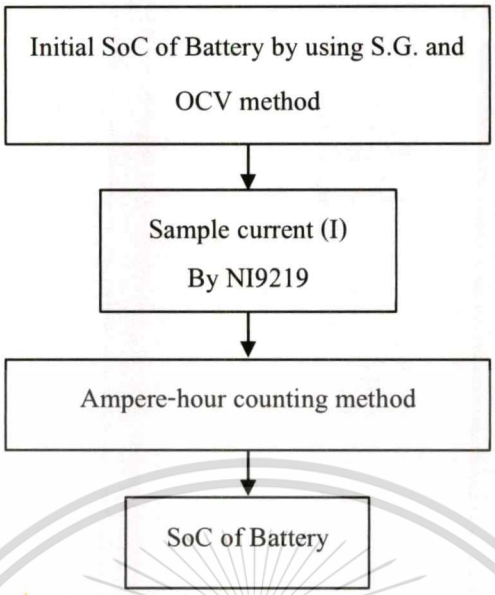

Figure 3.18 Flowchart to determine SoC of lead acid battery.

3.2.4 Mixed estimations: Specific gravity Measurement and Ampere-hour Counting with correcting factor

As presented in section 2.2.4, the discharge rate directly affects the actual available capacity of battery. As the discharge current increases, the less total capacity of battery (Ampere-hours) could be withdrawn from the battery. A factor α was introduced to improve the accuracy of Ampere-hour counting method, as present in equation 3.1.

$$SoC(t) = SoC(0) - \frac{1}{Ah_{total}} \int_0^t \alpha \, I(t)dt \tag{3.2}$$

Where,

$$\alpha = \frac{\text{Nominal capacity}}{\text{Available capacity}} \tag{3.3}$$

The available capacity is the capacity that could be withdrawn from the battery at each discharge rate. Then, the ampere-hour counting method with the value of α corresponding to discharge rate was used. The flowchart of the explained method is shown in Figure 3.19

This material is reserved for educational use only, not allowed for commercial use.
Forbidden to modify the content, and cite the document when use.

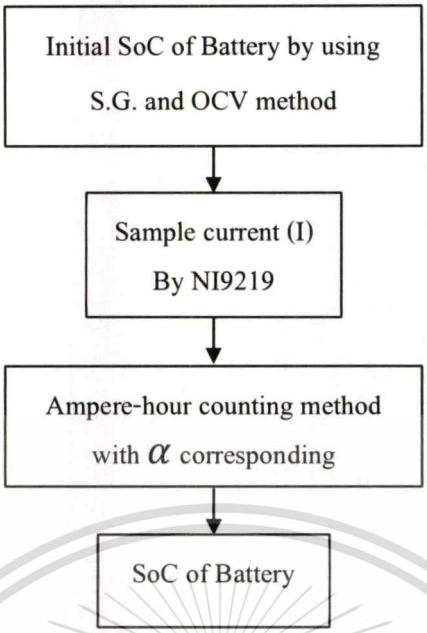

Figure 3.19 Flowchart to determine SoC of lead acid battery with correcting factor.

3.3 Main Experiments in real driving conditions

In driving tests, there were 4 driving configurations for studying both electrical behaviors and an estimating battery SoC of flooded lead-acid and VRLA type battery in dynamic conditions i.e. acceleration test, load test, fix driving range test (vary driving mode and drivers), and regenerative breaking test.

3.3.1 Acceleration Test & Load test

In order to study about battery behavior, acceleration test is the most important case. During acceleration test, a high current was flowing out from battery. The test started from a stand still, then pedal was fully pushed as maximum accelerate to reach 50km/hr.

During driving condition, the electric bus may carry passengers and some loads. An additional load about 800kg was added to the test. Load test is input for study battery behavior comparing to no-load condition.

This material is reserved for educational use only, not allowed for commercial use.
Forbidden to modify the content, and cite the document when use.

Figure 3.20 Additional load of 800kg during driving tests.

3.3.2 Fixed driving range test

In the fixed range test, the tests were done in NSTDA campus. The total run range is about 1.4 km/lap, including straight road and corner sections under real traffic conditions. The driving modes used in this study were maximum range, normal, and maximum power. Because driving style may also highly affect the available capacity, 4 drivers were also considered in these tests.

3.3.3 Regenerative breaking test

In general, electric vehicles could convert vehicle motions back into energy during braking by using regenerative breaking system. Due to energy conversion, kinetic energy could be recovered to energy storage. In this test, 2 modes of electric vehicles (slippery mode and regenerative mode) were studied.

3.4 Mixed estimation in real driving conditions

In electric vehicle, the batteries do not normally start from 100%SoC. By using mixed estimation, the initial SoC (SoC(0)) was estimated by OCV method or the lasted SoC (SoC(t)). During the driving test, the current flow was measured at in every second, then the corresponding α was used to collect the rate of capacity flow. The algorithm to determine SoC of Lead-acid battery in real driving conditions is shown in figure 3.21. The initial state of charge came from the manner of the last estimation, for example if the latest SoC measurement was grater or equal to

This material is reserved for educational use only, not allowed for commercial use.
Forbidden to modify the content, and cite the document when use.

30 minutes, SoC from OCV method would be used as an initial SoC data. On the other hand, if it were less than 30 minutes the SoC from the last estimation would be directly used. After the initial SoC has been identified, the current flow from battery would be measured and collected every second in order to get the accurate information. In the next process, the rate of discharge was grouped into range by relating with the raw data and the sensitivities of the α values. In the case of proximity current's values, the α used in calculating is barely effect to the result of the calculation (only two decimal places). Thus, by grouping the rate of discharge, it was reducing the complexities of the next step calculation while also matching the sensitivities of the values. Therefore, the discharge rate of specific battery was set as the references, then, the middle value of the different discharge rate was used as boundary of the range. Hence, the rate of discharge was classified into five ranges by equally range with the same ratio as in Figure 3.22 i.e. 0A-13A (Range of C_{10}), 14A-40A (Range of C_3), 41A-90A (Range of 1C), 91A-150A (Range of 2C), and more than 150A. In addition, for increasing the accuracy, the grouping of discharge rate may finely divided, while the value of α correcting factor increases linearly proportional to the discharge current. Finally, the ampere-hour counting method with the value of α corresponding factor would be applied to estimate the remaining SoC of batteries.

King Mongkut's Institute of Technology Ladkrabang

This material is reserved for educational use only, not allowed for commercial use.
Forbidden to modify the content, and cite the document when use.

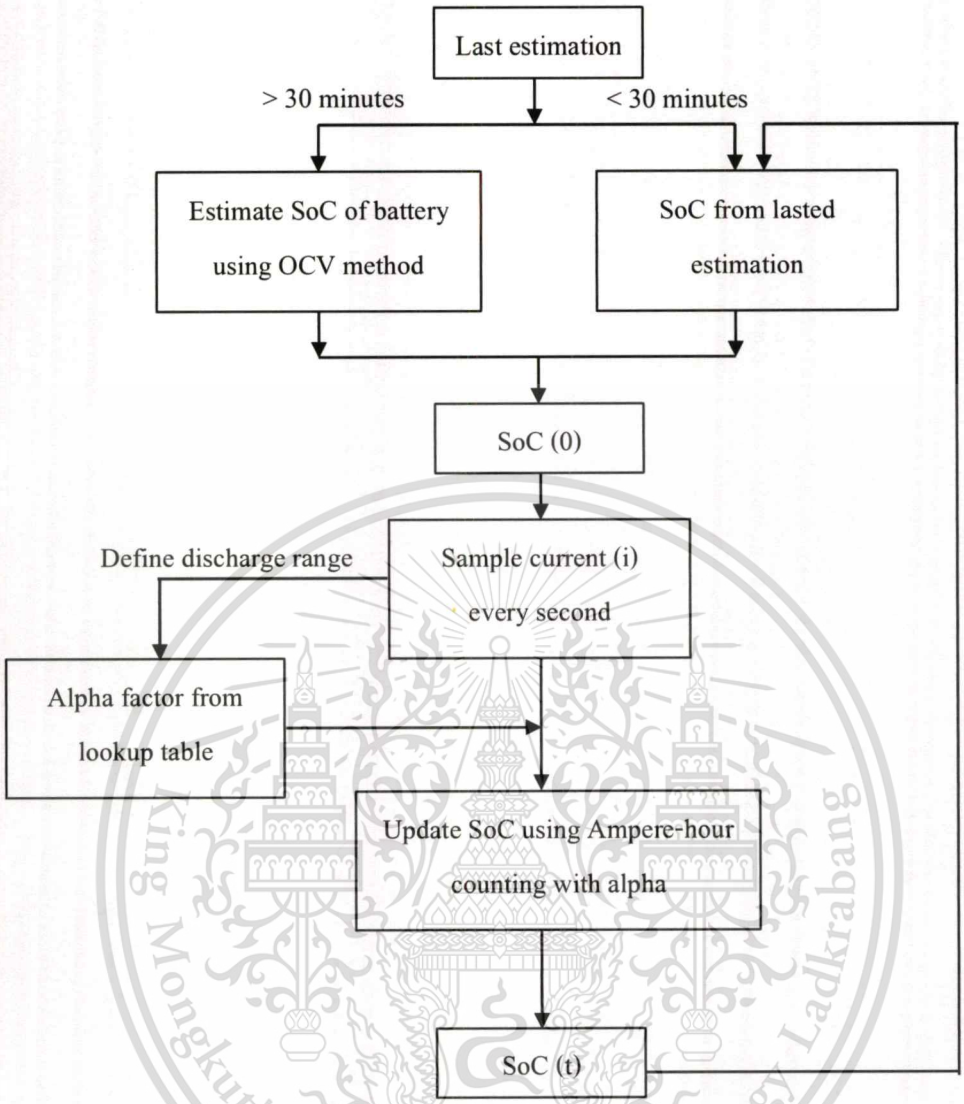

Figure 3.21 Algorithm to determine SoC of Lead-acid battery in real driving condition.

This material is reserved for educational use only, not allowed for commercial use.
Forbidden to modify the content, and cite the document when use.

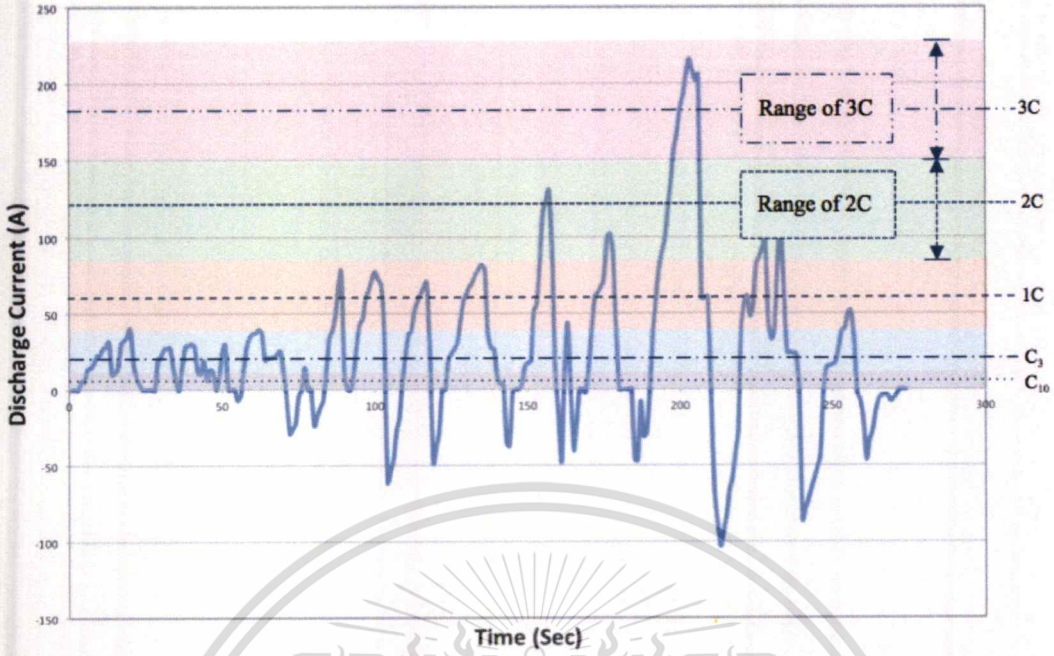

Figure 3.22 Characteristic of discharge current in real driving condition.

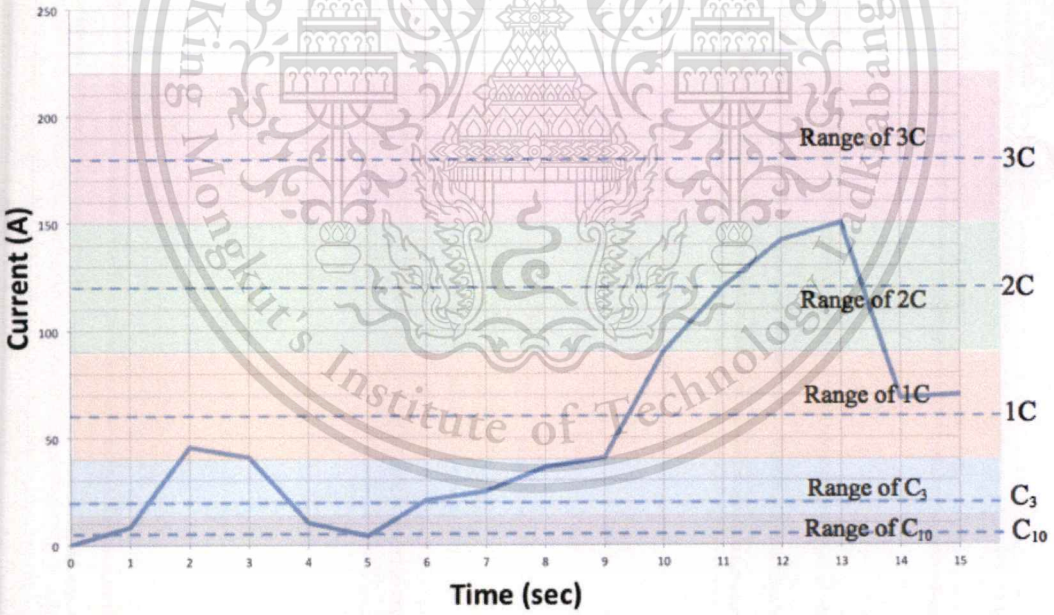

Figure 3.23 Example of the collecting data in real driving condition (VRLA Batteries).

The Figure 3.23 illustrates the example of collected data in real driving condition. The Table 3.2 is shown the example of ampere-hour counting method with the value of α corresponding. Thus, the equation for estimating SoC could be expressed as:

This material is reserved for educational use only, not allowed for commercial use.
Forbidden to modify the content, and cite the document when use.

$$SoC(t) = SoC(0) - \frac{1}{Ah_{total}} \sum_{t=0}^{n} (\propto_x I_t)$$
$$= SoC(0) - \frac{1}{Ah_{total}} ((\propto_x I_1) + (\propto_x I_2) + \ldots + (\propto_x I_n)) \quad (3.4)$$

Where: SoC(0) is initial SoC value,

I_t is the measured current.

$\propto_x$ is the correcting factor at I(t) (Table 4.3, and 4.4)

$Ah_{(total)}$ is amount of total charge

For example, at the 3rd second in figure 3.23, the batteries were spending 41A in the cruising period or part 2 of the grouped current range. Therefore, this sample current was multiplied by the corresponding α factor of 1.37. In addition, during the acceleration part (13rd second), the current flow was 150A, and hence the current was multiplied by the corresponding α factor of 1.56.

Table 3.2. Example of the collecting data by Ah-counting and α corresponding factor.

Time (sec)	Current (A)	Total current drawn	α Corresponding factor	Total current drawn with α Corresponding factor	SoC(t) (%) - with α Corresponding factor
0	0	0	0	0	100
1	8.2	8.2	1	8.2	99.996
2	45.7	53.9	1.37	70.80	99.967
3	41	94.9	1.37	126.97	99.941
4	10.2	105.1	1	137.17	99.936
5	4.3	109.4	1	141.47	99.934
6	20.7	130.1	1.37	169.83	99.921
7	25	155.1	1.37	204.08	99.905
8	36.3	191.4	1.37	253.81	99.882
9	40.6	232	1.37	309.44	99.856
10	90	322	1.41	436.34	99.797
11	120	442	1.41	605.54	99.719
12	142	584	1.41	805.76	99.626
13	150	734	1.56	1039.76	99.518
14	68.4	802.4	1.37	1133.46	99.475
15	69.9	872.3	1.37	1229.23	99.430

This material is reserved for educational use only, not allowed for commercial use.
Forbidden to modify the content, and cite the document when use.

CHAPTER 4
RESULTS

In this chapter, the battery behaviour; ability of discharge rate, available capacity, State of Charge (SoC), and battery behaviour in real driving condition are reported. After study and improvement of estimation technique an appropriated SoC estimation for electric bus was conducted. The results are given in this chapter.

4.1 Preliminary Test

The laboratory scale test is determined and performed as preliminary experiment; thus, the results of the test would be used as a battery reference data.

4.1.1 Discharge test

At constant current discharge, the terminal voltage of battery continuously decreased and sharply dropped when the cut-off is reached. In figure 4.1, the result shows the discharge characteristics of 12V -130Ah flooded lead-acid battery under 4 different constant discharge rates (C_{10}, C_5, C_3, and 1C). At C_{10} or 13A discharge current, the battery terminal voltage slightly decreased form fully-charged (12.6V) to cut-off voltage (10.4V) by 27000 seconds or about 7.5 hour. After the cut-off voltage is reached, the battery terminal voltage is dramatically decreased to risky zone (over-discharge). The total discharge time of C_5, C_3, and 1C is 14000 seconds (3.9 hour), 7500 seconds (2.1 hour) and 2100 seconds (0.6 hour) respectively.

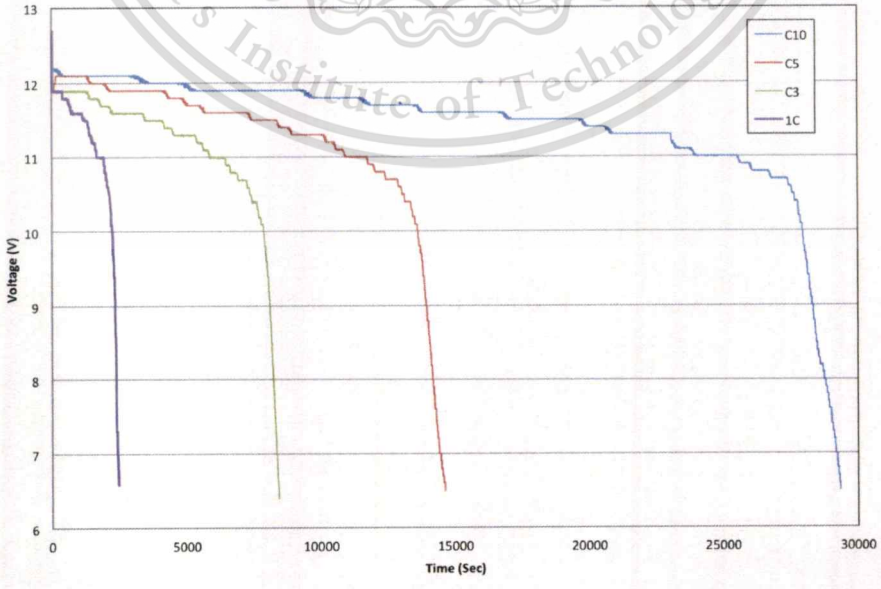

Figure 4.1 Discharge Characteristic of Flooded Lead-acid Battery.

This material is reserved for educational use only, not allowed for commercial use.
Forbidden to modify the content, and cite the document when use.

The discharge characteristic of 12V - 60Ah VRLA battery is shown in figure 4.2. As you can see from the graph, the first sample discharge at C_5 or 12A and reach to cut-off voltage 10.4V. The total discharge time is 15000 seconds or about 4.3 hour. While C_2 or 30Ah discharge test, the total discharge time is about 5500 seconds or about 1.5 hour.

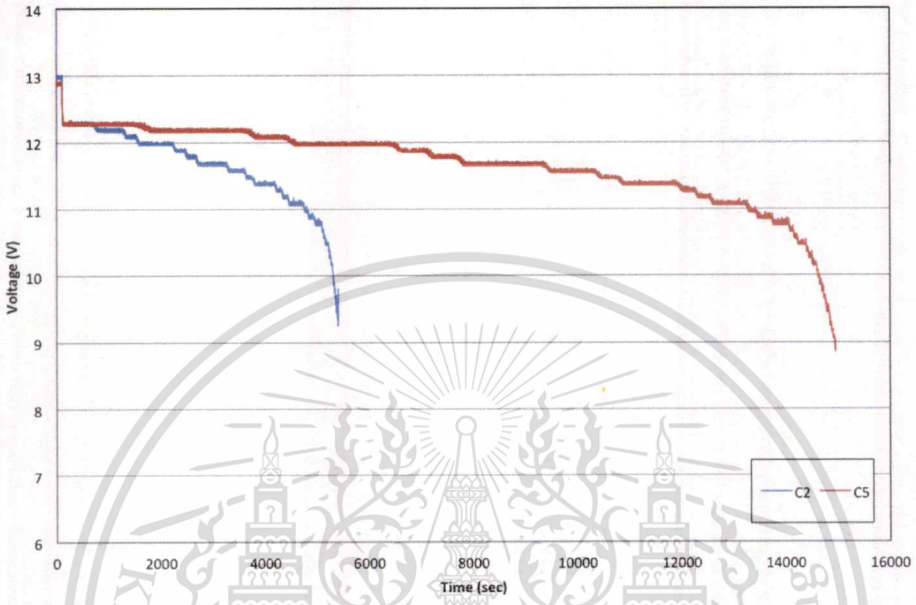

Figure 4.2 Discharge Characteristic of VRLA Battery

4.1.2 Specific gravity test

The specific gravity of flooded lead-acid battery was measured every half an hour and the observed relationship between specific gravity versus time under different discharge rate. The observed relationship between specific gravity, SoC and OCV is shown in figure 4.3. The graph shows the discharge characteristics of battery under 5-hours rate, C_5 constant discharge current. At the maximum capacity, corresponding OCV at measured S.G. of 1.27 was calculated to be 12.69V. After being discharged at C_5, a terminal voltage of 10.4V was reached (i.e. cut-off) the OCV was calculated to 11.07V and S.G. was decreasing to 1.0 by using hydrometer. The battery SoC is decreased from 100% to 0% as shown in the graph.

The measurement of electrolyte S.G. in each cell from new battery and old batteries is shown in figure 4.4. The test sample no.1 - 4 is about 2 years old battery, while sample no.5 is new battery. The specific gravity of new battery in every cell is equal and shown as 1.27. For old battery, the specific gravity of 100% SoC vary around 1.24 – 1.25 that is about 90% of new battery. There are some weaken in sample no.4, the specific gravity of cell no.4 was measured to be 1.225 (80%).

This material is reserved for educational use only, not allowed for commercial use.
Forbidden to modify the content, and cite the document when use.

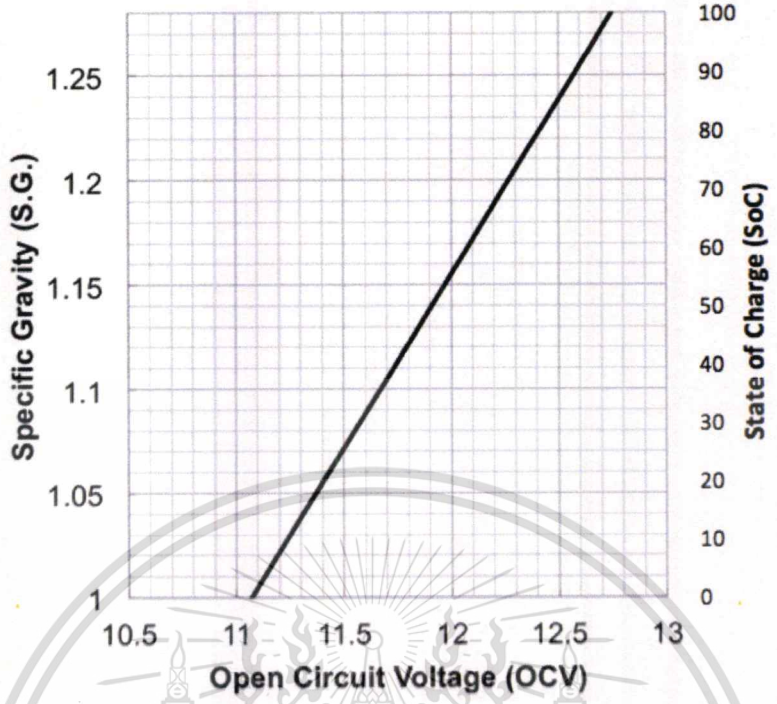

Figure 4.3 Open circuit voltage versus Specific gravity and State of Charge.

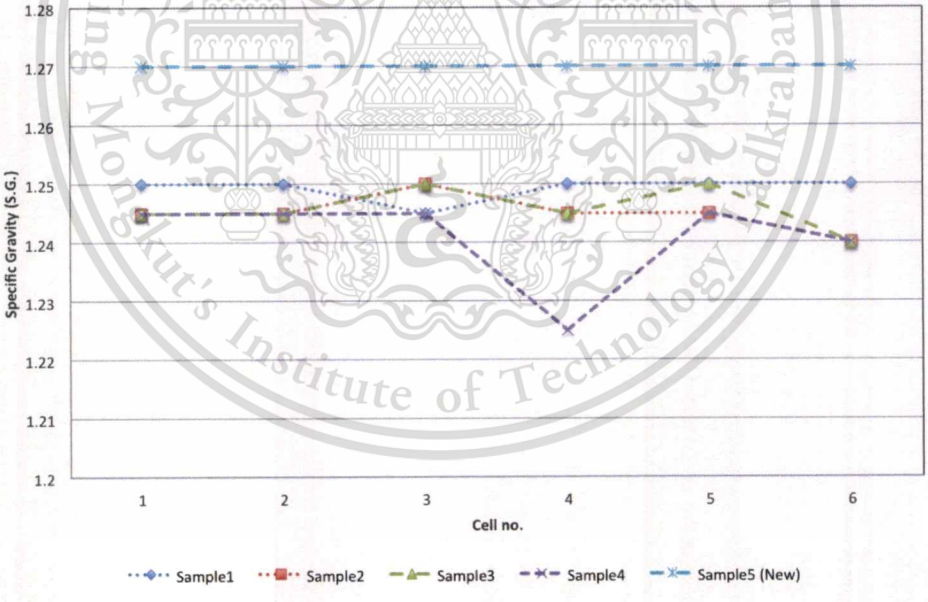

Figure 4.4 Measurement of electrolyte specific gravity between new battery and old battery.

4.1.3 Open Circuit Voltage (OCV)

For VRLA battery, the direct measurement of specific gravity cannot be measured, therefore the SoC estimation technique by using Open Circuit Voltage (OCV) method was used in this study. The voltage characteristic of VRLA battery is shown in figure 4.5. After completely

This material is reserved for educational use only, not allowed for commercial use.
Forbidden to modify the content, and cite the document when use.

discharged, the terminal voltage of battery swing back from cut-off voltage to 11.3V for C_2 and 10.9V for C_5 respectively. The open circuit voltage of battery is closed to stable in 5 minutes. Moreover, more than 30 minutes is required of battery to reach the steady state or OCV measurement. By applying open circuit voltage method, the relationship of OCV (after 30 minutes) and SoC of VRLA battery under C_5 (12V) discharge is presents in figure 4.6. At fully charged, OCV of VRLA battery is 12.9V and SoC is 100% and continuously decreases to 0%SoC (10.9V - OCV).

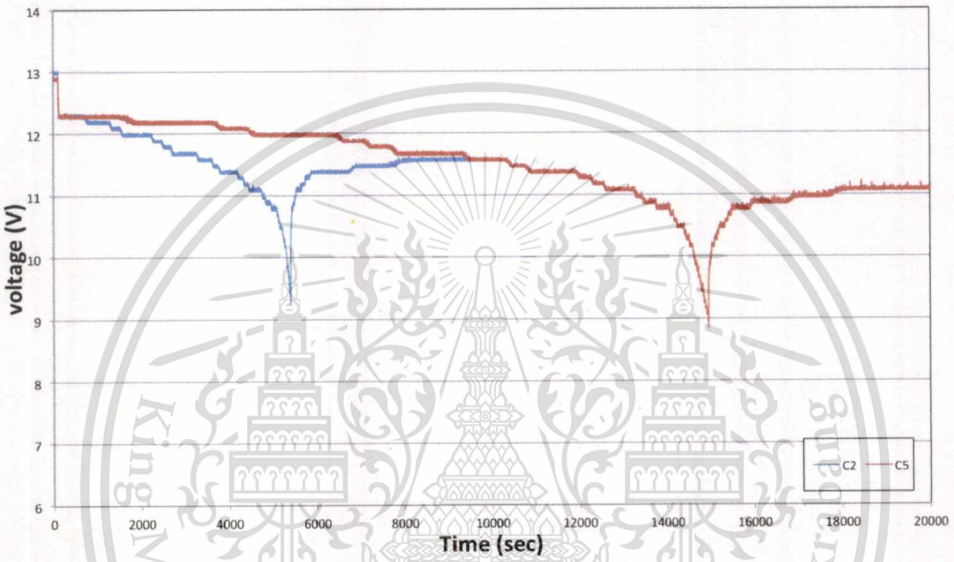

Figure 4.5 Battery voltage characteristics after open circuit.

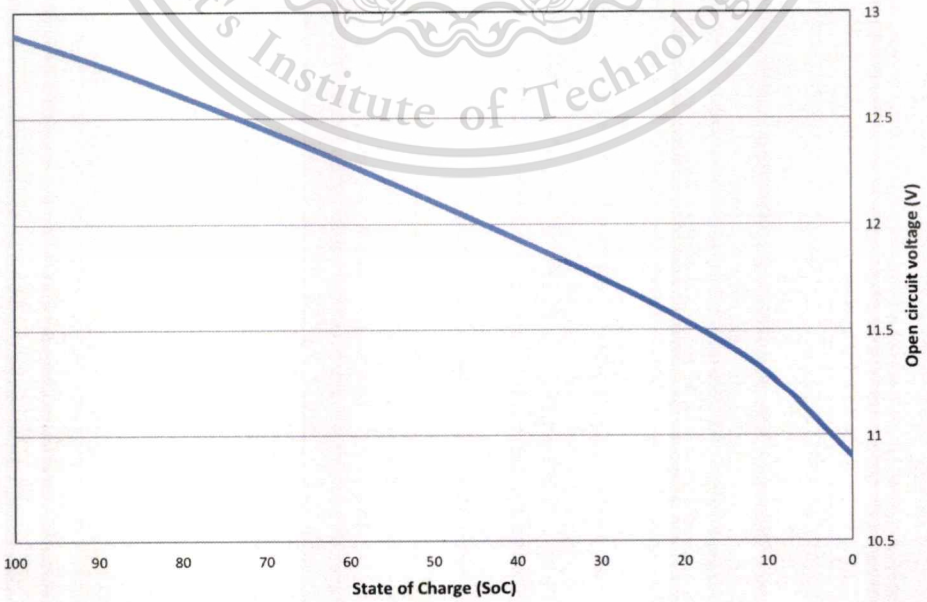

Figure 4.6 Open circuit voltage versus State of Charge of VRLA battery.

This material is reserved for educational use only, not allowed for commercial use.
Forbidden to modify the content, and cite the document when use.

4.1.4 Ampere-hour counting

By using Ampere-hour counting method, the relationship between SoC and time of flooded lead-acid battery was almost linearly proportional under constant current discharge as shown in figure.4.7. By using ampere-hour counting method, the initial SoC of battery was set to 100%. At C_{10}, the discharge test end at 27000 seconds (7.5 hour) after cut off voltage was reach. However, at the end of the test the SoC of C_{10} is not shown as 0%, about 28.2% remaining SoC is presented. Thus, the remaining SoC of 28.9%, 38.5% and 44.7% are presented for the discharge rate at C_5, C_3, and 1C respectively.

A capacity consumption of 93Ah, 92Ah, 80Ah and 72Ah was collected from the testing under C_{10}, C_5, C_3, and 1C discharge rates respectively, as shown Table 4.1. The obtained capacity percentage was calculated based on nominal capacity 130Ah fully charged battery. For VRLA battery, the total charge output from discharge test of C_5 and C_2 are equivalent at 43.5Ah. In Table 4.2, variation of available capacity of VRLA battery is shown. However, the available capacity of VRLA battery at C_{10} (60Ah), 1C (42.4Ah), and 2C (38.3Ah) are discharged test by manufacturer.

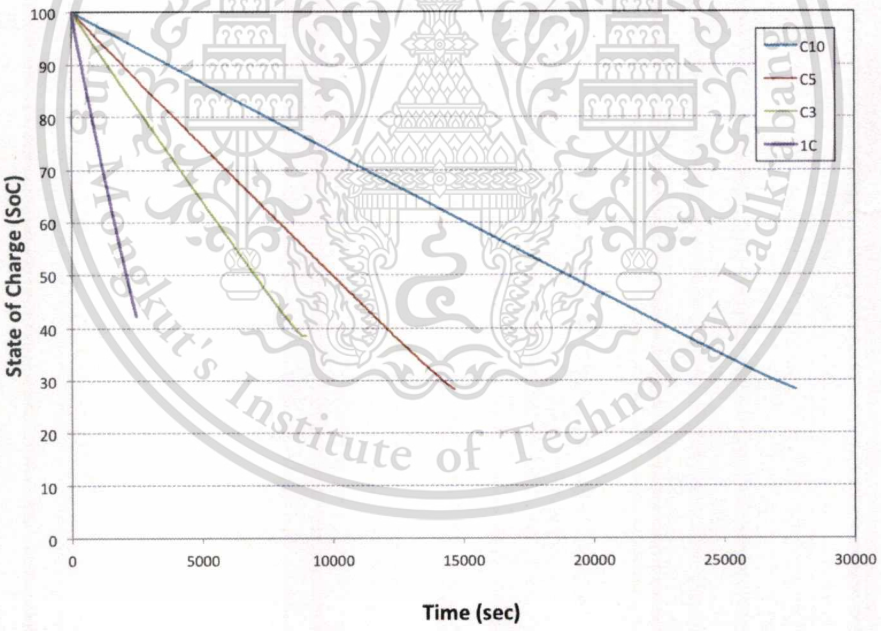

Figure 4.7 The SoC estimation at different discharge rates by Ampere-hour counting method.

Table 4.1 Variation of available capacity of flooded Lead-Acid battery.

Discharge rate	Available Capacity (Ah)
C_{10}	93
C_5	92
C_3	80
1C	72

This material is reserved for educational use only, not allowed for commercial use.
Forbidden to modify the content, and cite the document when use.

Table 4.2 Variation of available capacity of VRLA battery.

Discharge rate	Available Capacity (Ah)
C_{10}	60*
C_5	43.5
C_2	43.5
1C	42.4*
2C	38.3*

4.1.5 Ampere-hour counting with correcting factor

A factor α was introduced to improve the accuracy of Ampere-hour counting method. By the calculation α corresponding factor (section 3.2.4) at each rate of discharge of flooded lead-acid battery and VRLA battery is present in Table 4.3 and Table 4.4 respectively. In figure.4.8, the comparison of SoC estimation of flooded lead-acid battery by using Ampere-hour counting with and without the value of corresponding α is shown. Without α parameter, the SoC started at 100% and continuously decreased at different rate from the SoC estimated with α. At C_5, the battery was supposed to run out of charge with percentage of SoC using α parameter reached 0%, while SoC of 28.9% was predicted without α. It can be observed that while SoC of battery predicted with α reached 0%, all the estimations without α gave relatively overestimated values such as 28.2%, 38.5% and 44.7% for C_{10}, C_3 and 1C respectively. The SoC comparison at C_5 and C_2 of VRLA battery is present in figure 4.9. The SoC also start from 100%, without α corresponding factor the SoC is estimated as 28.5% when the cutoff voltage was reach. By using ampere-hour counting with correcting factor (α), at complete discharge the estimated SoC shown 1.64% and 1.17% for C_2 and C_5 respectively.

Table 4.3 Available capacity and α corresponding factor (Flooded Lead-Acid battery).

Discharge rate	Available Capacity (Ah)	Obtained % Capacity	α
C_{10}	93	71.5	1.39
C_5	92	70.7	1.40
C_3	80	61.5	1.62
1C	72	55.3	1.8

This material is reserved for educational use only, not allowed for commercial use.
Forbidden to modify the content, and cite the document when use.

Table 4.4 Available capacity and α corresponding factor (VRLA battery)

Discharge rate	Available Capacity (Ah)	Obtained % Capacity	α
C_{10}	60	100	1
C_5	43.5	72.5	1.37
C_2	43.5	72.5	1.37
1C	42.4	70.6	1.41
2C	38.3	63.8	1.56

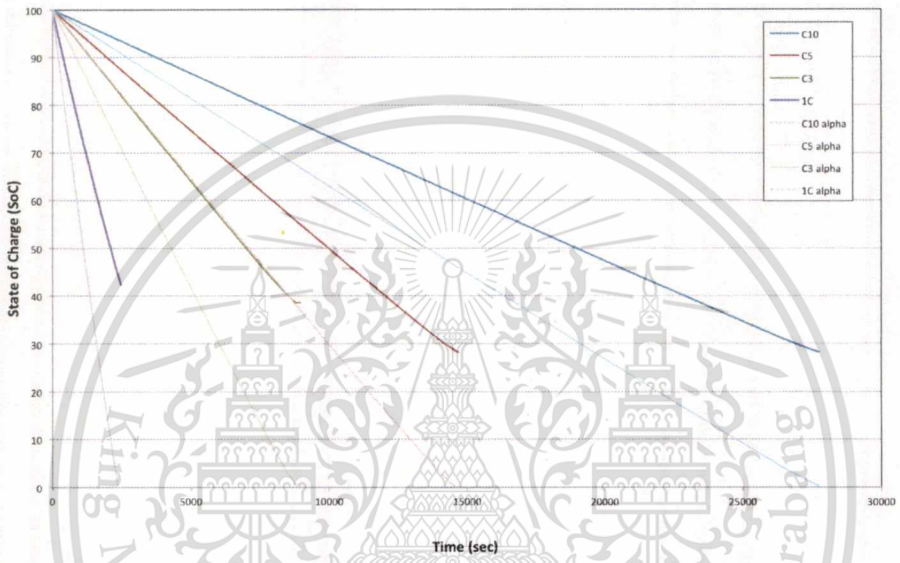

Figure 4.8 The comparison of SoC estimation at different discharge rates of flooded lead-acid battery.

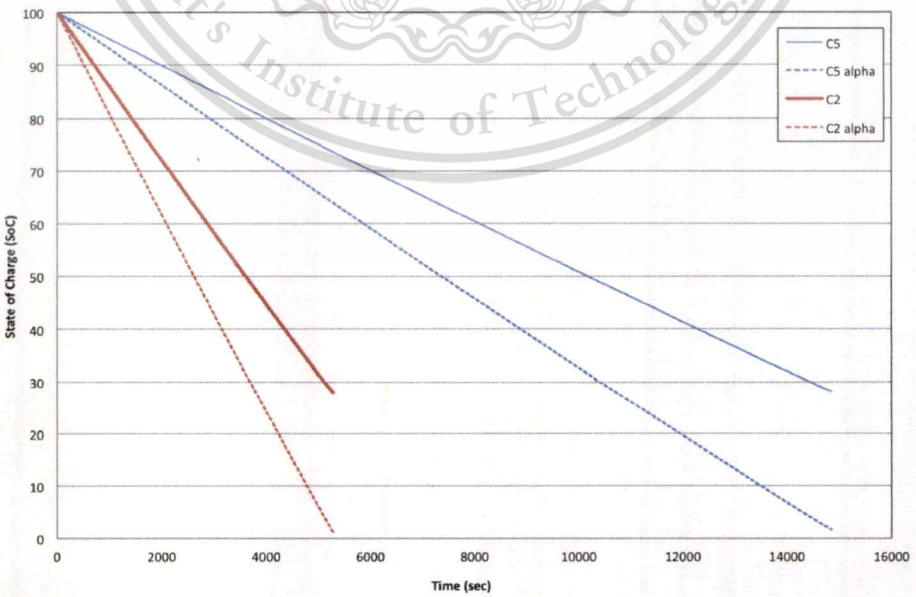

Figure 4.9 The comparison of SoC estimation at different discharge rates of VRLA battery.

This material is reserved for educational use only, not allowed for commercial use.
Forbidden to modify the content, and cite the document when use.

4.2 Driving test

In driving tests, both type of lead-acid battery (flooded lead-acid and VRLA battery) are tested in electric bus prototype. In the first part, the acceleration of electric bus prototype with under loading and no-loading condition is tested. In the next part, fixed driving range test by vary the driving mode, regenerative breaking system, and drivers are studied. The results of battery consumption and State of Charge (SoC) are presented in this section.

The total range of the driving cycle is about 1.4 km/lap, including straight road and corner under real traffic condition. Figure 4.10 and Figure 4.11 show initial driving test between flooded lead-acid battery and VRLA battery respectively. For 1 lap (1.4 km), average current for flooded lead-acid battery is 39.69A and total charge output is 1.92Ah, while 31.35A and 1.87Ah are for VRLA battery. For flooded Lead-Acid battery, the terminal voltage of battery varied form 280V - 300V, while 300V – 320V for VRLA battery. Torque of motor and power output is also varying with battery current or acceleration of the test vehicle. The heatsink temperature at inverter is a bit increasing with a driving time.

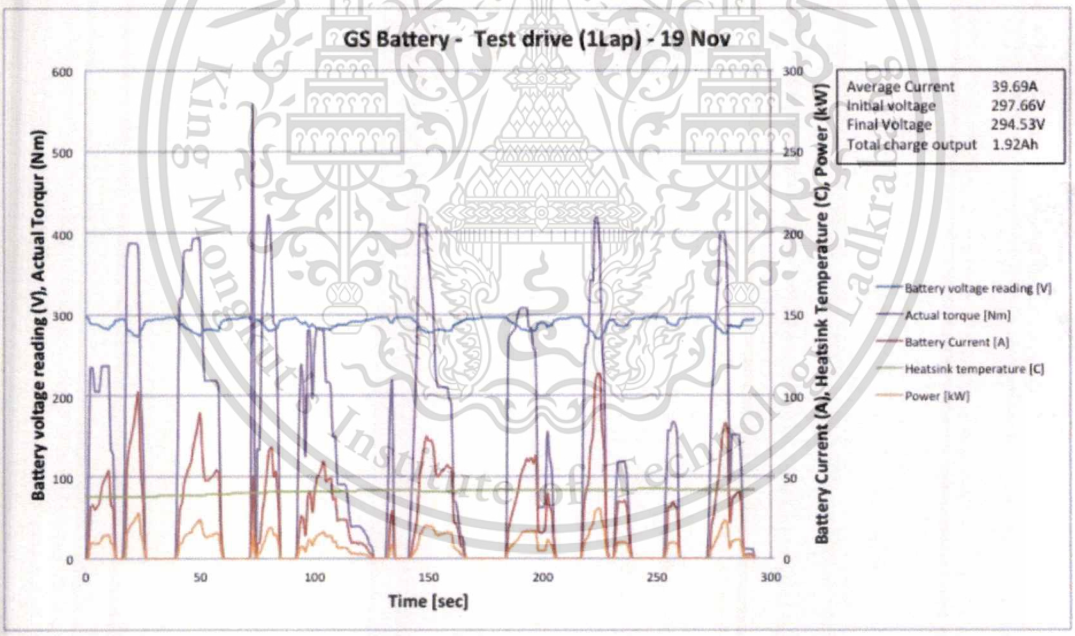

Figure 4.10 The driving test of Flooded lead-acid battery in real traffic condition.

This material is reserved for educational use only, not allowed for commercial use.
Forbidden to modify the content, and cite the document when use.

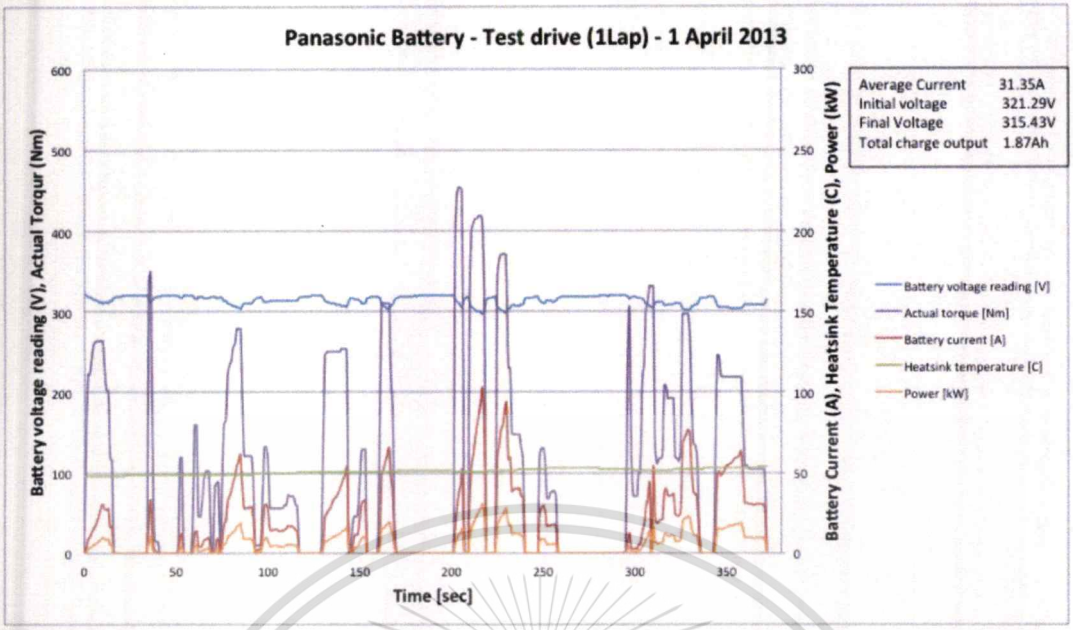

Figure 4.11 The driving test of VRLA battery in real traffic condition.

4.2.1 Acceleration test

In order to study about battery behaviour, acceleration test is one of the most important cases. The test start from stand still, then put pedal as maximum accelerate to reach 50km/hr. As you can see from the graph, to reach a speed of 50km/hr the motor revolution is about 1700rmp. At no-load condition the vehicle takes about 50 second to get a target speed, while 70 second or 40% longer used for vehicle under loading condition. Furthermore, under loading condition the electric vehicle used longer period of current discharge to reach 50km/hr. However, under no-loading condition the maximum discharge current is only 120A while 160A (33% higher) is used for loading as shown in figure 4.12.

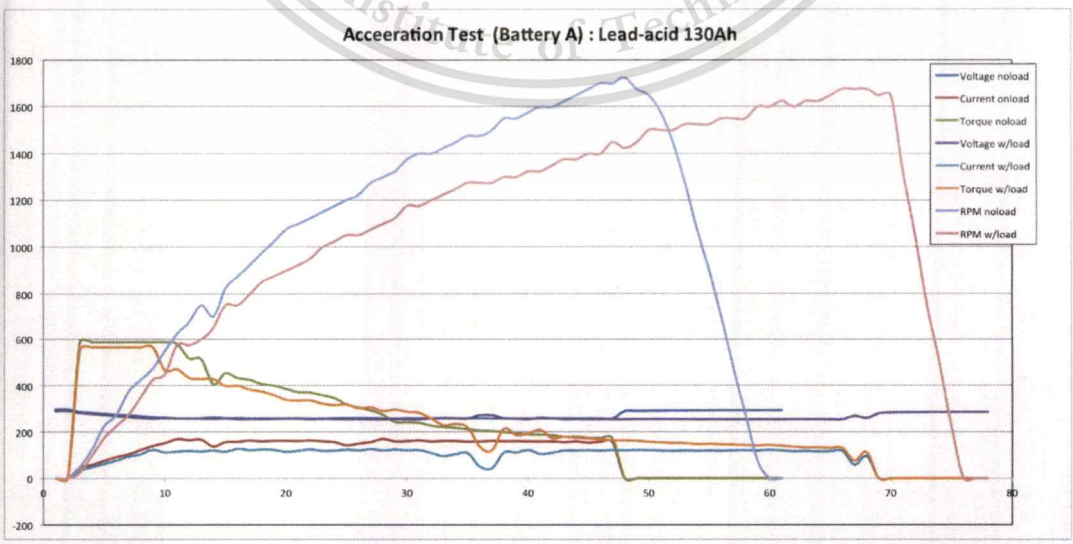

Figure 4.12 The acceleration test of flooded lead-acid battery.

This material is reserved for educational use only, not allowed for commercial use.
Forbidden to modify the content, and cite the document when use.

4.2.2 Fix driving range test

For study the behaviour of electric bus prototype, 12 different cases are observed. During the driving test 2 types of battery is used as sample. Moreover, 2 modes of regenerative braking system are studied separately at each type of battery. The study also focuses on the driving mode of the electric bus prototype, i.e. Max Range mode, Normal mode, and Max power mode. The overall of study case is summarise in Table 4.5

Table 4.5 The summarise of study cases in electric bus prototype.

Type of battery	Regenerative braking system	Driving Mode
Flooded Lead-Acid battery	Slippery	Max Range
		Normal
	Regenerative braking	Max Power
VRLA battery	Slippery	Max Range
		Normal
	Regenerative braking	Max Power

From the initial tests (figure 4.10, 4.11) and the case study requirement, the electric bus prototype driving cycle is set to 15laps (21km)/ day – 5 laps per a driving case. In figure 4.13, the battery voltage of Flooded Lead-Acid and VRLA battery in regenerative braking mode is presented. An initial voltage of Flooded Lead-Acid battery is started from about 302V, while about 332V is set as initial voltage of VRLA battery. During the test, the electric bus prototype will stops for 5 minutes after finish a single lap for collecting the OCV data. In regenerative braking mode, the battery terminal voltage decreasing during acceleration and increasing during deceleration and braking period. After 15 laps the final voltage of Flooded Lead-Acid battery is 294.92V and 302.34 for VRLA battery. In figure 4.14, the battery terminal voltage at slippery mode is shown. The initial voltage of both types of battery is almost the same with regenerative braking mode, but slippery mode the final voltage of flooded Lead-Acid battery is shown only 289.84V and 297.85V for VRLA battery.

This material is reserved for educational use only, not allowed for commercial use.
Forbidden to modify the content, and cite the document when use.

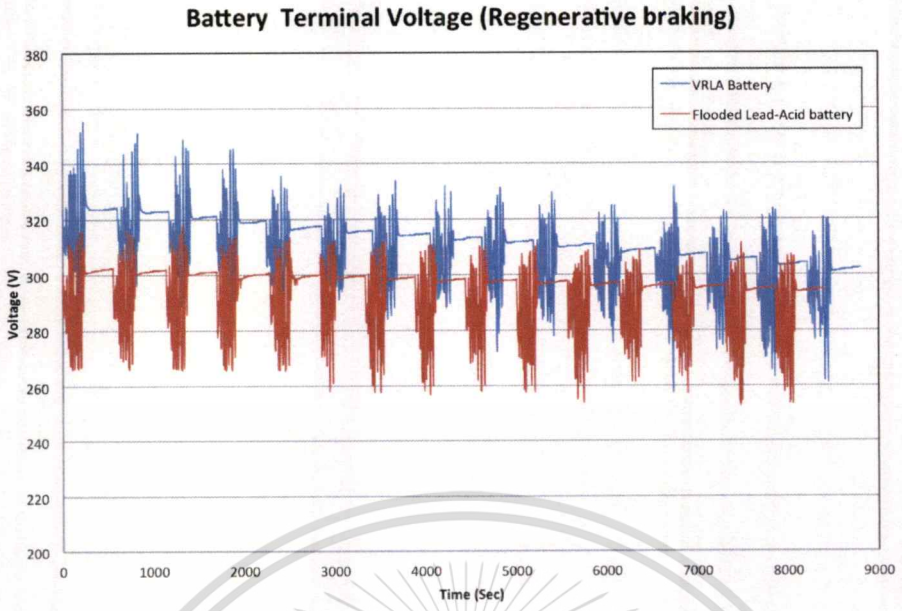

Figure 4.13 Battery terminal voltage of electric bus prototype (Regenerative braking)

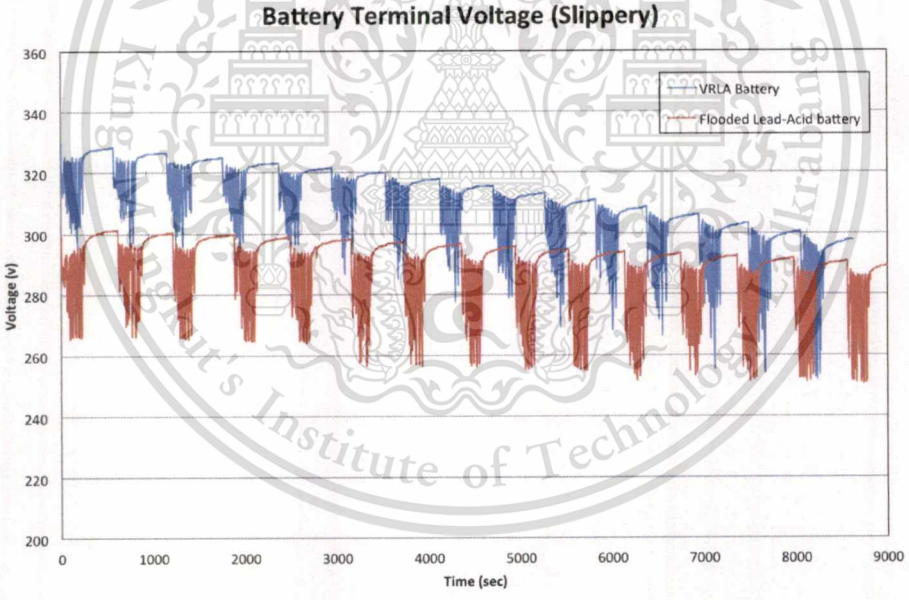

Figure 4.14 Battery terminal voltage of electric bus prototype (Slippery)

The total VRLA battery consumption of electric bus with regenerative breaking system is only 1.38Ah – 2.1Ah per lap as shown in figure 4.15. By using regenerative braking system, the energy can convert back to battery as shown as the negative value in the graph. Nevertheless, figure 4.16 shows the battery consumption of electric bus without regenerative breaking system 15 laps. The battery consumption is varying from 2Ah – 2.7Ah per lap. Moreover, the battery consumption of flooded lead-acid battery is shown in figure 4.17 and figure 4.18, with regenerative breaking and

This material is reserved for educational use only, not allowed for commercial use.
Forbidden to modify the content, and cite the document when use.

slippery respectively. The total battery consumption of flooded lead-acid battery in regenerative braking mode is about 1.7Ah – 2.3Ah per lap (signal lost for 1 minute in test no.21- column no.6 (1.4Ah)). In slippery mode, the total battery consumption of flooded lead-acid battery is varied from 2.4Ah – 3.1Ah.

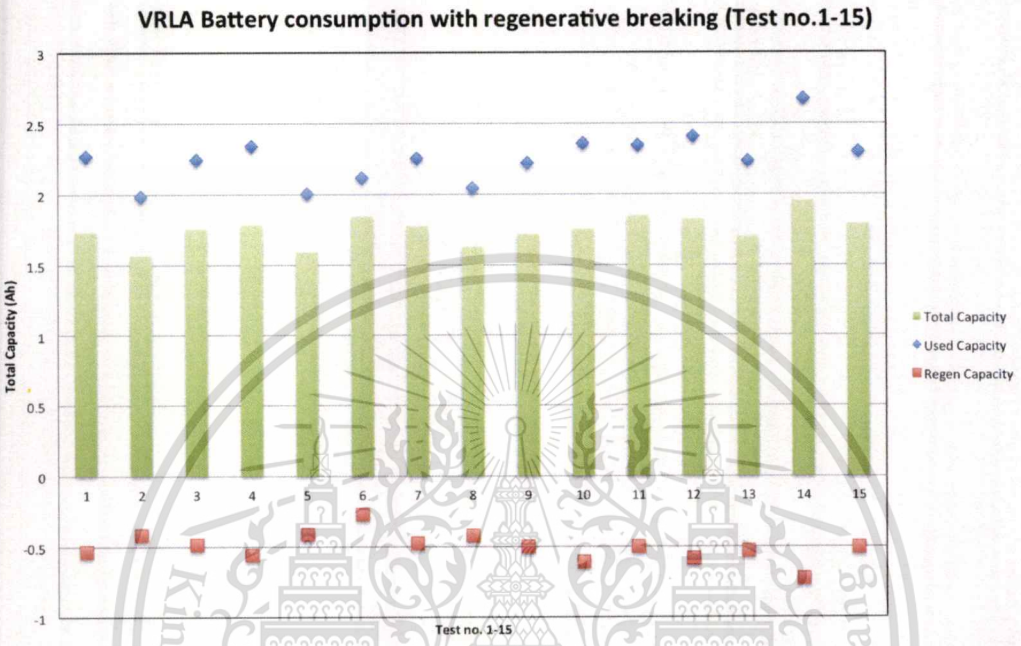

Figure 4.15 VRLA battery consumption (with regenerative breaking).

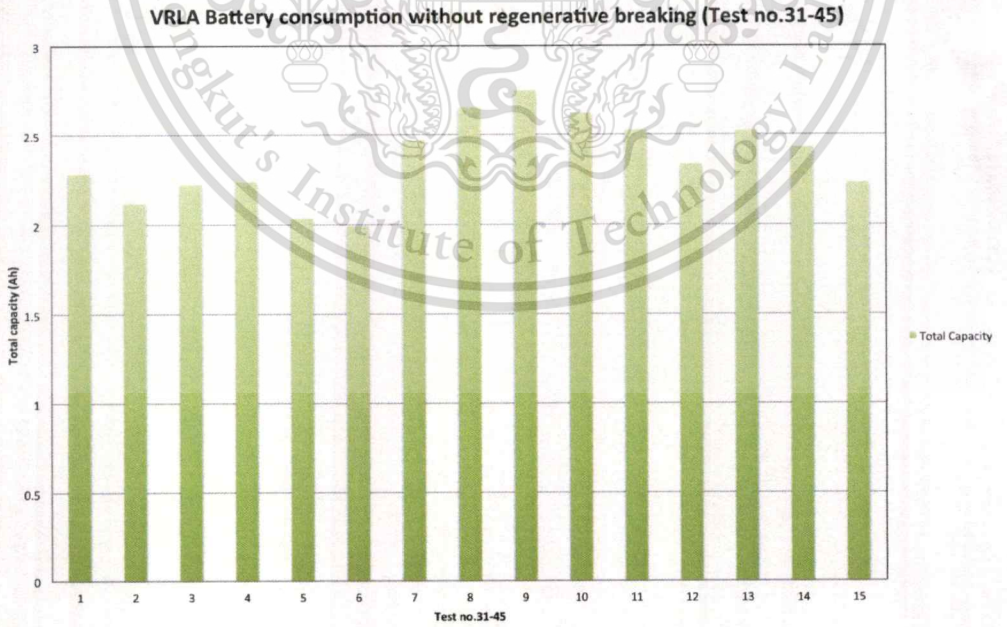

Figure 4.16 VRLA battery consumption without regenerative breaking (Slippery).

This material is reserved for educational use only, not allowed for commercial use.
Forbidden to modify the content, and cite the document when use.

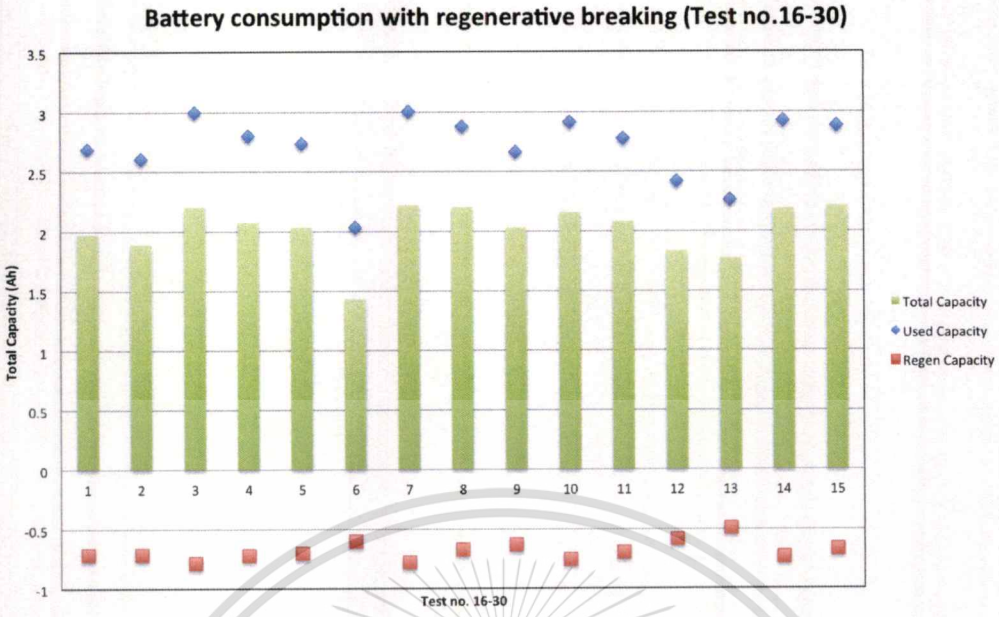

Figure 4.17 Flooded Lead-Acid battery consumption (with regenerative breaking).

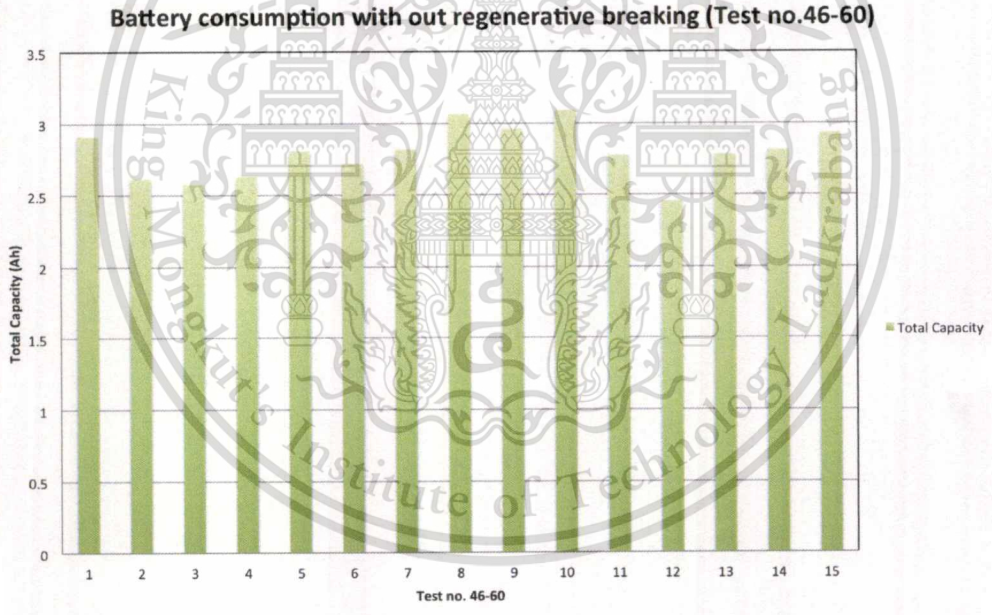

Figure 4.18 Flooded Lead-Acid battery consumption with out regenerative breaking (Slippery).

Nonetheless, the driving style is directly effects to battery consumption. In figure 4.19 and figure 4.20, a total capacity output of VRLA battery and flooded Lead-Acid battery by other drivers are shown. By using regenerative braking system, the total capacity output is always lower than slippery mode. The maximum battery consumption of VRLA battery in regenerative braking system is used by driver no.2 (30.2Ah) and 21.6Ah from driver no.4 is minimum value. At slippery mode, the maximum battery consumption is taken by driver no.3 40.4Ah is used, while minimum about 32.9Ah is used by driver no.2.

This material is reserved for educational use only, not allowed for commercial use.
Forbidden to modify the content, and cite the document when use.

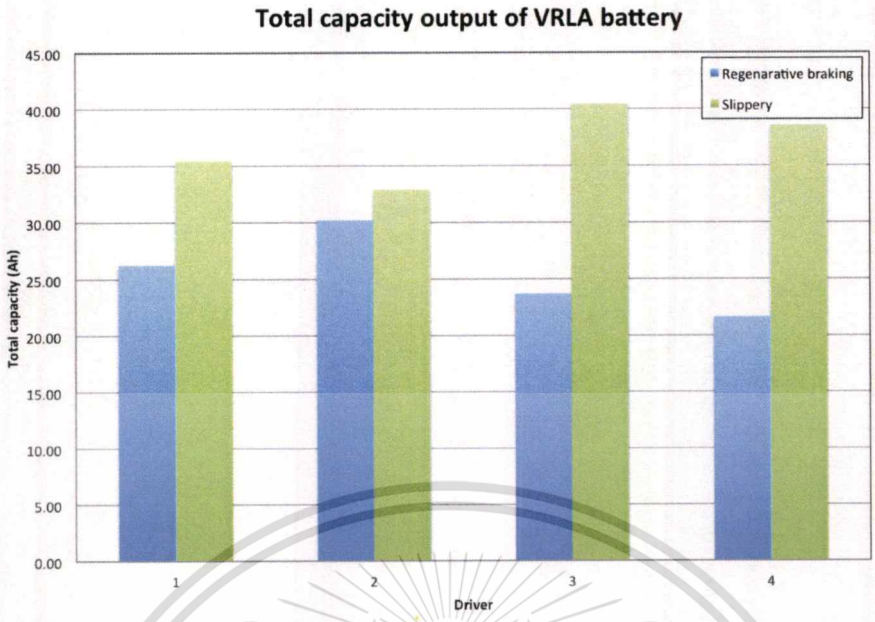

Figure 4.19 VRLA Battery consumption at different drivers.

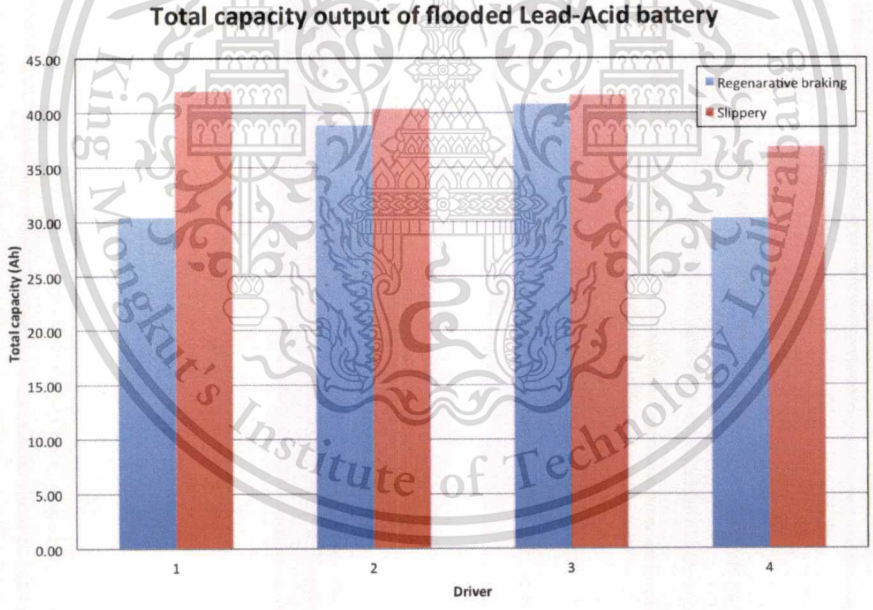

Figure 4.20 Flooded Lead-Acid Battery consumption at different drivers.

4.3 Battery State of Charge (SoC)

The parameters obtained from a driving test of VRLA battery are shown in figure 4.21. The battery current varied from -100A to 200A, depending on the driving situations. The results were obtained from a 15 laps test drive or about 21km. By using ampere-hour counting method, battery SoC was determined to decrease slightly from 100%SoC to 56.4%SoC. Nevertheless, by using α

This material is reserved for educational use only, not allowed for commercial use.
Forbidden to modify the content, and cite the document when use.

parameter from the discharge test (Table 4.4) the result of estimated SoC is show as the purple line. At the end of driving test the estimated remaining SoC is 30.7% and OCV is 302.34V.

For the discharge test in section 4.1.1, the relationship of SoC and OCV of single battery is express in figure 4.3. However, the figure 4.22 represents the relationship of SoC and OCV for using in electric bus prototype. From the final voltage of 302.34V, by using the reference OCV data a final SoC of the driving test is about 23%SoC.

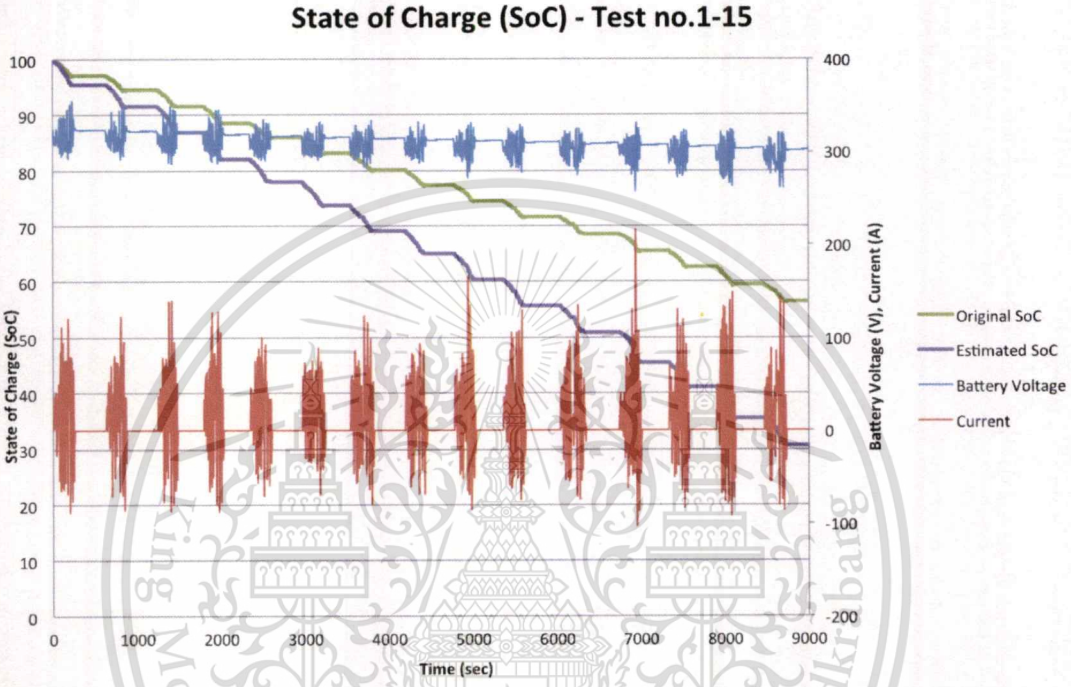

Figure 4.21 Battery parameters and SoC of VRLA battery (regenerative braking mode).

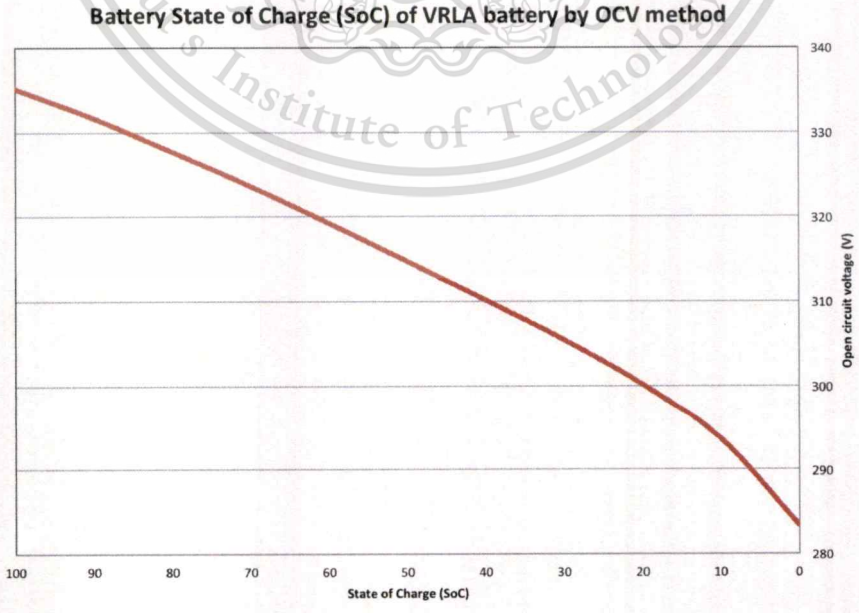

Figure 4.22 Battery SoC and OCV of VRLA battery.

This material is reserved for educational use only, not allowed for commercial use.
Forbidden to modify the content, and cite the document when use.

The test result of VRLA battery in slippery mode is displayed in figure 4.23. The final OCV voltage of the test vehicle is 297.85V or about 17%SoC. By using ampere-hour counting method the final SoC show 41%, while estimate SoC with α parameter represent 12% remaining.

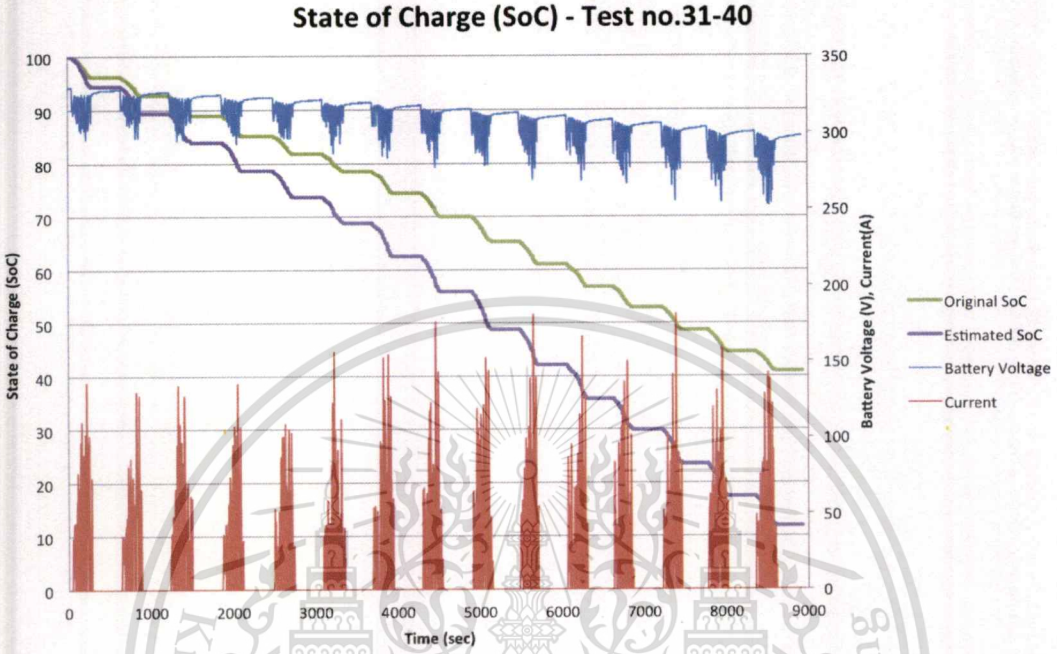

Figure 4.23 Battery parameters and SoC of VRLA battery.

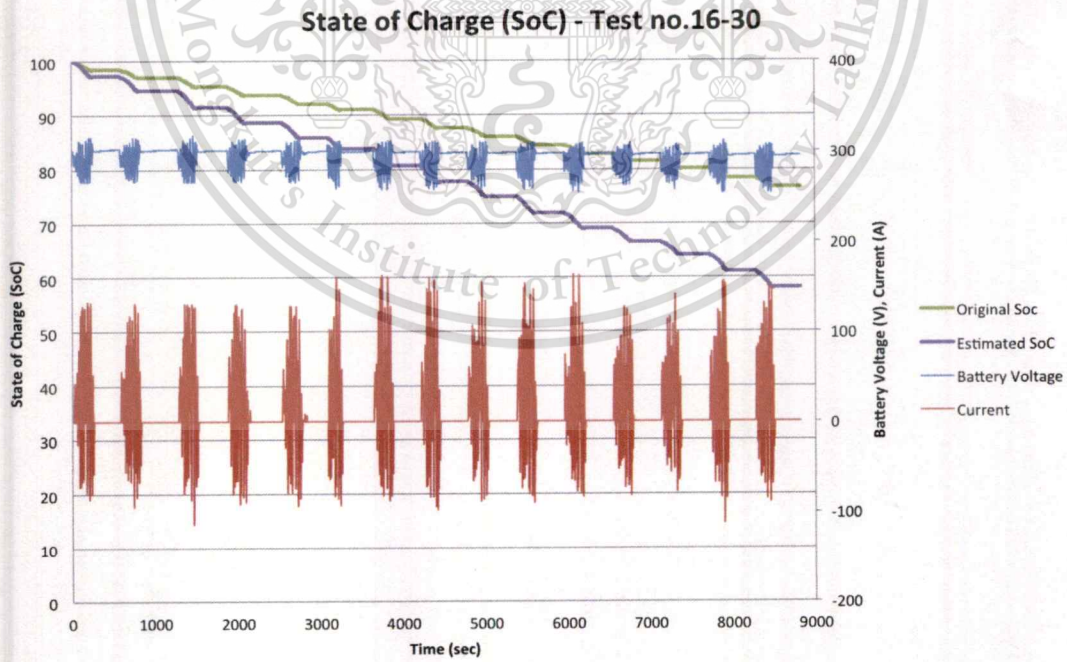

Figure 4.24 Battery parameters and SoC of flooded Lead-Acid battery (Regenerative braking mode).

This material is reserved for educational use only, not allowed for commercial use.
Forbidden to modify the content, and cite the document when use.

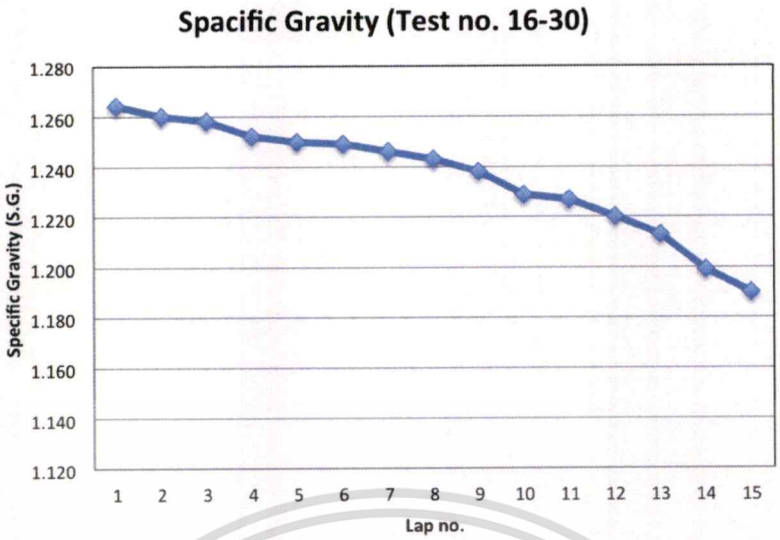

Figure 4.25 Specific gravity of flooded lead-acid battery (regenerative braking mode).

Figure 4.24 indicates the battery parameter and SoC of flooded lead-acid battery in regenerative breaking mode. From the graph the initial SoC start from 100% and slightly decrease, at final stage the estimated SoC from ampere-hour counting technique show 76.65%, while 58.0% remaining SoC estimated from ampere-hour counting with correcting factor. Moreover, the relationship of SoC and specific gravity measurement of concentration in flooded lead acid battery is shown in figure 4.25. The specific gravity of lead-acid battery starts from 1.262 or about 92%SoC and continuously decreases to 1.19 or 68%SoC.

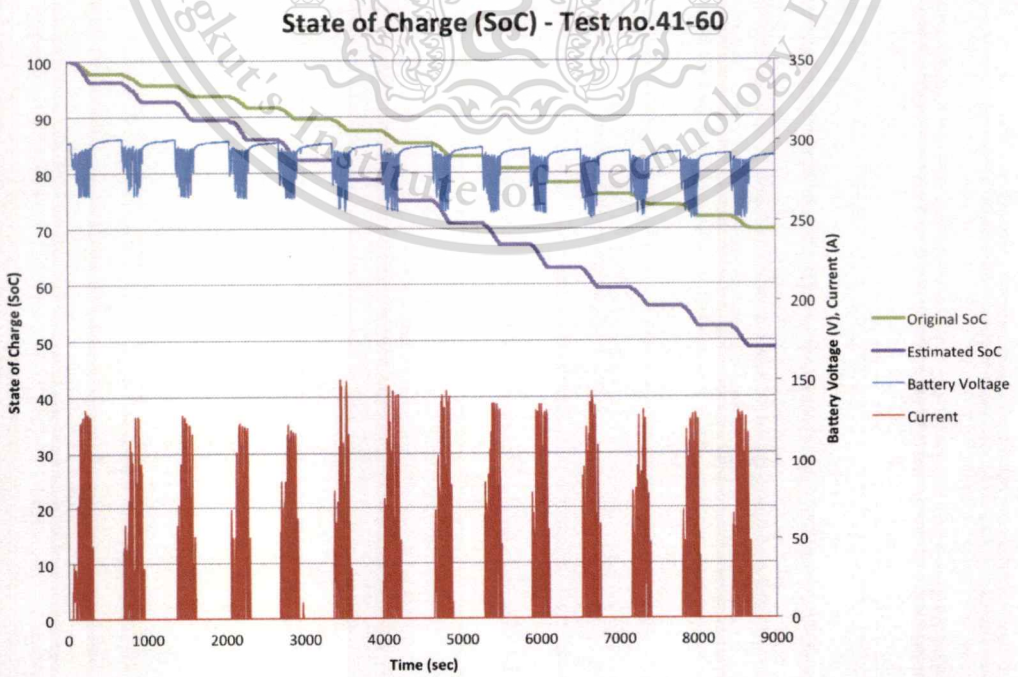

Figure 4.26 Battery parameters and SoC of flooded Lead-Acid battery (Slippery mode).

This material is reserved for educational use only, not allowed for commercial use.
Forbidden to modify the content, and cite the document when use.

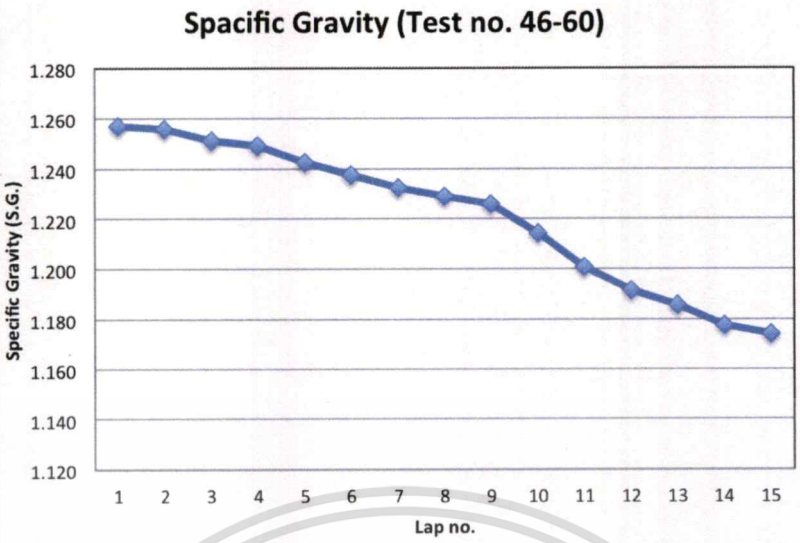

Figure 4.27 Specific gravity of flooded lead-acid battery (slippery mode).

In figure 4.26 and figure 4.27, the results of SoC and specific gravity measurement of flooded lead-acid in slippery mode are shown. The initial SoC also start from 100%, at the end of the test SoC from ampere-hour counting technique present 70% remaining, while with the correcting factor the remaining SoC of 48% is indicated. However, the initial SoC from specific gravity measurement displayed only 91%SoC (S.G. of 1.258) and final S.G. of 1.17 or equivalent to 60%SoC is notified.

This material is reserved for educational use only, not allowed for commercial use.
Forbidden to modify the content, and cite the document when use.

CHAPTER 5
DISCUSSIONS

In this chapter, the characteristics and behaviour of two different types of batteries, i.e. flooded lead-acid and VRLA battery, will be discussed. Moreover, the discussion regarding State of Charge (SoC) estimation technique that is appropriate to the current electric bus prototype is also given.

5.1 Preliminary test

In preliminary testing, the discharge test, specific gravity test, and open circuit voltage test of lead-acid batteries were performed. By using the results of discharge test, the estimation of State of Charge (SoC) of battery was presented. In addition, the comparison of the SoC of battery at different method is given.

5.1.1 Discharge test

From the discharge test, the available capacity (total capacity output) of battery was decreasing with the rate of discharge as shown in table 5.1. The results suggested that a higher discharge rate, a lower available charge from the battery was presented.

Table 5.1. The available capacity of flooded lead-acid battery and VRLA battery.

Discharge rate	Available Capacity (Ah)	
	Flooded lead-acid battery (130Ah)	VRLA battery (60Ah)
C_{10}	93	60*
C_5	92	43.5
C_3	80	43.5
1C	72	42.4*
2C	-	38.3*

The comparison of available capacity between flooded lead-acid battery and VRLA battery is shown in figure 5.1. At the same discharge rate test, the results showed that at high rate of discharge the available capacity of VRLA battery were almost the same (71.7%). At high discharge rate, the performance of VRLA is better than flooded lead-acid battery because of higher percentage of available capacity. More than 3C-rate could be obtained from VRLA, while only about 1.2C- rate was seen from flooded lead-acid battery. Then, the rate of discharge directly effects to the total charge output of flooded lead-acid battery.

This material is reserved for educational use only, not allowed for commercial use.
Forbidden to modify the content, and cite the document when use.

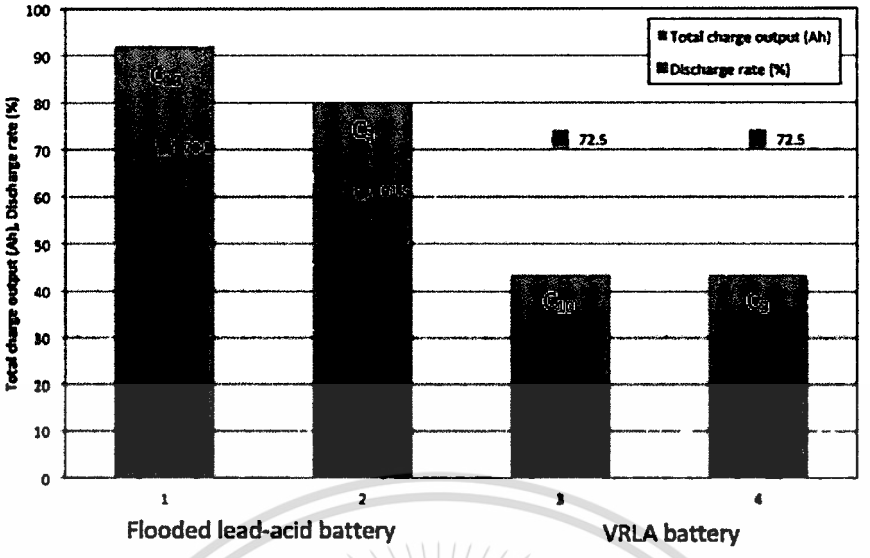

Figure 5.1. The comparison of available capacity between flooded lead-acid and VRLA battery.

5.1.2 Specific gravity test

There are 6 cells in a 12V flooded lead-acid battery. The measurements of electrolyte concentration were conducted at every cells. From figure 4.3, the observed relationship of specific gravity (S.G.), SoC, and OCV is presented. The relationship of S.G., SoC, and OCV was observed to be almost a linear relationship. Normally, the specific gravity of new flooded lead-acid battery is about 1.27-1.28 (100%SoC). However, the specific gravity of used battery varied around 1.24 – 1.25 which was about 90% of new battery as shown in figure 4.4. It could be seen that the S.G. of electrolyte in battery could present the change of battery characteristics due to an aging effect. In electric vehicles the initial SoC does not always begin from 100%, therefore the initial SoC of flooded lead acid battery could be estimated by using S.G. method. Moreover, the measurement of electrolyte in every cell could identify the abnormality of the cell that might lead to the damage of a device.

5.1.3 Open Circuit Voltage

Commonly, the battery terminal voltage is decreasing while discharging or being used in an electric device. At high discharge rate, the terminal voltage could dramatically dropped in a few minutes. After discharged (open circuit), the terminal voltage of battery will swing back to the open circuit voltage. After 5 minutes, the open circuit voltage of battery is closed to stable. Then, the measurement of battery could inform the State of Charge (SoC). Moreover, for more accurate prediction of SoC of battery, more than 30-minutes open circuit voltage is needed before a measurement. Nevertheless, the open circuit voltage of battery is quite different between

This material is reserved for educational use only, not allowed for commercial use.
Forbidden to modify the content, and cite the document when use.

manufacturers. The accurate SoC from OCV measurement should be referred to battery specific data or experiment in the laboratory.

5.1.4 Ampere-hour counting – Ampere-hour counting with correcting factor

From the discharge test, the SoC of battery could be estimated by ampere-hour counting method. By integrating the current flow over the time, the remaining capacity could be estimated as shown in figure 4.7. However, since the discharge rate was found to directly affect the available capacity of battery, the estimated SoC from this technique would usually over-estimate. To solve the over-estimated SoC in ampere-hour counting technique, a factor α was introduced to improve the accuracy of this technique. At completely discharge (cutoff voltage was reached) in the same discharge test, the a result of ampere-hour counting with correcting factor is closed to 0%SoC while about 30%-40% over-estimated is indicate in normal ampere-hour counting technique. The α correcting factor is increasing directly proportional to the rate of discharge. At the same discharge rate, the percentage of available capacity of flooded lead-acid battery was lower than VRLA battery, and then the α correcting factor of flooded lead-acid battery was higher than VRLA battery.

In the driving test, the discharge rate of electric bus was classified into 5 zones for reducing the complexities of calculation (Figure 3.22). The zoning of discharge current was defined by the discharge rate (C-Rate) by equally ranged with the same ratio. Generally, the discharge current of electric bus prototype was observed to be oscillating around 0A-80A, while the α correcting factor of battery almost increased in linear proportional to the discharge current. In addition, the division of discharge's current range could be adjusted and improved by researcher as appropriate. Furthermore, for more accurate result, the α correcting factor can be calculated by an interpolating technique.

5.1.5 A comparison of State of Charge (SoC) estimation techniques

A comparison of SoC in flooded lead-acid battery under 5 hours rate (common discharge rate for electric vehicles) is shown in figure 5.2. At the end of discharge, the SoC from specific gravity measurement show 8%SoC, while 28.9% and 0% was estimated by ampere-hour counting, and ampere-hour counting with correcting factor respectively. However, there might have been certain discrepancy in estimated SoC by using specific gravity measurement due to an error by reading scale of the hydrometer. There were 3 digits reading value at a hydrometer with increasing by 0.025, while 0.01 of S.G relative to 4%SoC different. Consequently, the reading value of S.G. by hydrometer could have been caused by a human error.

This material is reserved for educational use only, not allowed for commercial use.
Forbidden to modify the content, and cite the document when use.

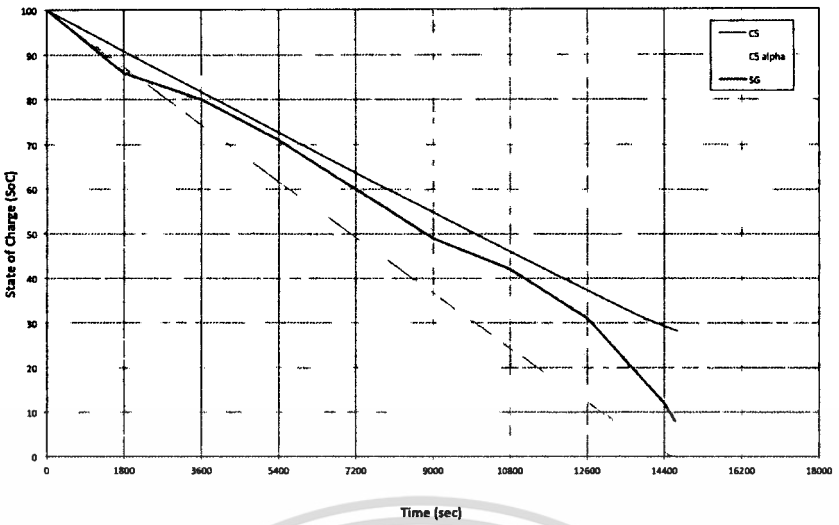

Figure 5.2 A comparison of SoC estimation technique (flooded lead-acid battery).

Figure 5.3 is the SoC comparison of VRLA battery under 5 hours rate. The OCV measurement is a general indicator and high accuracy for identifies SoC of battery. However, about 30 minutes time delays is necessary for OCV that makes it inconvenient for real time measurements. By ampere-hour counting with correcting factor, the estimated SoC was about 0% that very closed to %SoC by using OCV technique, while 28.5%SoC was estimated from general ampere-hour counting technique. By using α correcting factor with ampere-hour counting, the estimation of SoC appeared to be more accurate, convenience and did not require time delays for measurements.

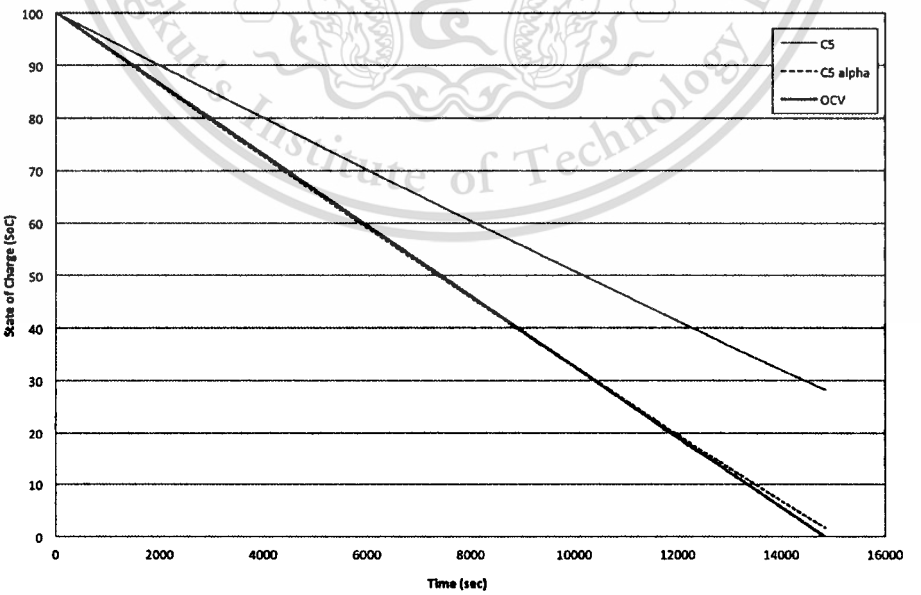

Figure 5.3 A comparison of SoC estimation technique (VRLA battery).

This material is reserved for educational use only, not allowed for commercial use.
Forbidden to modify the content, and cite the document when use.

5.2 Driving tests

Examples of motor parameters obtained from MTEC Electric bus prototype during initial test drive are shown in figure 5.4. The parameters of interest were the change of battery voltage, battery current, motor revolution, and torque. During acceleration test, high current was flowing out from battery. The battery voltage dramatically decreased while the motor revolution and torque were continuously increasing. At constant speed, all parameters were almost constant. During accelerating up the slope, high torque was required for this condition. As a result, high current was flowing out to create torque for motor while motor revolution was slightly increasing. In breaking condition, there was no significant change in battery voltage, no current flowing from battery while torque was zero. The motor revolution was sharply decreased to zero then the bus stopped.

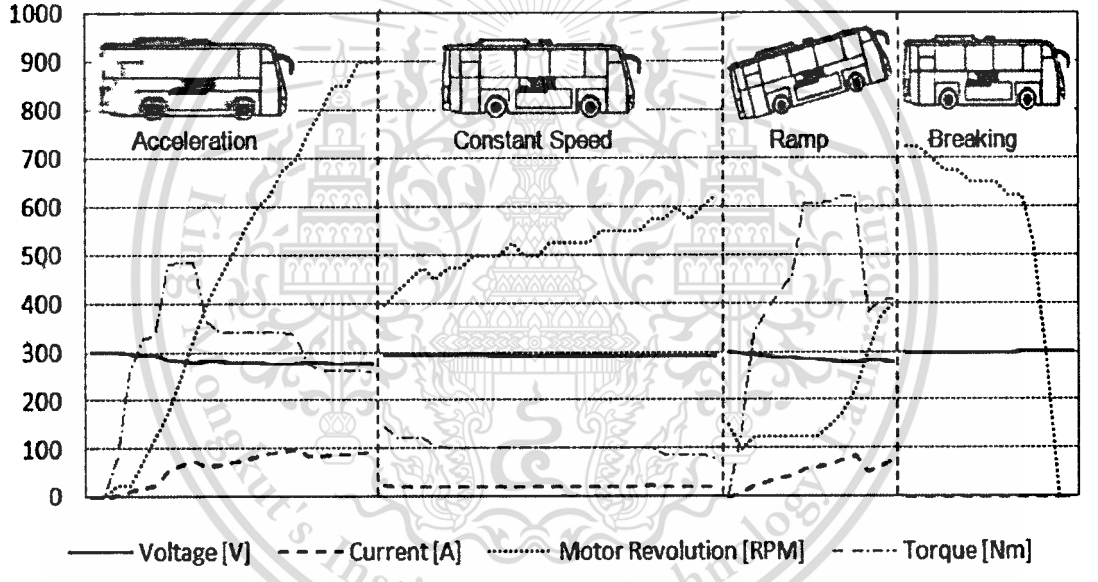

Figure 5.4 Motor characteristics of electric bus at various driving conditions.

From the initial test of electric bus prototype, a flooded lead-acid battery consumed higher total charge output than VRLA battery with the same distance. In the same way, the average current flow of flooded lead-acid battery was also higher. One of reasons might have come from the weight of flooded lead-acid battery packs, which was 540kg (49.4%) higher than that of VRLA battery.

5.2.1 Acceleration test

There were 2 cases in acceleration test i.e. no-loading condition, and full loading condition. The decreasing rate of battery terminal voltage in both cases was almost the same. From the

This material is reserved for educational use only, not allowed for commercial use.
Forbidden to modify the content, and cite the document when use.

initial voltage of 297V, the terminal voltage sharply decreased to about 257V during maximum acceleration (100% pedal). Under loading condition, the electric bus needed 25 seconds longer to reach the target speed. The maximum discharge current of electric bus under loading condition was 1.2C, while only 1C was maximum discharge rate for no-loading condition. Therefore, the weight of the vehicle had direct effect on the discharge rate as well as an acceleration and total distance per charge. In addition, VRLA battery could obtain the discharge current about 3C and the weight was lighter, the acceleration of VRLA was higher than that of the flooded lead-acid battery.

5.2.2 Fix driving range test

According to the 12 cases of driving condition for each driver, the result of different driving mode (max range, normal, max power) was slightly different. In the max range mode, the electric bus prototype could not go through high current zone. Therefore, limited current flows were advantages to the available capacity of battery, meaning that the bus could run in a longer distance per charge. A current about 200A (VRLA battery) could be drawn in the max power mode. In max power mode, an acceleration of electric bus prototype was the best. However, the bus required very high current in this mode that led to a shorter distance per charge.

5.2.2.1 Regenerative braking mode and Slippery mode

In regenerative braking mode, the current was reversed back to batteries during braking and no acceleration i.e. a movement by moment of inertia of the bus. The total consumption of VRLA battery in 1-lap driving test (1.4km) was about 2Ah-2.7Ah per lap or 1.43Ah-1.93Ah per km in both driving modes. The reverse capacity from regenerative braking system was about 0.5Ah per lap or 0.35Ah per km. For flooded lead-acid battery, about 1.43Ah-2.14Ah per km was taken from battery. Because of moment of inertia, the amount of reversed charge from regenerative braking system of flooded lead-acid battery was about 0.35Ah-0.71Ah per km.

From figure 4.15-4.18, the average consumption in 1 km of VRLA battery was 1.24Ah/km and 1.71Ah/km in regenerative braking mode and in slippery mode respectively. The average consumption in 1 km of flooded lead-acid battery in regenerative braking mode was 1.48Ah/km and 2.02Ah/km in slippery mode respectively. The percentage difference of average consumption between regenerative braking mode and slippery mode is 37.9% for VRLA battery, and 36.49% for flooded lead-acid battery. The result showed that, under real traffic conditions and driving cycle that included a lot of corners, the overall battery consumption of electric bus in regenerative braking mode was better than that obtained by the slippery mode. On the other hand, in straight route or constant speed the battery consumption of electric bus prototype in both cases was almost the same.

This material is reserved for educational use only, not allowed for commercial use.
Forbidden to modify the content, and cite the document when use.

5.2.2.2 Effect of battery consumption

At the same conditions, different drivers consumed different battery consumption, for VRLA, about 36.3% difference between highest and lowest battery consumption for regenerative braking mode and 22.7% for slippery mode, while 34.4% and 14.8% were obtained for flooded lead-acid battery. The table 5.2 shows the estimation of maximum distance by different drivers. The different of maximum and minimum distance by different drivers is about 10km. From the data collection, the total distance was inversely proportional to the averaged speed, and maximum speed of an electric bus prototype. At the same distance, the higher speed meant the higher acceleration was requested, then the batteries needed to supply a higher rate of discharge that directly affected the available capacity of battery. Therefore, the driving style of driver could be seen as the major effect to the maximum distance.

Table 5.2 The estimation of maximum distance.

		Diver 1	Diver 2	Diver 3	Diver 4
Regenerative braking	Flooded	88	70.9	66.6	88
	VRLA	48.5	42	52.5	57.3
Slippery	Flooded	65	67.4	65	73.8
	VRLA	35	38.7	31.5	33.2

5.3 State of Charge (SoC)

In fix-distance test, the electric bus prototype was set to start from 100%SoC. The estimate SoC was directly proportional to available capacity of battery. By using OCV technique, the equivalent SoC after 21 km was about 22%, while 30.7% and 56.4% was calculated for ampere-hour counting with correcting factor and general ampere-hour counting respectively as shown in figure 5.5. During driving in real driving condition, the vehicle movement was very fluctuated. The OCV measurement could identify the real SoC by the physical property of battery after 5 minutes delays. The equivalent SoC by specific gravity measurement also offered a good reference for flooded lead-acid battery. However, the measurement could not be measured to identify the battery SoC during driving test. Generally, the initial SoC of battery was not start from 100%, the flowchart of SoC estimation in electric bus prototype is presented in figure 5.6. A new SoC estimation for electric bus prototype is presented in figure 5.7. The initial SoC would be identified by OCV or S.G, and then the ampere-hour counting with correcting factor was used to estimate the remaining SoC.

This material is reserved for educational use only, not allowed for commercial use.
Forbidden to modify the content, and cite the document when use.

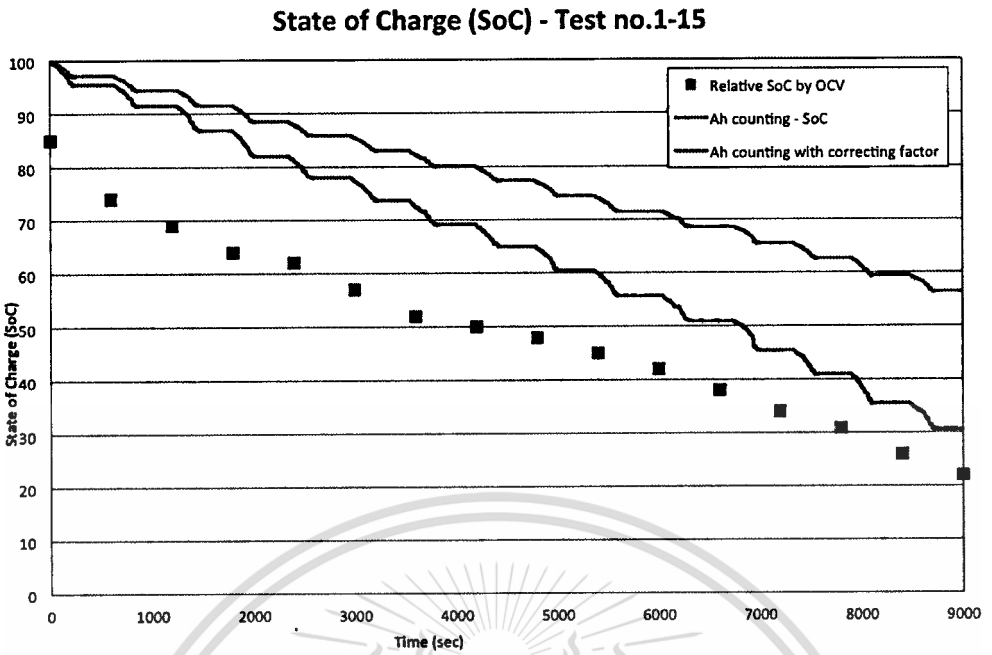

Figure 5.5 A comparison of state of charge estimation (VRLA battery).

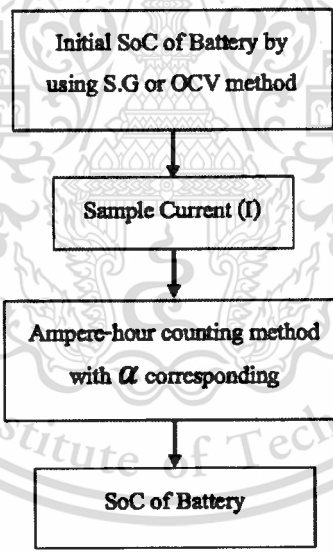

Figure 5.6 Flowchart to determine SoC of lead acid battery with correcting factor.

This material is reserved for educational use only, not allowed for commercial use.
Forbidden to modify the content, and cite the document when use.

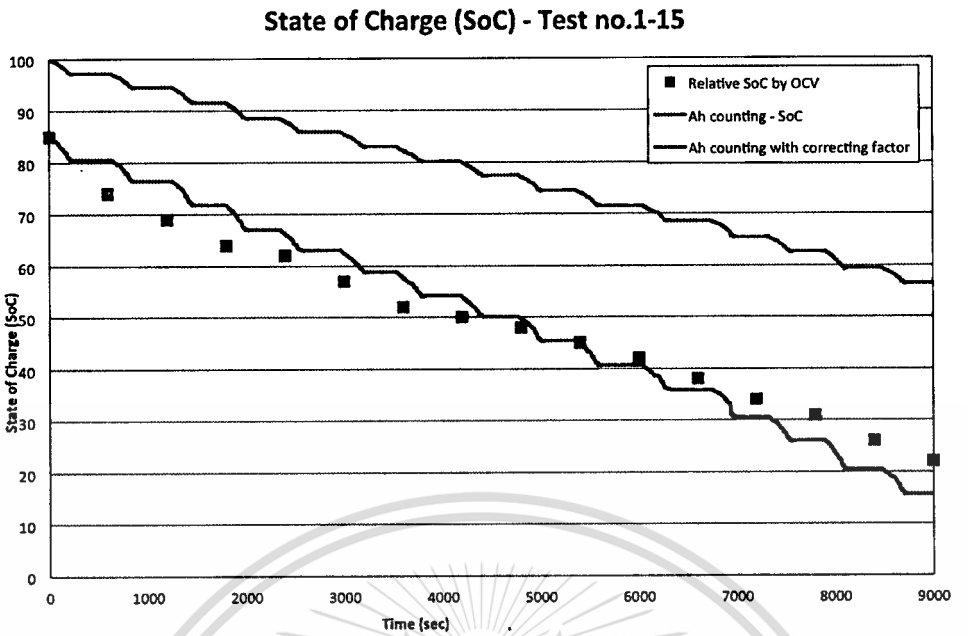

Figure 5.7 A comparison of state of charge estimation (VRLA battery).

An ampere-hour counting technique could not estimate the accurate SoC that was significantly affected by the fluctuation of the discharge rate. However, by using α corresponding factor, in which the discharge rate of electric bus prototype was concerned, the ampere-hour counting with correcting factor could estimate SoC of battery with a higher accuracy.

This material is reserved for educational use only, not allowed for commercial use.
Forbidden to modify the content, and cite the document when use.

CHAPTER 6
CONCLUSIONS AND SUGGESTIONS

6.1 Conclusions

This research focused on a practical estimation for the State of Charge (SoC) of battery in an electric vehicle. In an electric bus prototype, 78kW AC motor was used as driving system and the packs of lead-acid batteries were installed as the main power source. In this study, there were two types of lead-acid batteries i.e. flooded lead-acid battery GS BV-130, and valve regulated lead-acid (VRLA) battery Panasonic EC- FV1260. The novel approach of exploring the battery behavior in real driving conditions and investigating the practical SoC estimation techniques for electric bus were presented. First of all, the laboratory-scaled test was performed as preliminary experiment. Halogen Light Bulbs rated 12V, 50W were connected in parallel to be used as the constant current loads of battery. A hydrometer was used to measure the concentration of electrolyte in battery after battery being charged and during the discharge process. The results of the preliminary test would be used as a battery reference data (S.G, OCV, and α correcting factor) for estimation of a SoC in real driving condition. Next, in the real driving tests, the experiment was conducted by different drivers in many driving situations i.e. an acceleration test, load test, and the fixed distance on real traffic conditions. This research was also concentrated on the regenerative breaking system that could recover the kinetic energy back to energy storage. In the driving test, the current flow from battery was be measured and collected at every second and a factor α was introduced to improve the accuracy of ampere-hour counting method for the estimations of SoC.

Form the laboratory scale; it was observed that a constant discharge rate had a direct effect on the capacity of battery. On the other hand, the variety of discharge behaviors was obtained in real traffic conditions. High current was demanded when the vehicle was accelerating or climbing up slope, whereas relatively fewer amount of current was consumed during cruising. An ampere-hour counting method is the method that could be used to predict the remaining available run-time or driving range per charge of the vehicle. However, the main problems of ampere-hour counting technique are the unknown initial SoC and the error from rate of discharge effect. In this work, the S.G. and OCV was employed to identify an initial SoC and combined with an ampere-hour counting method using α corresponding. As a result, the more accurate SoC could be appropriately estimated. The main conclusions of this study can be summarized as followed:

This material is reserved for educational use only, not allowed for commercial use.
Forbidden to modify the content, and cite the document when use.

- At the same driving cycle, the remaining SoC of flooded lead-Acid battery - 130Ah was higher than VRLA battery. Nevertheless, the average consumption per lap of flooded lead-Acid battery was higher than that of VRLA battery.
- A regenerative braking mode offered better overall battery consumption than slippery mode (no regenerative braking) in real traffic conditions, and driving routes that include a lot of cornering. The percentage different of average capacity between regenerative braking mode and slippery mode is 37.9% for VRLA battery, and 36.49% for flooded lead-acid battery. On the other hand, the battery consumption of electric bus prototype in both cases was almost the same in straight route or constant speed.
- The driving style of driver was observed as one of the major effects to the battery consumption and maximum driving distance. Different drivers demanded different battery capacity output (VRLA), about 36.3% different between highest and lowest battery consumption for regenerative braking mode and 22.7% for slippery mode (34.4% and 14.8% for flooded lead-acid battery).
- By using mixed estimations "Ampere-hour Counting with correcting factor", the final SoC was estimated as 16%SoC while 22% could be acquired from the reference OCV technique. Thus, the results showed that the ampere-hour Counting with correcting factor led to an error of about 6% for SoC estimation, while 34.4% error was obtained by using general ampere-hour counting technique.

The findings revealed that by using the mixed estimations technique (Ampere-hour Counting with correcting factor), the result of battery estimation tended to get closer to the value of reference (S.G. measurement and OCV method) and was more practical to employ. Nevertheless, the research also showed that the battery type, traffic conditions or even the driver's driving style were the factors that could not be neglected in order to get more accurate results.

6.2 Suggestions

Although this current work was finished, it was only the first step of the study practical estimation for the State of Charge (SoC) of battery in electric vehicle by using Ampere-hour Counting with correcting factor. Below are some suggestions to this work in order to improve the result further as followed:

- In this study, only 2 types of lead-acid batteries were used as test samples. In order to ensure the mixed estimation technique, different types of batteries test is suggested to be considered.
- For increasing the accuracy of battery SoC estimation technique, the proximity of α

This material is reserved for educational use only, not allowed for commercial use.
Forbidden to modify the content, and cite the document when use.

corresponding factor and a grouping of discharge rate could be precisely defined.

- In practical of electric vehicle, the state of health of battery that has direct effect on the performance of batteries should be observed.

This material is reserved for educational use only, not allowed for commercial use.
Forbidden to modify the content, and cite the document when use.

REFERENCES

[1] V. Pop, H.J. Bergveld, D. Danilov, P.P.L Regtien, P.H.L Notton (2008), *Battery Management Systems, Accurate State-of-Charge Indication for Battery Powered Applications*, Philips Research Book Series, 9, ISBN: 978-1-4020-6944-4, Springer publishing.

[2] R.C. Bansal (2005), in A. Emadi (ed.) *Handbook of Automotive Power Electronics And Motor Drives.* London: Taylor & Francis Group.

[3] L.C. Rosario (2007), *Power and Energy Management of Multiple Energy Storage Systems in Electric Vehicles*, Department of Aerospace Power & Sensors, Cranfield University.

[4] M. Ehsani, Y. Gao, S. E. Gay, A. Emadi (2005) , *Modern Electric, Hybrid Electric, and Fuel Cell Vehicles*, CRC Press.

[5] J. Larminie J. Lowry (2003), *Electric Vehicle Technology Explained*, ISBN: 0-470-85163-5, John Wiley & Sons Ltd, England.

[6] M. Maskey, M. Parten, D. Vines, and T. Maxwell (1999), *An intelligent battery management system for electric and hybrid electric vehicles*, 49(2), pp. 1389–1391.

[7] A. Emadi, M. Ehsani, and J. M. Miller (2004), *Vehicular Electric Power Systems.* New York: Marcel Dekker.

[8] C.C. Han and K.T. Chau (2001), *Modern Electric Vehicle Technology.* England: oxford science publications

[9] Ng. Kong, M. Chin-Sien, C. Yi-Ping, H. Yao-Ching (2009), *Enhanced coulomb counting method for estimating state-of-charge and state-of-health of lithium-ion batteries*, Applied Energy, 86, pp. 1506-1511.

[10] S. Dhameja (2002), *Electric Vehicle Battery Systems*, ISBN: 0-7506-9916-7, Newnes.

[11] Jeevan Reddy N, 2011

[12] M. Ehsani, Y. Gao, S. E. Gay, A.Emadi (2005), *Modern electric, hybrid electric, and fuel cell vehicles: fundamentals, theory, and design.* London: CRC Press LLC

[13] G. Yonglang (2005) ,A sensor of sulfuric acid specific gravity for lead-acid batteries, Sensor and Actuator B 105, pp. 194-198.

[14] D. G. Vutetakis (2007) *Avionics: Elements, Software and Functions.* London: Taylor & Francis Group.

[15] I. Buchmann (2011), *What is the C-rate?* [Online]. Available at: http://www.batteryuniversity.com.

[16] A. Fasih (2006), *Modeling and Fault Diagnosis of Automotive Lead-Acid Batteries*, College of Engineering, The Ohio State University Columbus.

This material is reserved for educational use only, not allowed for commercial use.

Forbidden to modify the content, and cite the document when use.

REFERENCES (CONT.)

[17] CRC (2005) *Chapter9 Battery*. London: CRC Press LLC.

[18] W.He, N. Williard, C. Chen, M. Pecht (2012), *State of charge estimation for electric vehicle batteries using unscented kalman filtering.*

[19] S. Piller, M.Perrin, A. Jossen (2001), *Methods for state-of-charge determination and their applications*, J. Power Sources, 96, pp. 113-120.

[20] F. Codecà, S. M. Savaresi, and G. Rizzoni, "On battery State of Charge estimation: a new mixed algorithm", 17th IEEE International Conference on Control Applications, Part of 2008 IEEE Multi- conference on Systems and Control, San Antonio, Texas, USA, pp. 102-107, Sep. 2008.

[21] M. S. (Steve) Clark (2010), State of charge: Specific gravity vs. battery charging current, *Battcon 2010 Conference, Hollywood,* FL.

[22] G. Plett (2004), *Extended Kalman filtering for battery management systems of LiPB-based HEV battery packs. Part 1.* Background, J. Power Source. 134 (2), pp. 252–261.

[23] B. BS, P. Bently, DA Stone, CM Bingham (2005), *Nonlinear observers for predicting State of Charge and State of Health of lead-acid batteries for Hybrid-Electric Vehicles*, IEEE Trans Vehicular Technology, Vol. 54.

[24] H. A. Kiehne (2000), *Battery Technology Handbook*, 2nd Edition, ISBN: 0-8247-4249-4, Expert Verlag, Renningen-Malsheim, Germany.

[25] GS BV-130Z, Lead-Acid Battery datasheet.

[26] R. Kalman (1960), *A new approach to linear filtering and prediction problems*, Transactions of the ASME— Journal of Basic Engineering, vol. 82 (Series D), pp. 35–45.

This material is reserved for educational use only, not allowed for commercial use.
Forbidden to modify the content, and cite the document when use.

APPENDIX A

DATA ACQUISITION SPECIFICATIONS

- UNIVERSAL ANALOG INPUT MODULE –NI 9219
- PORTABLE BUS-POWERED USB CARRIER FOR NI C SERIES I/O MODULES
- AC/DC CURRENT TRANSDUCER DRH100-C10

King Mongkut's Institute of Technology Ladkrabang

This material is reserved for educational use only, not allowed for commercial use.
Forbidden to modify the content, and cite the document when use.

NI 9219

4-Channel, 24-Bit, Universal Analog Input Module

Français Deutsch 日本語 한국어 简体中文

ni.com/manuals

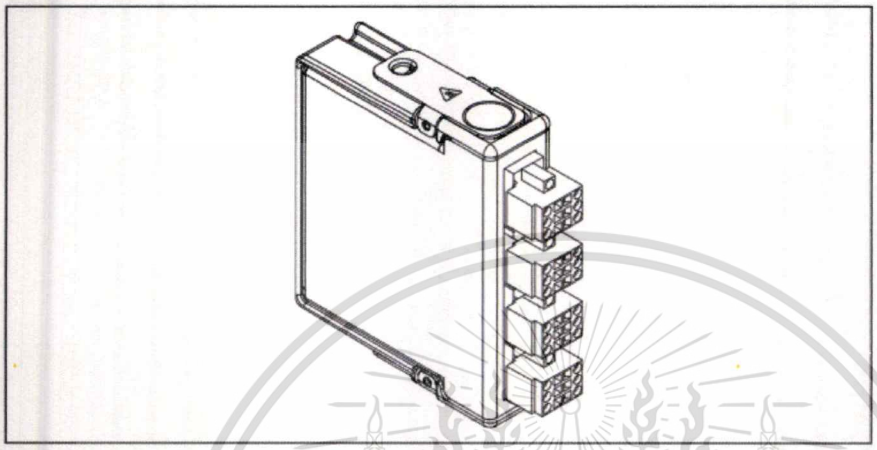

Mode input ranges

Mode	Nominal Range(s)	Actual Range(s)
Voltage	±60 V, ±15 V, ±4 V, ±1 V, ±125 mV	±60 V, ±15 V, ±4 V, ±1 V, ±125 mV
Current	±25 mA	±25 mA
4-Wire and 2-Wire Resistance	10 kΩ, 1 kΩ	10.5 kΩ, 1.05 kΩ
Thermocouple	±125 mV	±125 mV
4-Wire and 3-Wire RTD	Pt 1000, Pt 100	5.05 kΩ, 505 Ω
Quarter-Bridge	350 Ω, 120 Ω	390 Ω, 150 Ω
Half-Bridge	±500 mV/V	±500 mV/V
Full-Bridge	±62.5 mV/V, ±7.8 mV/V	±62.5 mV/V, ±7.8125 mV/V
Digital In	—	0–60 V
Open Contact	—	1.05 kΩ

This material is reserved for educational use only, not allowed for commercial use.
Forbidden to modify the content, and cite the document when use.

Mode, Range	Gain Error (Percent of Reading)	Offset Error (ppm of Range)
	Typ (25 °C, ±5 °C), Max (–40 to 70 °C)	
Half-Bridge, ±500 mV/V	±0.03, ±0.07	±300, ±450
Full-Bridge, ±62.5 mV/V	±0.03, ±0.08	±300, ±1000
Full-Bridge, ±7.8 mV/V	±0.03, ±0.08	±2200, ±8000
* 2-Wire Resistance mode accuracy depends on the lead wire resistance. This table assumes 0 Ω of lead wire resistance.		

Cold-junction compensation
sensor accuracy.....±1°C typ

This material is reserved for educational use only, not allowed for commercial use.
Forbidden to modify the content, and cite the document when use.

NI USB-9162

Portable Bus-Powered USB Carrier for NI C Series I/O Modules

This user guide describes how to use the National Instruments USB-9162 and lists specifications.

Figure 1. NI USB-9162 and C Series I/O Module

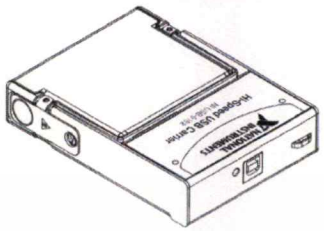

Specifications

The following specifications are typical for the range 0 to 60 °C unless otherwise noted.

Power Requirements

Caution The protection provided by the NI USB-9162 carrier can be impaired if it is used in a manner not described in this document.

Current consumption from USB ..... 500 mA, max

Suspend mode ..... 2.5 mA, max

Bus Interface

USB specification ..... USB 2.0 Hi-Speed

Physical Characteristics

Weight ..... 101 g (3.5 oz)

Dimensions ..... 114.6 mm × 85.7 mm × 25.1 mm
(4.51 in. × 3.37 in. × 0.99 in.)

If you need to clean the module, wipe it with a dry towel.

Safety Voltages

Connect only voltages that are within these limits.

Isolation

Channel-to-channel

Continuous ..... 250 VAC, Measurement Category II

Withstand ..... 1500 VAC, verified by a 5 s dielectric withstand test

Channel-to-earth ground

Continuous ..... 250 VAC, Measurement Category II

Withstand ..... 3000 VAC, verified by a 5 s dielectric withstand test

Measurement Category II is for measurements performed on circuits directly connected to the electrical distribution system. This category refers to local-level electrical distribution, such as that provided by a standard wall outlet, for example, 115 V for U.S. or 230 V for Europe. Do *not* connect the NI USB-9162 to signals or use for measurements within Measurement Categories III or IV.

This material is reserved for educational use only, not allowed for commercial use.
Forbidden to modify the content, and cite the document when use.

AC/DC Current Transducer DHR-C10

I_{PN} = 100 .. 1000 A

The transducer for the electronic measurement of DC & distorted AC waveform currents, with galvanic isolation between the primary circuit (power) and the secondary circuit (measurement). True RMS 0-10V voltage output.

Electrical data

Primary Nominal DC & AC Current I_{PN} (A.t.RMS)	Primary AC Current Max. Peak Value [1] I_P (A)	Output voltage (Analog) V_{OUT} (VDC)	Type
100	600	0-10	**DHR 100 C10**
200	600	0-10	**DHR 200 C10**
300	1000	0-10	**DHR 300 C10**
400	1000	0-10	**DHR 400 C10**
500 [2]	1800	0-10	**DHR 500 C10**
600 [2]	1800	0-10	**DHR 600 C10**
1000 [2]	1800	0-10	**DHR 1000 C10**

R_L	Load resistance	≥ 10	kΩ
V_C	Supply voltage	+ 20 .. 50	V DC
I_C	Current consumption	30	mA
V_{SL}	Output voltage limitation (0 - 10 V)	< 14	V
I_P	Overload capability (Ampere Turns)	30000	A.t

Performance data

X	Accuracy @ I_{PN}, T_A = 25°C (excluding offset)	< ± 1	% of I_{PN}
ε_L	Linearity error (1% of I_{PN} .. ± I_{PN})	< ± 1.0	% of I_{PN}
V_{OE}	Electrical offset voltage, T_A = 25°C	< ± 1.0	% of I_{PN}
TCV_{OE}	Temperature coefficient of V_{OE} (0..+60 °C)	± 2.0	mV/K
	(-40..+70 °C)	± 4.0	mV/K
TCV_{OUT}	Temperature coefficient of V_{OUT} (% of reading)	± 0.1	%/K
t_r	Response time to 90 % of I_{PN} step	< 150	ms
BW	Frequency bandwidth (± 1 dB)	DC 20..6000	Hz

General data

T_A	Surrounding operating temperature	- 40 .. + 70	°C
T_S	Surrounding storage temperature	- 40 .. + 85	°C
m	Mass	260	g
IPxx	Protection degree	IP20	

Notes : [1] The Max. Peak AC Current is the highest peak level of the primary signal that is taken into account for accurate True RMS calculation. Yet the device is designed for maximum continuous True RMS value equal to I_{PN}, whereas the output is limited by the above specified output limitation.

[2] According to the UL 508 Standard for Safety for Industrial Control Equipment the primary current must not exceed 475 A.t.RMS through the transducer hole.

Features

- VFD and SCR waveforms current measurement
- True RMS output
- Panel mounting
- Eliminates insertion loss
- Isolated plastic case recognized according to UL94-V0

Advantages

- Large aperture for cable up to Ø32mm
- High isolation between primary and secondary circuits
- Easy installation

Applications

- ***VFD Controlled Loads***
  VFD output indicates how the motor and attached load are operating.
- ***SCR Controlled Loads***
  Acurate measurement of phase angle fired or burst fired (time proportioned) SCRs. Current measurement gives faster response than temperature measurement.
- ***Switching Power Supplies and Electronic Ballasts***
  True RMS sensing is the most accurate way to measure power supply or ballast input power.

Application domain

- Energy and Automation

This material is reserved for educational use only, not allowed for commercial use.
Forbidden to modify the content, and cite the document when use.

Current Transducer DHR-C10

Isolation characteristics

V_b	Rated isolation voltage rms [3]	300	V
	according to the standard IEC 61010-1 and with the following conditions:		
	- Reinforced isolation		
	- Over voltage category CAT III		
	- Pollution degree PD2		
	- Heterogeneous field		
V_d	Rms voltage for AC isolation test [4], 50 Hz, 1min	4.0	kV
V_w	Impulse withstand voltage [4], 1.2/50 uS	7.3	kV
dCp	Creepage distance	7.2	mm
dCl	Clearance distance	7.2	mm
CTI	Comparative tracking index (Group I)	> 600	

Notes :[3] Between primary conductor voltage and ground. The voltage category could be improved according to the insulation characteristic given by the cable manufacturer. The UL 508 Standard for Safety for Industrial Control Equipment requires that only insulated conductors are used as primary circuit with this transducer.

[4] Between primary (completely filling the aperture) and secondary.

Transfer characteristics

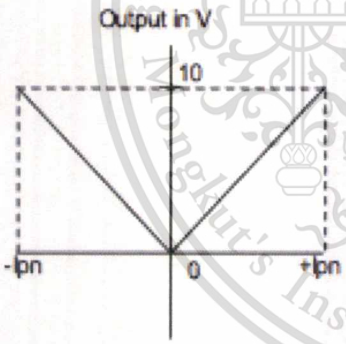

This material is reserved for educational use only, not allowed for commercial use.
Forbidden to modify the content, and cite the document when use.

APPENDIX B

PROCEEDINGS

- **Appendix B-1:** Battery Behavior of Electric Bus at Different Discharge Rate in Real Driving Condition
- **Appendix B-2:** Progressive State of Charge Estimation for Electric Bus
- **Appendix B-3:** Correcting Factor on State of Charge Estimation for Lead-Acid Batteries

This material is reserved for educational use only, not allowed for commercial use.
Forbidden to modify the content, and cite the document when use.

Appendix B-1: Battery Behavior of Electric Bus at Different Discharge Rate in Real Driving Condition

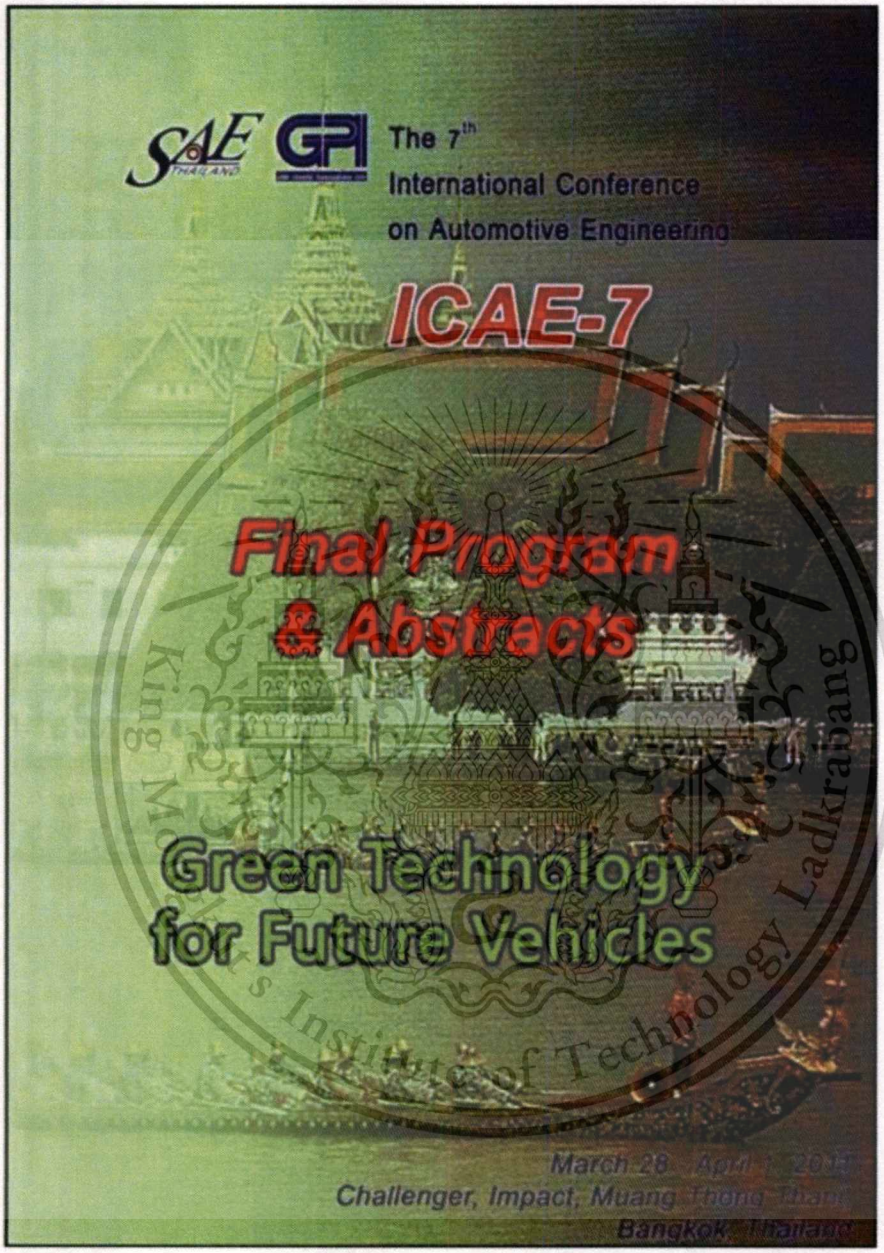

This material is reserved for educational use only, not allowed for commercial use.
Forbidden to modify the content, and cite the document when use.

The 7th International Conference on Automotive Engineering (ICAE-7)
March 28 – April 1, 2011, Challenger, Impact, Muang Thong Thani, Bangkok, Thailand

Battery Behavior of Electric Bus at Different Discharge Rate in Real Driving Condition

Nathapol Taweewong
Automotive Engineering, King Mongkut's Institute of Technology Ladkrabang (KMITL), Thailand

Chi-na Benyajati, Piyapong Premvaranon
Automotive Laboratory, National Metal and Materials Technology Center (MTEC), Thailand

Chinda Charoenphonphanich
Faculty of Engineering, King Mongkut's Institute of Technology Ladkrabang (KMITL), Thailand

Masaki Yamakita
Department of Mechanical and Control Engineering, Tokyo Institute of Technology, Japan

ABSTRACT

In order to use electric vehicles (EVs) and get the most efficiency out of it, the information about the battery status is important for drivers. The aim of this paper is to present battery behavior in an electric bus and the change of battery capacity in real driving conditions. Moreover, it is of significant importance to improve the existing battery monitoring system of electric vehicles. As a battery monitoring system is a major part in electric vehicles in similar way a fuel gauge is in internal combustion engine vehicles, a high-accuracy State of Charge (SoC) monitor is needed. The change of battery capacity under different discharge rates and available battery percentage were studied as a reference in a battery monitoring system.

INTRODUCTION

Because of recent global warming phenomena and petroleum price crisis, there has been a clear sign that majority of next generation vehicles will be powered by electricity. History of electric vehicles (EVs) development dated back to 1834 [1]. Due to the improvements of the performance of internal combustion engine vehicles and lack of technology about battery and electric motor in electric vehicles, the interest in electric vehicles was reduced and temporarily ended in early 20th century. However, as petroleum price was increasing and environmental problems were more evident in late 20th century, the electric vehicles have become popular again. In 2008, the automotive laboratory of National Metal and Materials Technology Center (MTEC) has started the EVs project with the goal of developing a medium-size bus prototype that can be produced in Thailand.

In internal combustion engine vehicles, a fuel gauge is an important part for displaying the remaining fuel in the fuel tank of vehicle. Similar to electric vehicles, it is necessary to know the amount of remaining charges in battery in order to know how far the vehicle can still travel and to preserve the overall battery life. Thus, the importance of a battery monitoring system to electric vehicles is in the same way of how a fuel gauge is important to internal combustion vehicles.

This paper presents a battery behavior in an electric bus and the change of battery capacity in real driving conditions. The battery discharge test was carried out in many driving conditions such as designed routes, real traffic conditions. The battery data such as the battery voltage, battery charge and discharge current, battery temperature, and motor revolution were measured using data acquisition tools.

BACKGROUND OF BATTERY

Nowadays, electric devices have become a major part of our life. All portable electric devices use battery as electricity storage for operation. The first battery was invented in 1800. There have been many researches and developments about performance and abilities of battery over 200 years. In the most basic terms, a battery is an electrochemical cell in which an electric potential (voltage) is generated at the battery terminals by a difference in potential between the positive and negative electrodes [2]. Today, there are many various types and sizes of batteries such

This material is reserved for educational use only, not allowed for commercial use.
Forbidden to modify the content, and cite the document when use.

as; Lead-acid batteries (Pb-acid), Nickel-based batteries, Sodium-based batteries, and more recently, Lithium batteries. The different types of battery depended on different applications. There are some requirements for electric vehicles batteries such as; specific power, specific energy, efficiency, cost, maintenance, safety, and environmental friendly. Lead-acid battery is the most popular type of battery for over century. It is also the cheapest battery per kilo-watt-hour of charge widely used for storage in applications such as; SLI (starting, lighting, ignition), UPS (uninterruptible power supply), and stationary applications. However, lead-acid battery has low specific power compared to other types of batteries. Lithium-ion battery is the most commonly used in portable device, with the highest specific power, but it is very expensive and still has a problem about safety of battery during charge/discharge. Unfortunately, only few types of commercial battery are appropriate for use in electric vehicles. At the present, those types are lead acid, nickel iron, nickel cadmium, nickel metal hydride, lithium polymer and lithium ion, sodium sulphur and sodium metal chloride [3].

BATTERY PARAMETER

Electrochemical reaction

Batteries are electrochemical devices that convert electrical energy into potential chemical energy during charging, and convert chemical energy into electric energy during discharging [4]. Overall reaction of Lead-acid can be generally expressed by

$$PbO_2 + Pb + 2H_2SO_4 \rightleftharpoons 2PbSO_4 + H_2O \quad (1)$$

In the discharge of a lead-acid battery, the lead dioxide and lead react with the sulfuric acid in the electrolyte to form the lead sulfate on the positive and negative plates, respectively. During charge process, the sulfuric acid revert back into the solution state again as shown in Figure.1 [3, 6]

Battery Capacity

By electrochemical reaction, batteries store and produce the electric energy during charging and discharging. The amount of charge of battery is normally presented in term of amp-hours (Ah), defined as the integral product of current (Amperes) and time (hours), as expressed below:

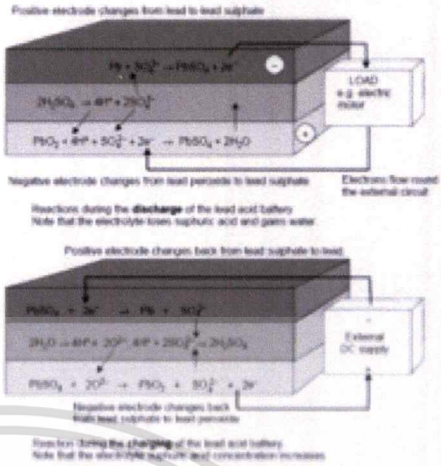

Figure.1 Electrochemical reactions during the charge and discharge of the lead acid battery

$$Ah = \int_0^t I(t)dt \quad (2)$$

The battery industry conventionally uses C-rate to scale the charge and discharge current of a battery [5]. For example, 10Ah battery can generate 1A for 10 hours (0.1C), or 5A for 2 hours (0.5C), or in theory 10A for 1 hour (1C). Battery manufacturers usually specify the battery with coulometric capacity (amp-hours), which is defined as the number of amp-hours gained when discharging the battery from a fully charged state [6].

BATTERY STATE OF CHARGE

All modern electronic devices that use battery as a main power source require battery status to display battery capacity or remaining run-time information. In electric vehicles, battery statuses, such as the battery remaining capacity, remaining run-time, and range, are also important for drivers. Normally, in electric vehicles, the remaining capacity of battery is displayed as SoC. Technically, a unique definition for SoC does not exist. Accordingly, SoC can be defined as the percentage of the maximum possible charge that is present inside a rechargeable battery [7]. By using Ampere counting, SoC of battery can be expressed as:

$$SoC(t) = SoC(0) - \frac{1}{Ah_{nom}} \int_0^t I(t)dt \quad (3)$$

Where: SoC(0) is initial SoC value;
Ah_{nom} is the nominal battery capacity;
I(t) is the measured current.

This material is reserved for educational use only, not allowed for commercial use.
Forbidden to modify the content, and cite the document when use.

The 7th International Conference on Automotive Engineering (ICAE-7)
March 28 – April 1, 2011, Challenger, Impact, Muang Thong Thani, Bangkok, Thailand

In Lead-Acid battery, the relationship between sulfuric acid's specific gravity and SoC is almost linear. Thus, it can be used to indicate the remaining charge in the battery. Normally, hydrometer is manually used to measure the electrolyte concentration in lead-acid battery.

RESEARCH EXPERIMENT

The experiments were divided in to 2 main parts. First, the preliminary experiment was performed in a laboratory. The result data would be used as a battery reference data. For the other part, the battery was tested to monitor its behavior in real traffic conditions. The overall research diagram is shown in Figure. 2

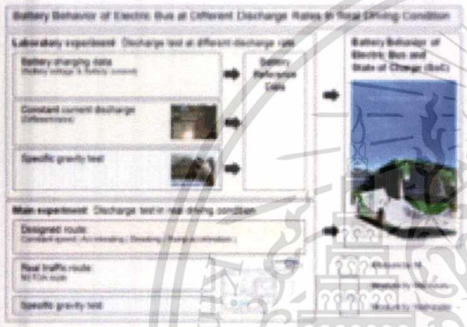

Figure.2 The overall diagram of research

PRELIMINARY EXPERIMENT

The set up of laboratory-scaled experiment is shown in Figure.3. In order to conveniently calculate the percentage of the maximum possible charge that was presented inside a rechargeable battery, the constant current discharge was used as loads of battery. 40 units of Halogen Light Bulb rated 12V, 50W were connected in parallel to achieve a maximum discharge current of 132A.The test samples were GS BV-130 12V lead acid battery which are the same as those used on MTEC bus. A constant voltage charger was used to charge the batteries. A hydrometer was used to measure the concentration of electrolyte in battery after battery being charged and during discharge process. However, a direct measurement could not be done in a high current discharge rate test. Therefore, the LEM DHR100-C10 current transformer was needed to measure the current flow. The K-type thermocouple was used in measuring battery temperature. Two units of digital meter were used for displaying battery voltage and current flow. The data acquisition hardware by National Instrument (NI 9219) was used to measured battery data. Signal Express by National Instruments was used as software for monitoring and collect the battery data. This methodology can be further specified into following aspects:

1. Validate battery consumption behavior using discharge test.
2. Use Hydrometer for measuring specific gravity of battery.
3. Use data acquisition hardware to collect battery referent data.
4. Vary the discharge rate by controlling the load.

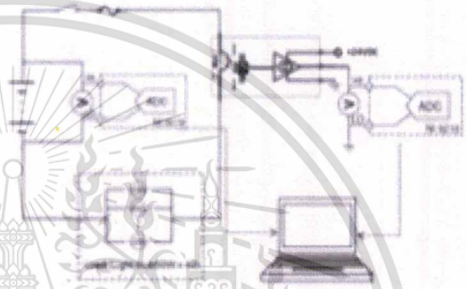

Figure. 3 Schematic diagram of laboratory-scaled experiment

MAIN EXPERIMENT

In main experiment, a test drive on MTEC electric bus prototype was carried out in controlled driving conditions. In this bus, 24 units of 12V, 130Ah lead acid batteries were used as power source for AC drive motor (maximum rated power 90kW) and the other 24 units of batteries were used for other electrical devices in the bus. The AC invertors needs high voltage for operate. Therefore, batteries were connected in series to achieve nominal 288V DC source and 130Ah. The data acquisition tools was used to collect battery discharging data such as battery voltage, battery current, battery temperature, motor revolution, and torque, as shown in Figure.4.

EXPERIMENTAL RESULT AND DISCUSSION

In Figure.5, the result of preliminary experiment is shown. The graph shows the discharge characteristics of battery under constant discharge current. Two different discharge current of 13A (0.1C) and 26A (0.2C) was studied.

This material is reserved for educational use only, not allowed for commercial use.
Forbidden to modify the content, and cite the document when use.

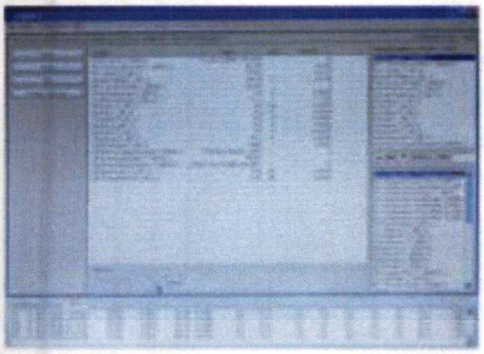

Figure.4 The battery data of electric bus by data acquisition tools

At the maximum capacity, corresponding specific gravity (SG) at the battery voltage of 12.3V was measured to be 1.25. After discharged at 0.1C for 8 hours, the voltage and specific gravity were continuously decreasing to 6.8V and 1.05 respectively.

This experimental result indicated a capacity consumption of 95Ah. However, according to battery specification, a theoretical capacity consumption of 104Ah was expected for 80% depth of discharge. The SG was measured every half an hour and the observed relationship between specific gravity versus time under different discharge rate is shown in Figure.6.

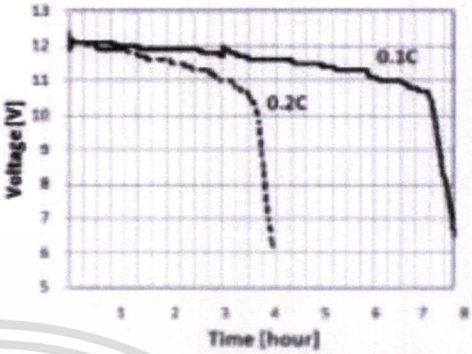

Figure.5 Discharge characteristic of battery

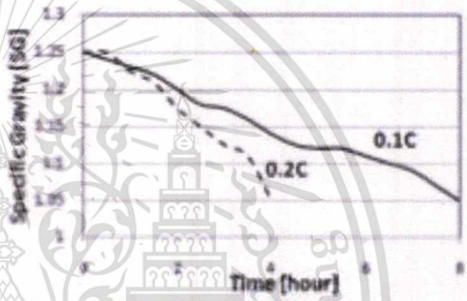

Figure.6 The change of specific gravity

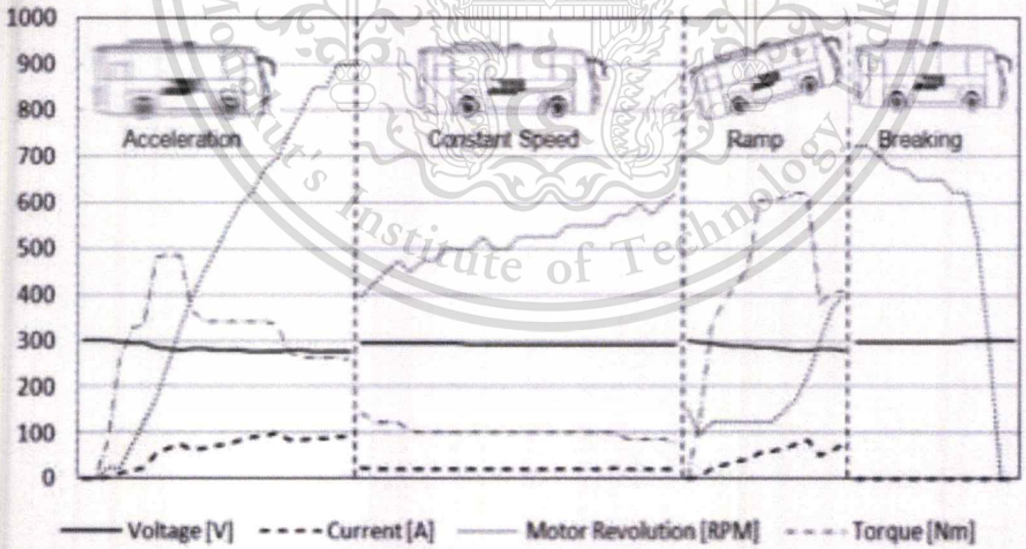

Figure.7 Motor characteristics of electric bus at various driving conditions

This material is reserved for educational use only, not allowed for commercial use.
Forbidden to modify the content, and cite the document when use.

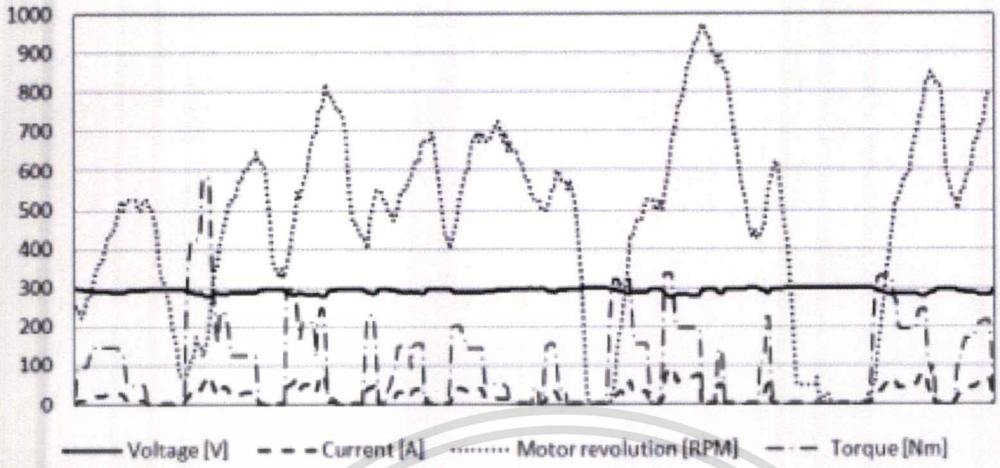

Figure.8 Electric vehicle characteristic in real traffic condition

The motor parameters obtained from MTEC Electric bus prototype during initial test drive are shown in Figure.7. The parameters of interest were the change of battery voltage, battery current, motor revolution, and torque. During acceleration test, high current was flowing out from battery. The battery voltage dramatically decreased while the motor revolution and torque were continuously increasing. At constant speed, all parameters were almost constant. During accelerating up the slope, high torque was needed for this condition. As a result, high current was flowing out to create torque for motor while motor revolution was slightly increasing. In breaking condition, there was no significant change in battery voltage without current flowing from battery while torque was zero. The motor revolution was sharply decreased to zero then the bus stopped. Nonetheless, a regenerative braking function was not employed in the present work. The parameters obtained from real traffic condition are shown in Figure. 8. All parameters varied depending on the driving situations. In real traffic condition test, the average speed was 14km/hr, the energy consumption was about 1.4 Ah/km. From this information, a maximum range could be determined to be 70 km/charge.

The results from laboratory-scaled showed that the discharge rate would directly affect the capacity of battery. Furthermore, variation of discharge rates observed during the test drive (Figure.8) would suggest that predicting the remaining available run-time of the vehicle might not be that straight forward. In addition, there were some discrepancies in the battery capacity consumption between that of theoretical specification and that observed during the lab-scaled tests. This could be due to the variation in the setups between different discharge tests. Therefore, the necessity in carrying out individual battery capacity study was obvious in order to develop a potent SoC monitoring system for any EVs applications.

In future work, the test results obtained from current work would be used to estimate the SoC monitoring systems of electric bus. There are currently many proposed techniques to estimate the SoC of battery. In general, the Coulomb counting is the closest concept idea for determining battery SoC. However, the main problem of coulomb counting technique is an initial SoC and a battery life. Since the SG is relatively easy to measure in a lead-acid battery, the correlation between SG data and SoC will be the key for accuracy of Battery Monitoring System of lead-acid battery.

CONCLUSIONS

In conclusion, the results of preliminary experiments are presented including the characteristics of lead-acid battery in many discharge conditions, both in laboratory and in actual driving test. In laboratory scale, the remaining capacity of battery could be easily calculated by counting the current flow over time coupled with a specific gravity measurement of battery electrolyte. It was observed that a discharge rate had a direct effect on the capacity of battery. However, real traffic conditions resulted in variety of discharge behaviors. High current was needed when the vehicle was accelerating and

This material is reserved for educational use only, not allowed for commercial use.
Forbidden to modify the content, and cite the document when use.

climbing up slope whereas relatively small current was consumed during cruise. As a result, the estimation of remaining battery capacity and vehicle remaining run-time becomes more complicated. Therefore, an in-depth knowledge about battery capacity becomes very crucial for accurate SoC estimation.

ACKNOWLEDGMENTS

The author wishes to express his gratitude to his advisors also wishes to thank all at the Automotive Laboratory, National Metal and Materials Technology Center (MTEC), for their support and recommendations.

REFERENCES

1. Leon C Rosario, *Power and Energy Management of Multiple Energy Storage Systems in Electric Vehicles*, Department of Aerospace Power & Sensors, Cranfield University,2007.
2. S. Dhameja, *Electric Vehicle Battery Systems*, Newnes, 2002.
3. J. Larminie J. Lowry, *Electric Vehicle Technology Explained*, John Wiley & Sons Ltd, 2003.
4. M. Ehsani, Y. Gao, S. E. Gay, A. Emadi, Modern *Electric, Hybrid Electric, and Fuel Cell Vehicles*, CRC Press, 2005.
5. I. Buchmann, *What is the C-rate?*, http://www.batteryuniversity.com, 2011.
6. G. Yonglang, *A sensor of sulfuric acid specific gravity for lead-acid batteries*, Sensor and Actuator B 105, pp. 194-198, 2005.
7. V. Pop, H.J. Bergveld, D. Danilov, P.P.L Regtien, P.H.L Notton, *Battery Management Systems, Accurate State-of-Charge Indication for Battery Powered Applications*, Philips Research Book Series, 9, Springer publishing, 2008.

CONTACT

Mr. Nathapol Taweewong
Automotive Engineering, King Mongkut's Institute of Technology Ladkrabang (KMITL), Thailand. Email: goblin30@hotmail.com.

This material is reserved for educational use only, not allowed for commercial use.
Forbidden to modify the content, and cite the document when use.

Appendix B-2: Progressive State of Charge Estimation for Electric Bus

This material is reserved for educational use only, not allowed for commercial use.
Forbidden to modify the content, and cite the document when use.

ETM 24
The Second TSME International Conference on Mechanical Engineering
19-21 October, 2011, Krabi

Progressive State of Charge Estimation for Electric Bus

Nathapol Taweewong[1*], Chi-na Benyajati[2], Piyapong Premvaranon[2], Chinda Charoenphonphanich[3] and Masaki Yamakita[4]

[1] Automotive Engineering, International College, King Mongkut's Institute of Technology Ladkrabang, Bangkok, Thailand 10520
[2] Automotive Laboratory, National Metal and Materials Technology, Pathumthani Thailand 12120
[3] Department of Mechanical Engineering, King Mongkut's Institute of Technology Ladkrabang, Bangkok, Thailand 10520
[4] Department of Mechanical and Control Engineering, Tokyo Institute of Technology, Japan
* Corresponding Author: E-mail: gotdin30@hotmail.com, Tel: 089 991 1798

Abstract

In order to use electric vehicles (EVs) and get the most efficiency out of it, the information about the battery status is significant for drivers. As a battery monitoring system is a major part in electric vehicles, a high-accuracy State of Charge (SoC) monitor is needed. The aim of this paper is to present the progressive State of Charge estimation for deep cycle lead-acid batteries powering an electric bus prototype.

In this study, the SoC of battery was estimated by means of a discharge test and a specific gravity test. An ampere-hour counting method was used in a discharge test. While this method could provide an accurate physical remaining capacity of battery, it was inconvenient in real automotive application and can only be used with flood-type lead acid battery. Alternatively, the Kalman Filter method was also considered in this study in an attempt to improve the current battery SoC estimation technique. The results of proposed study can be used initially in an electric bus prototype and can be used as a guideline for development of other electric vehicle projects in Thailand.

Key words: State of Charge, Lead-Acid Battery, Ampere-hour counting.

1. Introduction

Nowadays, electric devices have become a major part of our life. All portable electric devices use battery as electricity storage for operation. In the most basic terms, a battery is an electrochemical cell in which an electric potential (voltage) is generated at the battery terminals by a difference in potential between the positive and negative electrodes [1]. Today, there are many various types and sizes of batteries such as; Lead-acid batteries, Nickel-based batteries, Sodium-based batteries, and more recently, Lithium batteries.

Because of recent global warming phenomena and petroleum price crisis, there has been a clear sign that majority of next generation vehicles will be powered by electricity. History of electric vehicles (EVs) development dated back to 1834 [2]. In internal combustion engine vehicles, a fuel gauge is an important part for displaying the remaining fuel in the fuel tank of vehicle. Similar to electric vehicles, it is necessary to know the amount of remaining charges in battery

This material is reserved for educational use only, not allowed for commercial use.
Forbidden to modify the content, and cite the document when use.

ETM 24
The Second TSME International Conference on Mechanical Engineering
19-21 October, 2011, Krabi

in order to know how far the vehicle can still travel and to preserve the overall battery life. Thus, the importance of a battery monitoring system to electric vehicles is in the same way of how a fuel gauge is important to internal combustion vehicles.

In this paper, an ampere-hour counting method was used in a discharge test to estimate SoC of tested batteries. An initial study of Kalman Filter method for lead acid battery is presented. In section 2, some existing battery SoC estimation techniques are reviewed. The implementation of discharge test, the calculations for battery initial parameters for SoC estimation in Kalman Filter method are presented in section 3. During all the experiment, data acquisition tools were used to collect various battery-discharging data such as battery voltage, battery current, and battery temperature.

2. State of Charge Estimation Techniques

Technically, a unique State of Charge (SoC) definition does not exist. Accordingly, The SoC is defined as the percentage of the maximum possible charge that is present inside a rechargeable battery [3]. The determination of the SoC of a battery may be a problem of more or less complexity depending on the battery type and on the application in which the battery is used, as reviewed by Piller *et al* [4].

2.1 Specific Gravity

Batteries are electrochemical devices that convert electrical energy into potential chemical energy during charging, and convert chemical energy into electric energy during discharging [5]. When considering flooded lead-acid cells, the specific gravity (S.G.) of the electrolyte is known to be a good measure of SoC [6]. In [7], the individual cell open circuit voltage (OCV) is measured and the S.G. is calculated using the following equation:

$$OCV = S.G. + 0.845 \quad (1)$$

The S.G. measurement with the use of a hydrometer is a simple and easy way, with a high accuracy, to indicate SoC. However, it is impossible to measure the specific gravity of each battery cells during driving period and can be used only in a flooded lead-acid type.

2.2 Open Circuit Voltage

The open circuit voltage (OCV) of battery varies almost linearly to the battery SoC. For flooded lead-acid battery, the OCV can be determined from S.G. as shown in previous section. However, a direct measurement of OCV cannot be operated under loading condition. Especially in valve-regulated lead-acid (VRLA) batteries, considerable amount of times, such as several hours, are needed to reach a steady state after loading [4].

2.3 Ampere-hour Counting

Ampere-hour counting or Coulomb counting is a method to measure a delivered current during charge or discharge. The SoC of battery can be estimate as:

$$SoC(t) = SoC(0) - \frac{1}{Ah_{nom}} \int_0^t I(t)dt \quad (2)$$

Where: SoC (0) is initial SoC value;

Ah_{nom} is the nominal battery capacity;

I(t) is the measured current.

However, this technique could present only a change in battery capacity. Lack of knowledge of initial value of SoC and an accumulated error results in a limited accuracy of the estimation.

2.4 Kalman Filter Method

Kalman filter theory was introduced in 1960 [8]. Kalman Filters are an optimal-means for estimating a present value of the time-varying "state" of a dynamic system [9].

This material is reserved for educational use only, not allowed for commercial use.
Forbidden to modify the content, and cite the document when use.

ETM 24
The Second TSME International Conference on Mechanical Engineering
19-21 October, 2011, Krabi

2.4.1 Battery Model

To use Kalman Filter techniques to estimate battery SOC, a mathematical state-space model of the cell is needed. A dynamic model of lead-acid battery that was necessary for Kalman Filter technique to predict the SoC is shown in "Fig.2" [6]. The battery model is consisted of two capacitors and three resistors; C_{bulk} (bulk capacitor), $C_{surface}$ (surface capacitor), R_t (terminal resistance), R_s (surface resistance), and R_e (end resistance). The V_{Cb} and V_{Cs}, are voltage across the bulk capacity and surface capacitors respectively. The SoC can then be determined from the voltage present across the bulk capacitor (V_{Cb}).

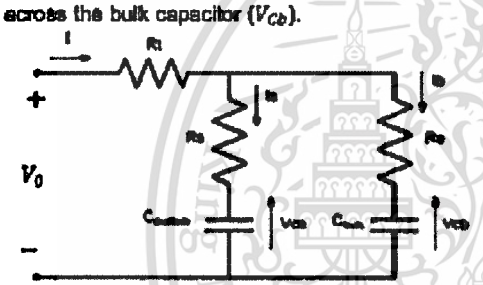

Fig. 2 RC Battery Model schematic [6]

From RC battery model schematic "Fig. 2", the characteristics equation of voltages and currents can be express as:

$$V_0 = IR_t + I_bR_e + V_{Cb} \quad (5)$$

$$V_0 = IR_t + I_sR_s + V_{Cs} \quad (6)$$

After some algebraic manipulation and Kirchoff's laws application, the complete state variables of the model were presented in [6]. The determinations of initial parameters in battery model in this study are presented in section 3.1.

3. Implementations

The test samples were 12 V lead-acid batteries with 130Ah capacity. In order to conveniently calculate the percentage of the maximum possible charge that was presented inside a rechargeable battery, the constant current discharge was used as battery loads. Three different rates of discharge were employed i.e. C_{20}, C_5 and C_3, among which the second rate is a common discharge rate for electric vehicles [10]. The data acquisition hardware by National Instrument (NI 9219) was used to measure battery data. Signal Express by National Instruments was used as a tool for monitoring and collect the battery data. However, a direct measurement could not be done in a high current discharge rate test. Therefore, the LEM DHR100-C10 current transformer was needed to measure the current flow. The Schematic diagram of the experiment is shown in "Fig. 3". A hydrometer was used to measure the concentration of electrolyte in battery during discharge process. The S.G. was measured every half an hour during the tests.

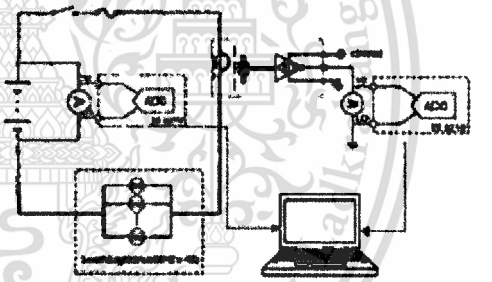

Fig. 3 Schematic diagram of the experiment

Furthermore, by using Ampere-hour counting method, a true SoC was directly obtained. The discharge test was started at fully charged condition where the SoC was considered to be 100%. The battery was discharged until the cut off voltage as presented in the battery datasheet [11] was reached. The discharge current pulses of C_5 were applied for 1800 s at 3600-s intervals. Nevertheless, in an actual electric bus prototype, batteries were connected in series to achieve a nominal 288V DC source and 130Ah. Hence, the SoC estimation in real driving conditions using Ampere-hour counting

This material is reserved for educational use only, not allowed for commercial use.
Forbidden to modify the content, and cite the document when use.

ETM 24
The Second TSME International Conference on Mechanical Engineering
19-21 October, 2011, Krabi

method was also investigated.

3.1 Calculation of Initial Battery Parameters

From section 2.A, the initial battery parameters are required for Kalman Filter technique. A summery of battery initial parameters is given in Table. 1.

3.1.1 Battery Resistance

The total internal resistance (R) of the battery can be estimated by [12]:

$$R = No.\,of\ cell \times \frac{0.022}{C_{10}} \quad (8)$$

The R_s and R_d is assumed to be equivalent and accounted for 75% of total internal resistance [6]. Therefore, from "Fig.3" R_t can be expressed by:

$$R = R_t + \left(\frac{1}{R_d} + \frac{1}{R_s}\right) \quad (9)$$

3.1.2 Battery Capacitors

The C_{bulk} (bulk capacitor) is obtained from OCV of battery at 0% SoC and 100% SoC, as express in "Eq. (10)":

$$C_{bulk-initial} = \frac{Rate(Amp-Sec)\times V_{100\%SoC}}{\frac{1}{2}\left(V^2_{100\%SoC} - V^2_{0\%SoC}\right)} \quad (10)$$

The $C_{surface}$ (surface capacitor) is obtained from a pulse discharge test [13]. The time constant is determined by:

$$C_{surface} = \frac{\tau}{(R_d+R_s)} \quad (11)$$

Where;

$$\tau = -\Delta T \ln\left(1 - \frac{V_4 - V_3}{V_1 - V_3}\right) \quad (12)$$

Table.1 Summery of battery initial parameters.

Initial Parameters				
$R_t(\Omega)$	$R_s(\Omega)$	$R_d(\Omega)$	$C_{bulk}(F)$	$C_{Surface}(F)$
0.00073	0.00087	0.00087	269016.9	587.54

4. Result and Discussions

The observed relationship between specific gravity and OCV is shown in "Fig. 4". The graph shows the discharge characteristics of battery under 5-hours rate, C_5 constant discharge current. At the maximum capacity, corresponding OCV at measured S.G. of 1.25 was calculated to be 12.57V. After being discharged at C_5, the OCV was continuously decreasing to 11.07V after a terminal voltage of 10.2V was reached (i.e. cut-off) and S.G. was decreasing to 1.0. The battery SoC is decreased from 100% to 0% as shown in the graph. Nonetheless, in EVs the initial SoC is not always beginning from 100%. A study of S.G. can be used for identifies the initial SoC.

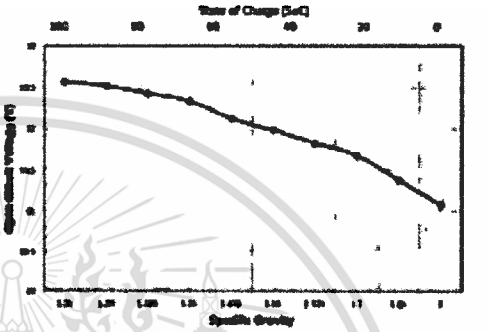

Fig. 4 OCV versus S.G. and SoC

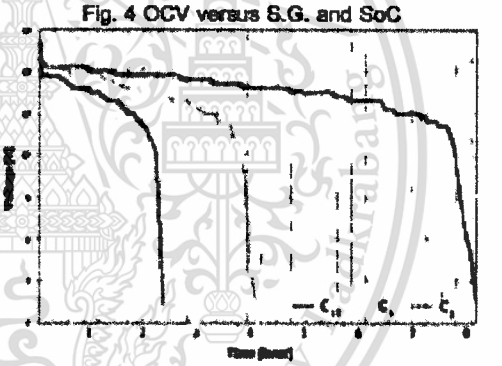

Fig.5 Discharge Characteristic of Battery

In "Fig.5", the result shows the discharge characteristics of battery under 3 different constant discharge rates (C_{10}, C_5, and C_3). By using ampere-hour counting method, the initial SoC was set to 100%. The result of SoC was determined by integral of current over the time as stated in "Eq. (2)". At constant current discharge, the SoC of battery continuously decreased. This experimental result indicated a capacity consumption of 93Ah, 83Ah, and 80Ah at C_{10}, C_5, and C_3 respectively. The relationship between SoC and time was almost linear-relationship under constant current discharge as shown in

This material is reserved for educational use only, not allowed for commercial use.
Forbidden to modify the content, and cite the document when use.

ETM 24
The Second TSME International Conference on Mechanical Engineering
19-21 October, 2011, Krabi

"Fig. 6". The battery voltage rapidly dropped at a cut-off voltage (0%SoC) in 8 hours, 4 hours, and 2.5 hours for C_{10}, C_5, and C_3 respectively.

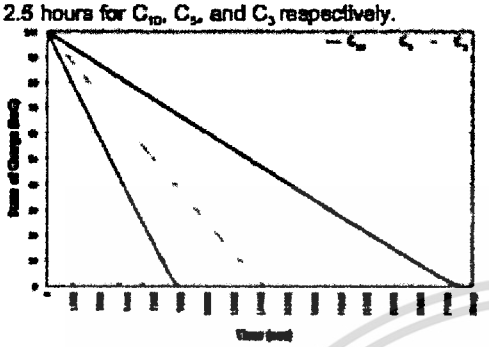

Fig.6 Calculated SoC of Battery using ampere-hour counting method

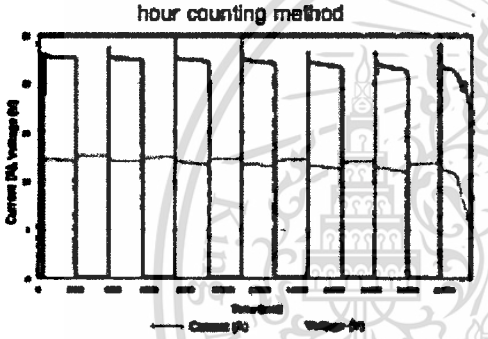

Fig.7 Battery voltage and current variation from pulse discharge test

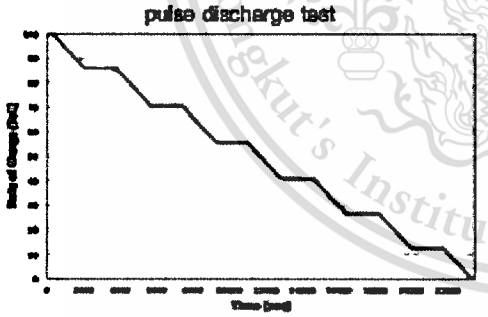

Fig.8 Calculated corresponding State of Charge from pulse discharge test

"Fig. 7-8" display a battery voltage, current and SoC obtained from a pulse discharge test. While a discharge current pulse of C_5 was applied, a battery voltage was inversely proportional to a drawn current as shown in "Fig. 7". During an open circuit, there was some voltage recovery in battery. However, after 50%SoC a gap between open circuit voltages were increased and a terminal voltage continuously decrease after 20%SoC was reached. Then, the battery could no longer supply electric charge to loads. As shown in "Fig. 8", the SoC results showed that the ampere-hour counting method could predict the remaining available run-time of the vehicle.

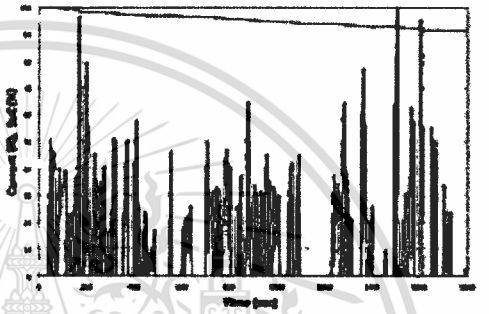

Fig.9 Battery current and SoC in real driving conditions

The parameters obtained from a real traffic condition are shown in "Fig. 9". The battery current varied from 0-100A, depending on the driving situations. The results were obtained from a 30-minutes test drive. Battery SoC was determined to decrease slightly from 100%SoC to 90%SoC over a travel distance of 7km resulting in an average consumption of 1.4Ah/ km. From this information, a remaining range could be determined to be 63km or a maximum operating range of 70km per charge.

In addition, there were some discrepancies in the battery capacity consumption between that of theoretical specification and that observed during the lab-scaled tests. The decreasing rates of SoC were changed by battery consumption and directly effected a total capacity. Therefore, the necessity in carrying out individual battery capacity study was obvious in order to

This material is reserved for educational use only, not allowed for commercial use.
Forbidden to modify the content, and cite the document when use.

develop a potent SoC monitoring system for any EVs applications.

5.Conclusion

All modern electronic devices that used battery as a main power source required battery status to display battery capacity or remaining run-time information. There are many techniques for estimating the battery status. Some techniques are appropriated with electric vehicles while some techniques are not.

- An ampere-hour counting method could predict the remaining available run-time of the vehicle.
- The S.G. measurement could be employed to identify an initial SoC and, by combining with ampere-hour counting method, could be used to estimate the real-time SoC.
- The constant current and pulse discharge test result showed that the rate of discharge could directly affect to the available charge in battery and also affect the estimation of SoC.

In future work, the Kalman Filter Method would be considered in this study in an attempt to improve the current battery SoC estimation technique. By using the battery model and initial battery parameters as presented in this paper, the estimation by Kalman Filter technique will be presented.

6. Acknowledgement

The author wishes to express his gratitude to his advisors also wishes to thank all at the Automotive Laboratory, National Metal and Materials Technology Center (MTEC), for their support and recommendations.

7. References

[1] S. Dhameja (2002), *Electric Vehicle Battery Systems*, ISBN: 0-7506-9916-7, Newnes.

[2] Leon C Rosario (2007), *Power and Energy Management of Multiple Energy Storage Systems in Electric Vehicles*, Department of Aerospace Power & Sensors, Cranfield University.

[3] V. Pop, H.J. Bergveld, D. Danilov, P.P.L Regtien, P.H.L Notten (2008), *Battery Management Systems, Accurate State-of-Charge Indication for Battery Powered Applications*, Philips Research Book Series, 9, ISBN: 978-1-4020-6944-4, Springer publishing.

[4] S. Piller, M.Perrin, A. Jossen (2001), *Methods for state-of-charge determination and their applications*, J. Power Sources, 96, pp. 113-120.

[5] Ng. Kong, M. Chin-Sien, C. Yi-Ping, H. Yao-Ching (2009), *Enhanced coulomb counting method for estimating state-of-charge and state-of-health of lithium-ion batteries*, Applied Energy, 86, pp. 1506-1511.

[6] Bhangu BS, Bentley P, Stone DA, Bingham CM (2005), *Nonlinear observers for predicting State of Charge and State of Health of lead-acid batteries for Hybrid-Electric Vehicles*, IEEE Trans Vehicular Technology, Vol. 54.

[7] M. S. (Steve) Clark (2010), State of charge: Specific gravity vs. battery charging current, *Battcon 2010 Conference, Hollywood*, FL.

[8] R. Kalman (1960), *A new approach to linear filtering and prediction problems*, Transactions of the ASME— Journal of Basic Engineering, vol. 82 (Series D), pp. 35–45.

[9] G. Plett (2004), *Extended Kalman filtering for battery management systems of LiPB-based HEV battery packs. Part 1.* Background, J. Power Source. 134 (2), pp. 252–261.

[10] H. A. Kiehne (2000), *Battery Technology Handbook*, 2nd Edition, ISBN: 0-8247-4249-4, Expert Verlag, Renningen-Malsheim, Germany.

[11] GS BV-130Z, Lead-Acid Battery datasheet.

This material is reserved for educational use only, not allowed for commercial use.
Forbidden to modify the content, and cite the document when use.

[12] J. Larminie J. Lowry (2003), *Electric Vehicle Technology Explained*, ISBN: 0-470-85163-5, John Wiley & Sons Ltd, England.

[13] W. Yan, Y. Tian-ming, L. Bao-jie (2006), Lead-acid Power Battery Management System Basing on Kalman Filtering, *IEEE Vehicle Power and Propulsion Conference (VPPC), Harbin, China.*

King Mongkut's Institute of Technology Ladkrabang

This material is reserved for educational use only, not allowed for commercial use.
Forbidden to modify the content, and cite the document when use.

Appendix B-3: Correcting Factor on State of Charge Estimation for Lead-Acid Batteries

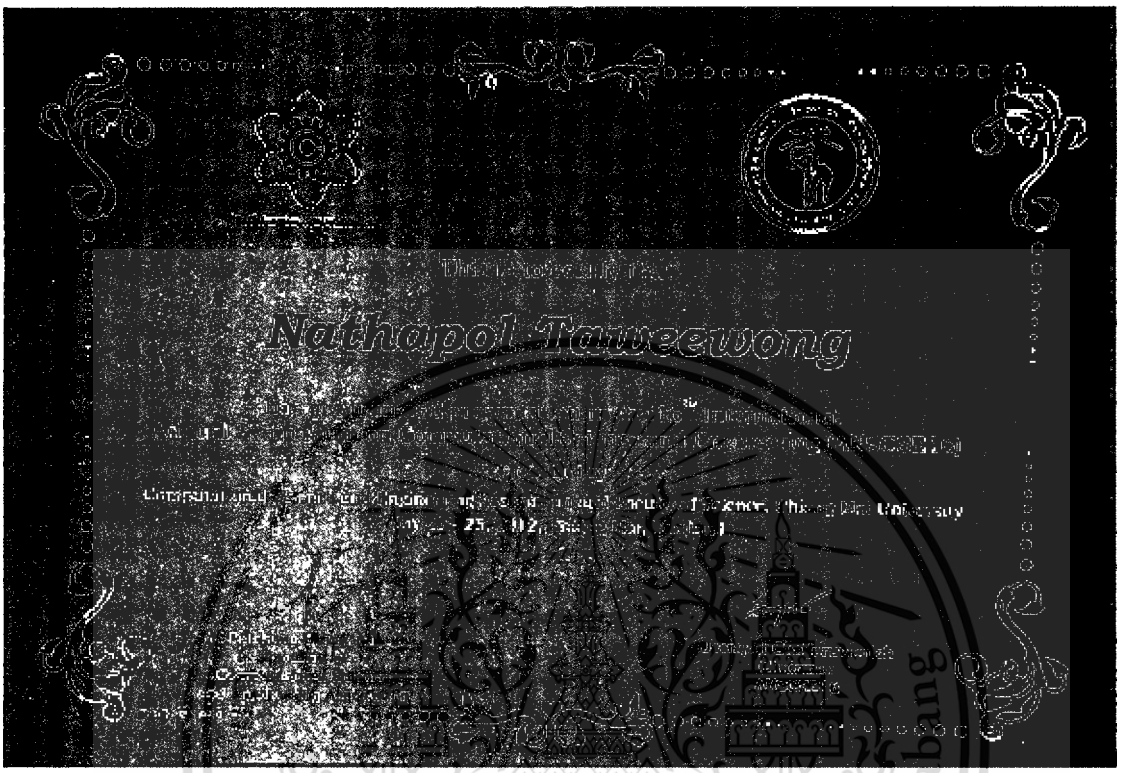

This material is reserved for educational use only, not allowed for commercial use.
Forbidden to modify the content, and cite the document when use.

Correcting Factor on State of Charge Estimation for Lead-Acid Batteries

N. Taweewong[1,C], C. Benyajati[2], P. Premvaranon[2], C. Charoenphonphanich[3], M. Yamakita[4]

[1]*Automotive Engineering, International College, King Mongkut's Institute of Technology Ladkrabang, Thailand*
[2]*Automotive Laboratory, National Metal and Materials Technology Center (MTEC), Thailand*
[3]*Faculty of Engineering, King Mongkut's Institute of Technology Ladkrabang (KMITL), Thailand*
[4]*Department of Mechanical and Control Engineering, Tokyo Institute of Technology, Japan*
E-mail: ntaweewong@gmail.com; **Tel.** 089-9911798

ABSTRACT

Lead-acid batteries are widely used in electric vehicles (EVs) among other various fields of application. Accurate information about State of Charge (SoC) of each individual cell is one of important factors in developing a reliable battery monitoring system. However, unlike other physical properties of battery, SoC cannot be measured directly from battery. The method for determining SoC varies depending on the battery type and on the application in which the battery is used. While many methods could provide an accurate remaining SoC of battery, it was inappropriate in real automotive application. Therefore, the aim of this paper was to discuss and present the SoC estimation of deep cycle lead-acid batteries for electric bus application by using combined techniques.

Keywords: Lead-acid battery, State of Charge

1. INTRODUCTION

In the most basic terms, a battery is an electrochemical cell in which an electric potential (voltage) is generated at the battery terminals by a difference in potential between the positive and negative electrodes [1]. Many types of batteries are used as electricity storage to operate various kings of portable electric devices. The different types of battery are suitable for different applications. Today, there are various types and sizes of batteries such as Lead-acid batteries, Nickel-based batteries, Sodium-based batteries, and more recently, Lithium batteries.

In internal combustion engine vehicles, a fuel gauge is an important part for displaying the remaining fuel in fuel tank of a vehicle. Similarly for electric vehicles, it is necessary to know the amount of remaining charges in battery in order to know how far the vehicle can still travel and to preserve the overall battery life. Thus, the importance of a battery monitoring system to electric vehicles is in the same way as how a fuel gauge is important to internal combustion vehicles. Furthermore, there are some requirements that need to consider for batteries in electric vehicle applications such as specific power, specific energy, efficiency, cost, maintenance, safety, and environmental friendly. As a result, only few types of commercial battery are appropriate for use in electric vehicles. At the present, those types are lead acid, nickel iron, nickel cadmium, nickel metal hydride, lithium polymer and lithium ion, sodium sulphur, and sodium metal chloride [2].

In this paper, a battery discharge test was carried out under constant current discharge conditions. A specific gravity measurement, open circuit voltage (OCV), and ampere-hour counting method were used in a discharge test to estimate SoC of tested batteries. In section 2, some existing battery SoC estimation techniques are reviewed. The combined techniques of SoC estimation are presented in section 3. The battery data such as the battery terminal

This material is reserved for educational use only, not allowed for commercial use.
Forbidden to modify the content, and cite the document when use.

voltage, battery charge and discharge current, and battery temperature were measured using data acquisition tools.

2. BACKGROUND OF BATTERY AND STATE OF CHARGE (SoC)

Batteries are electrochemical devices that convert electrical energy into potential chemical energy during charging, and convert chemical energy into electric energy during discharging [3]. Battery manufacturers usually specify the battery with coulometric capacity (amp-hours, Ah), which is defined as the number of amp-hours gained when discharging the battery from a fully charged state [4]. In theory, the capacity of battery is normally defined as the integral product of current (Amperes) and time (hours), as expressed below:

(1)

Technically, there has been no general definition of SoC. This was mainly because SoC cannot be measured directly from battery. Accordingly, The SoC is defined as the percentage of the maximum possible charge that is present inside a rechargeable battery as expressed in equation (2) [5]. Furthermore, the method for determining state of charge varies depending on the battery type and on the application in which the battery is used.

(2)

2.1 State of Charge Estimation

A decent overview of SoC estimation methods was presented in [6]. Some methods are appropriated with electric vehicles while some techniques are not. This is because they cannot estimate the value in real time and require disconnection of the battery. In this work, SoC estimation method for lead-acid batteries was a purpose of study and would be described below.

2.1.1 Specific Gravity Method

When considering flooded lead-acid cells, the specific gravity (S.G.) of the electrolyte is known to be a good measure of SoC [7]. During the discharge of a lead-acid battery, the discharge consumes sulfuric acid (H_2SO_4) and converts it to water (H_20). In charge process, the sulfuric acid reverts back into the solution state again [2, 4]. Overall reaction of lead-acid battery can be generally expressed by

$$PbO_2 + Pb + 2H_2SO_4 \rightleftharpoons 2PbSO_4 + H_2O \quad (3)$$

The S.G. measurement with the use of a hydrometer is a simple and easy way, with a high accuracy, to indicate SoC of battery. The relationship between sulfuric acid's specific gravity and SoC is almost linear. The general S.G of H_2O and H_2SO_4 is 1 and 1.28 respectively [8]. However, it is impossible to measure the specific gravity of each battery cells during a driving period wild the method can also be used only in a flooded-type lead-acid.

2.2.2 Open Circuit Voltage Method

The open circuit voltage (OCV) of battery varies almost linearly to the battery SoC. The specific relationship of OCV and SoC of each battery is usually identified by manufacturer in data sheet. However, a direct measurement of OCV cannot be operated under loading condition. Because of surface charge, the voltage measured just after discharge would drop lower than an actual voltage of a battery. If the surface layers of the plates have a much lower concentration of charged chemical species than deeper in the plate, it may take several hours before a charge is evenly distributed through the electrode [9]. Especially in valve-regulated lead-acid (VRLA) batteries, considerable amount of times, such as several hours, are needed to reach a steady state after loading [6]. In [10], the individual cell open circuit voltage (OCV) was measured and the S.G. was calculated using the following equation:

$$OCV = S.G. + 0.845 \quad (4)$$

2.3 Ampere-hour Counting Method

This material is reserved for educational use only, not allowed for commercial use.
Forbidden to modify the content, and cite the document when use.

Ampere-hour counting or Coulomb counting is a method to measure and summing the amount of delivered current during charge or discharge. By using Ampere counting, SoC of battery can be expressed as:

$$SoC(\tau) \quad SoC(0) \quad \frac{\cdot}{Ah_{(total)}} \int_0^t I(\tau)d\tau \qquad (5)$$

Where: SoC(0) is initial SoC value;

$Ah_{(total)}$ is amount of total charge;

I(t) is the measured current.

A current is measured by current sensor, which is inserted into the loop and integrated over time. The current sensor is generally either a Hall-Effect sensor or a current shunt [11]. However, this technique could present only a change in battery capacity. Lack of knowledge of initial value of SoC and an accumulated error results in a limited accuracy of the estimation.

3. IMPLEMENTATIONS

The test samples were lead-acid batteries 12V-130Ah capacity. The data acquisition hardware by National Instrument (NI 9219) was used to measure battery data (terminal voltage, load current, and battery temperature). Signal Express by National Instruments was used as a tool for monitoring and collect the battery data. Additionally, the LEM DHR100-C_{10} current transformer was needed to measure the current flow. The K-type thermocouple was used in measuring battery temperature. Two units of digital meter were used for displaying battery voltage and current flow. The Schematic diagram of the experiment is shown in Figure.1.

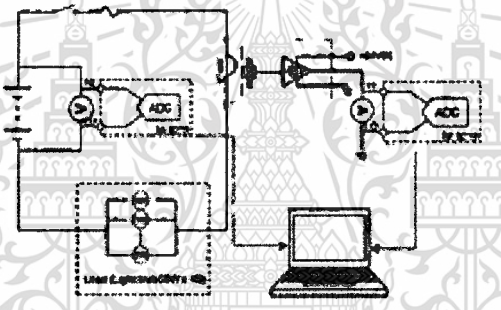

Figure. 1 Schematic diagram of laboratory-scaled experiment

3.1 Experimental Setup

3.1.1 Charging

AC/DC charger was used to charge the test samples. Normally, it took 6-8 hours for fully charge state. When fully charged (100% SoC), the presented battery voltage was 12.3V while corresponding specific gravity (SG) was measured to be 1.26.

Technically, battery characteristics change due to aging and directly affect the maximum capacity of battery. However, the discharge test was started at fully charged condition where the SoC was considered to be 100%.

3.1.2 Discharging

In order to conveniently calculate the percentage of the maximum possible charge that was presented inside a rechargeable battery, the constant current discharge was used as battery loads. The battery industry conventionally uses C-rate to scale the charge and discharge current of a battery [12]. For example, 10Ah battery can generate 1A for 10 hours (C_{10}), or 5A for 2 hours (C_2), or in theory 10A for 1 hour (C_1). Three different rates of discharge were employed i.e. C_{10}, C_2 and C_3, among which the second rate was a common

This material is reserved for educational use only, not allowed for commercial use.
Forbidden to modify the content, and cite the document when use.

discharge rate for electric vehicles [13]. The battery was discharged until the cut off voltage, as presented in the battery datasheet [14], was reached. Normally, the battery was considered to be completely discharge when the voltage reached 10.2V.

3.2 State of Charge Estimation by Using Combined Techniques

As preview in section 2, each method has some advantages and drawbacks. To improve the accuracy of the SoC estimation, the combined technique was presented.

3.2.1 Combining Specific Gravity and Ampere-hour Counting method.

In electric vehicles the initial SoC does not always begin from 100%. A study of S.G. could be used to identify the initial SoC. The measurement of electrolyte S.G. in each cell from new battery and old batteries is shown in Figure.2.

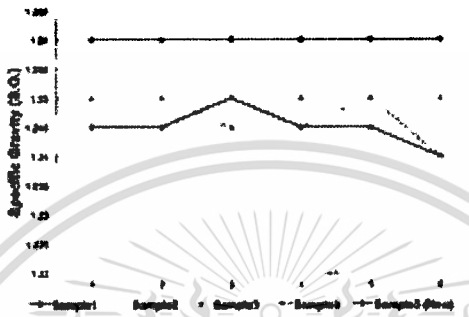

Figure.2 Measurement of electrolyte specific gravity.

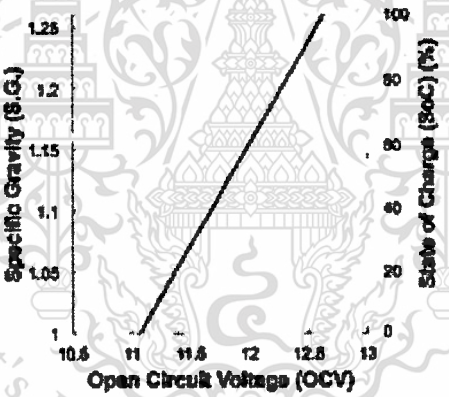

Figure. 3 Open circuit voltage VS Specific Gravity and State of Charge

The observed relationship between specific gravity and OCV is shown in Figure.3. The graph displayed the discharge characteristics of battery under 5-hours rate, or C_5 constant discharge current.

In Figure.4 and 5, the result showed the discharge characteristics and available capacity of battery under 3 different constant discharge rates (C_{10}, C_5, and C_3). By using ampere-hour counting method, the initial SoC was set to 100%. From the discharge characteristics of the samples, the result of available capacity at different discharge rate is shown in Table.1.

This material is reserved for educational use only, not allowed for commercial use.
Forbidden to modify the content, and cite the document when use.

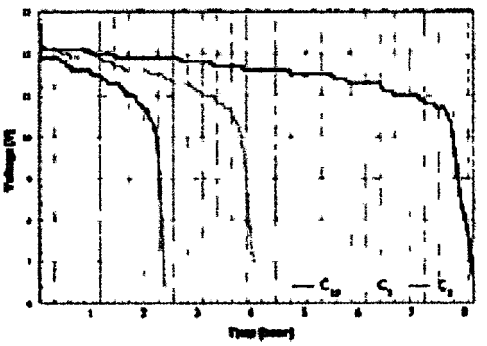

Figure.4 Discharge Characteristic of Battery

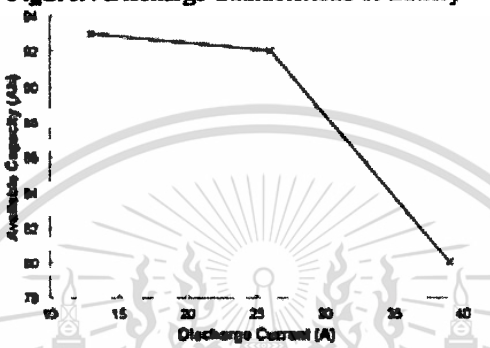

Figure.5 Available Capacity at different discharge rates.

Table.1 Variation of Available capacity with different discharge rates

Discharge rate	Available Capacity (Ah)	Obtained % Capacity	α
C_{10}	93	71.5	1.39
C_5	92	70.7	1.40
C_3	80	61.5	1.62

A factor α was introduced to improve the accuracy of Ampere-hour counting method [15].

$$SoC(t) = SoC(0) - \frac{1}{Ah_{rated}} \int_0^t \alpha I(t)dt \quad (6)$$

Where,

$$\alpha = \frac{Ah_{rated}}{Available\ capacity} \quad (7)$$

By using specific gravity and open circuit voltage data, the initial SoC of battery could be estimated. Then, the ampere-hour counting method with the value of α corresponding to discharge rate was used. The flowchart of the explained method is shown in figure.6.

This material is reserved for educational use only, not allowed for commercial use.
Forbidden to modify the content, and cite the document when use.

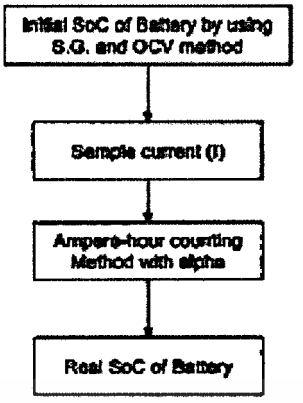

Figure.6 Flowchart to determine SoC of lead acid

4. EXPERIMENTAL RESULTS AND DISCUSSION

It can be seen from Figure.2 that the S.G of electrolyte in battery could present the change of battery characteristics due to aging. So, the initial SoC of flooded lead acid battery could be estimated by using S.G method. However, the measurement of S.G is impossible for VRLA battery. Moreover, the test result of S.G and OCV showed that the relationship between the two values was linear. At the maximum capacity, corresponding OCV at measured S.G. of 1.26 was calculated to be 12.57V. After being discharged at C_3, the OCV was continuously decreasing to 11.07V after a terminal voltage of 10.2V was reached (i.e. cut- off) and S.G. was decreasing to 1.0. The battery SoC decreased from 100% to 0% as shown in Figure.3.

At constant current discharge, the terminal voltage of battery continuously decreased and sharply dropped when the cut-off is reached (Figure.4). As shown in Figure.5 and Table.1, a capacity consumption of 93Ah (or 71.5% obtained capacity), 92Ah (70.7%), and 80Ah (61.5%) was collected from the testing under C_{10}, C_5, and C_3 discharge rates respectively. The obtained percentage capacity was calculated based on 130Ah fully charged battery. The results suggest that a higher discharge rate, a lower available charge from the battery.

In Figure.7, the comparison of SoC estimation by using Ampere-hour counting with and without the value of corresponding α is shown. Without α parameter, the SoC started at 100% and continuously decreased at different rate from the SoC estimated with α. After 4hr, the battery was supposed to run out of charge with percentage of SoC using α parameter reached 0%, while SoC of 28.9% was predicted without α. The results of SoC prediction under different discharge rates with and without corresponding α are shown in figure.8. It can be observed that while SoC of battery predicted with α reached 0%, all the estimations without α gave relatively overestimated values such as 28.2% and 38.5% for C_{10} and C_3 respectively.

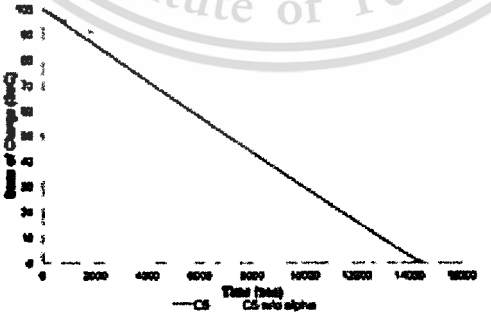

This material is reserved for educational use only, not allowed for commercial use.
Forbidden to modify the content, and cite the document when use.

Figure.7 The comparison of SoC estimation at C_3

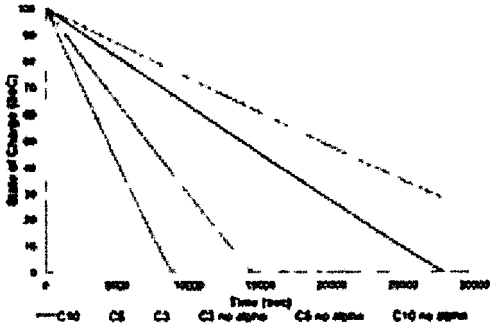

Figure.8 The comparison of SoC estimation at different discharge rates

5. CONCLUSION

In conclusion, there are many techniques for estimating the battery status. Some techniques are appropriated with electric vehicles while some techniques are not. The results showed that the discharge rate would directly affect the capacity of battery. Therefore, the necessity in carrying out individual battery capacity study was obvious in order to develop a potent SoC monitoring system for any EVs applications.

In general, the ampere-hour counting is the closest concept idea for determining battery SoC. However, the main problems of ampere-hour counting technique are an initial SoC and an available charge. Since the S.G. and OCV could be employed to identify an initial SoC, then by combining with an ampere-hour counting method using α corresponding, the real-time SoC could be appropriately estimated.

REFERENCES

1. S. Dhameja, *Electric Vehicle Battery Systems*, Newnes, 2002.
2. J. Larminie J. Lowry, *Electric Vehicle Technology Explained*, John Wiley & Sons Ltd, 2003.
3. M. Ehsani, Y. Gao, S. E. Gay, A. Emadi, Modern *Electric, Hybrid Electric, and Fuel Cell Vehicles*, CRC Press, 2005.
4. G. Yonglang, *A sensor of sulfuric acid specific gravity for lead-acid batteries*, Sensor and Actuator B 105, pp. 194-198, 2005.
5. V. Pop, H.J. Bergveld, D. Danilov, P.P.L Regtien, P.H.L Notton, *Battery Management Systems, Accurate State-of-Charge Indication for Battery Powered Applications*, Philips Research Book Series, 9, Springer publishing, 2008.
6. S. Piller, M.Perrin, A. Jossen, *Methods for state-of-charge determination and their applications*, J. Power Sources, 96, pp. 113-120, 2001.
7. B.S.Bhangu, P. Bently, D.A. Stone, C.M. Bingham, *Nonlinear observers for predicting State of Charge and State of Health of lead-acid batteries for Hybrid-Electric Vehicles*, IEEE Trans Vehicular Technology, Vol. 54, 2005.
8. H.A. Catherino, F.F. Feres, F. Trinidad, *Sulfation in lead-acid batteries*, Journal of Power Sources, Vol. 129, pp. 113-120, 2004
9. A. Fasih, *Modeling and Fault Diagnosis of Automotive Lead-Acid Batteries*, College of Engineering, The Ohio State University Columbus, 2006.
10. M. S. (Steve) Clark, *State of charge: Specific gravity vs. battery charging current*, Battcon 2010 Conference, Hollywood, FL. 2010.
11. W. Michael, *Design of a Battery State Estimation using a Dual Extended Kalman Filter*, Master of Applied Science in Mechanical Engineering, University of Waterloo,

This material is reserved for educational use only, not allowed for commercial use.
Forbidden to modify the content, and cite the document when use.

2010.
12. I. Buchmann, *What is the C-rate?*, http://www.batteryuniversity.com, 2011.
13. H. A. Kiehne, *Battery Technology Handbook*, 2nd Edition, Expert Verlag, Renningen-Malsheim, Germany. 2000.
14. GS BV-130Z, Lead-Acid Battery datasheet.
15. D.J. Deepti, V. Ramanarayanan, *State of Charge of Lead Acid Battery*, India International Conference on Power Electronics, 2006.

ACKNOWLEDGMENTS

The author wishes to express his gratitude to his advisors and also wishes to thank all at the Automotive Laboratory, National Metal and Materials Technology Center (MTEC), for their support and recommendations.

King Mongkut's Institute of Technology Ladkrabang

This material is reserved for educational use only, not allowed for commercial use.
Forbidden to modify the content, and cite the document when use.

BIOGRAPHY

Name: Mr. Nathapol Taweewong

Date of Birth: March 30, 1987

Place of Birth: Bangkok, Thailand

Education:

2005-2008	B. Eng. in Mechanical Engineering, Sirindhorn International Institute of Technology, Thammasat University (TU)
2009-2013	M. Eng. in Automotive Engineering (International program), International College, King Mongkut's Institute of Technology Ladkrabang (KMITL)

Honour and Scholarship:

2009-2011	TAIST-Tokyo Tech scholarship, the Master's Degree in Automotive Engineering funded by National Science and Technology Development Agency (NSTDA), Thailand

Proceeding:

1. **Taweewong N.**, Benyajati C., Charoenphonphanich C., Yamakita M., Premvaranon P. 2011. *"Battery Behavior of Electric Bus at Different Discharge Rate in Real Driving Condition"* The 7th International Conference on Automotive Engineering, Bangkok, Thailand.

2. **Taweewong N.**, Benyajati C., Charoenphonphanich C., Yamakita M., Premvaranon P. 2011. *"Progressive State of Charge Estimation for Electric Bus"* The 2nd TSME International Conference on Mechanical Engineering, Krabi, Thailand.

3. **Taweewong N.**, Benyajati C., Charoenphonphanich C., Yamakita M., Premvaranon P. 2012. *"Correcting Factor on State of Charge Estimation for Lead-Acid Batteries"* The 16th International Annual Symposium on Computational Science and Engineering (ANSCSE16), Chiang Mai, Thailand.

This material is reserved for educational use only, not allowed for commercial use.
Forbidden to modify the content, and cite the document when use.